Multi-scale optimization for heterologous biosynthesis of the nonribosomal peptide antibiotic valinomycin in *Escherichia coli*: from strain to bioprocess engineering

vorgelegt von

M. Sc. Jian Li

aus Anhui (China)

von der Fakultät III – Prozesswissenschaften
der Technischen Universität Berlin
zur Erlangung des akademischen Grades

Doktor der Naturwissenschaften
- Dr. rer. nat. -

genehmigte Dissertation

Promotionsausschuss:

Vorsitzender	Prof. Dr.-Ing. Vera Meyer
Gutachter	Prof. Dr. Peter Neubauer
Gutachter	Dr. rer. nat. Uwe Horn

Tag der wissenschaftlichen Aussprache: 11.09.2013

Berlin 2013
D83

Abstract

Nonribosomal peptides (NRPs), belonging to a large family of natural products, are assembled by multimodular nonribosomal peptide synthetases (NRPSs) from various microorganisms like bacteria and fungi. These naturally originated compounds are of great interest since they possess numerous crucial bioactivities such as antiviral, antimicrobial and anticancer activity. However, pharmaceutical applications of these products are often impeded because many native producers are difficult to cultivate or show a low productivity. The recombinant production of natural products in a surrogate host like *Escherichia coli* has emerged as a strategy to overcome these limitations. Although a few NRPs have been produced heterologously in *E. coli*, the yields were mostly unsatisfactory. In this study, based on the NRP valinomycin production platform in *E. coli*, multiple strategies from strain improvement to bioprocess optimization were employed to investigate the production conditions and increase the productivity.

Nine compatible expression vectors for coexpression of valinomycin synthetase, Vlm1 and Vlm2, were constructed, followed by a production screening. Batch and enzyme-based fed-batch cultivations were compared for valinomycin production, indicating the fed-batch mode can easily reach high cell densities and significantly improve volumetric valinomycin titers up to mg per liter levels compared to the low levels (µg per liter) obtained in batch cultivations. A design of experiments (DoE) driven optimization revealed that the following parameters had a significant positive impact on the volumetric yield of valinomycin: (i) the addition of nutrients to the medium, (ii) a higher enzyme concentration relating to faster glucose feeding and (iii) a lower culture volume allowing better oxygen supply. Repeated glucose polymer feeding to the culture dramatically increased cell densities and valinomycin titers. Coexpression of the repairing enzyme type II thioesterase (TEII) together with the valinomycin synthetase further improved valinomycin titers. The maximum titer of valinomycin obtained in this study was 13 mg L^{-1}. Fed-batch cultivation in lab-scale bioreactors confirmed that the valinomycin production in the mg per liter range is also possible in pure glucose based mineral salt medium and that this process reacts robust to nutrient oscillations. This might suggest that a scaling of the process to large industrial scale should be possible.

This study provides a feasible approach and example to optimize and enhance heterologous biosynthesis of valinomycin, which may be generally applicable for the development and production of other complex natural products in *E. coli*.

Zusammenfassung

Nichtribosomale Peptide (NRPs) gehören zu einer großen Familie von Naturstoffen und werden von multimodularen Nichtribosomalen Peptidsynthetasen (NRPSs) in verschiedenen Mikroorganismen wie Bakterien und Pilzen synthetisiert. Diese natürlich vorkommenden Verbindungen sind von großem Interesse, da sie zahlreiche bedeutende antivirale, antimikrobielle und tumor-inhibierende Bioaktiviäten besitzen. Die pharmazeutische Anwendung dieser Produkte wird dadurch erschwert, dass viele der natürlichen Produzenten schwer zu kultivieren sind oder eine geringe Produktivität aufweisen. Die rekombinante Produktion derartiger Naturstoffen in einem Ersatzorganismus wie *Escherichia coli* ist eine mögliche Strategie, diese Probleme zu umgehen. Obwohl bereits einige NRP in *E. coli* produziert wurden, sind die Ausbeuten generell unbefriedigend. In der vorliegenden Studie wurden am Beispiel der Produktion von Valinomycin in *E. coli* verschiedene molekularbiologische und bioverfahrenstechnische Strategien getestet, und die Produktivität zu steigern.

Neun kompatible Expressionsvektoren wurden zur Koexpression der Valinomycinsynthetasegene Vlm1 und Vlm2 konstruiert, und in einem Screeningansatz paralleleingessetzt. Batch- und enzymbasierte Fed-Batch-Kultivierungen wurden im Hinblick auf die Valinomycinproduktion verglichen. Hierbei zeigte es sich, dass unter Fed-Batch-Bedingungen höhere Zelldichten und damit eine signifikant erhöhte volumetrische Valinomycinkonzentration im Milligramm pro Liter Bereich erzielt werden kann, verglichen mit den niedrigen Ausbeuten (µg pro Liter) in den Batch-Kultivierungen. Eine auf statistischer Versuchsplanung beruhende Optimierung führte zu der Erkenntnis, dass die volumetrische Valinomycinausbeute durch folgende Faktoren positiv beeinflusst wird: (i) Zusatz komplexer Nährstoffe zum Kulturmedium, (ii) eine höhere Enzymkonzentration und dadurch höhere Glukose-Fütterungsrate, (iii) ein geringeres Kulturvolumen und damit eine bessere Sauerstoffversorgung. Eine Verlängerung der Produktionsphase durch wiederholte Zugabe von Glukosepolymer bei der EnBase-Kultivierung führte zu einer weiteren Steigerung der Zelldichte um einen Faktor von zwei und erhöhte auch die Valinomycin-Produktion um denselben Faktor. Koexpression des Korrekturenzyms Typ II Thioesterase (TEII) zusammen mit der Valinomycinsynthetase verbesserte die Valinomycinausbeute weiter. Als maximale Valinomycinkonzentration wurden 13 mg L^{-1} in dieser Arbeit erreicht.

Fed-Batch-Fermentationen im Bioreaktor im Labormaßstab zeigten, dass eine Valinomycinausbeute im mg pro Liter-Bereich prinzipiell auch im Mineralsalzmedium möglich ist und ein derartiger Prozess robust auf Nährstoffoszillationen reagiert, d.h. in den industriellen Maßstab skalierbar sein sollte.

Diese Studie bietet einen anwendbaren Ansatz und ein Beispiel dafür, wie die heterologe Biosynthese von Valinomycin optimiert und erhöht werden kann, und lässt sich auf die Entwicklung und die heterologe Produktion anderer komplexer Naturstoffe in *E. coli* übertragen.

The present work was performed from October 2010 – September 2013 in the research group of Prof. Dr. Peter Neubauer (Chair of Bioprocess Engineering) at the Department of Biotechnology, Technische Universität Berlin.

Publications

J. Jaitzig*, J. Li*, R. Süssmuth, P. Neubauer. Reconstituted biosynthesis of the nonribosomal macrolactone antibiotic valinomycin in *Escherichia coli*. 2013, submitted (*equal contribution)

J. Li*, J. Jaitzig*, F. Hillig, R. Süssmuth, P. Neubauer. Enhanced production of the nonribosomal peptide antibiotic valinomycin in *Escherichia coli* through small-scale high cell density fed-batch cultivation. 2013, submitted (*equal contribution)

Conference contributions

Oral presentation

J. Li, J. Jaitzig, R. Süssmuth, P. Neubauer. Total biosynthesis of the nonribosomal peptide antibiotic valinomycin in *Escherichia coli*: from gene to product. The 7th Conference on Recombinant Protein Production (RPP7) 2013, March 6-8, Laupheim, Germany

J. Li, J. Jaitzig, R. Süssmuth, P. Neubauer. Advanced cell engineering: making very large proteins and keeping them active – an example valinomycin. UniCat Symposium: Consistent Bioprocess Development -- New Expression Systems and Technologies 2013, March 1, Berlin, Germany

P. Neubauer, J. Li, R. Süssmuth, J. Jaitzig. Where “difficult to express” proteins and metabolic engineering meet: reconstituted biosynthesis of the antibiotic valinomycin in *E. coli*. International Workshop on New and Synthetic Bioproduction Systems 2012, December 6-7, Hamburg-Harburg, Germany

Poster presentation

J. Li, J. Jaitzig, R. Süssmuth, P. Neubauer. Enhanced production of the nonribosomal peptide antibiotic valinomycin in *Escherichia coli* through fed-batch cultivation in parallel milliliter-scale 24-well plates. International Workshop on New and Synthetic Bioproduction Systems 2012, December 6-7, Hamburg-Harburg, Germany

J. Li, J. Jaitzig, R. Süssmuth, P. Neubauer. Whole-cell production of the nonribosomal peptide valinomycin in the heterologous host *Escherichia coli*. Catalyzing Bio-Economy -- Biocatalysts for Industrial Biotechnology, Annual meeting of the DECHEMA-VAAM-Section Biotransformations 2012, April 24-25, Frankfurt, Germany

Table of Contents

Abbreviations

A	Adenylation (domain)
aa	Amino acid(s)
ACP	Acyl carrier protein
amp	Ampicillin
att	Attachment site
bp	Base pair(s)
C	Condensation (domain)
cm	Chloramphenicol
CoA	Coenzyme A
DMSO	Dimethyl sulfoxide
DNA	Deoxyribonucleic acid
dNTP	Deoxyribonucleoside triphosphate
DO	Dissolved oxygen
DoE	Design of experiments
DTT	Dithiothreitol
D-Hiv	D-α-Hydroxyisovalerate
E	Epimerization (domain)
EDTA	Ethylenediaminetetraacetic acid
IPTG	Isopropyl β-D-1-thiogalactopyranoside
kb	Kilo base pairs
kDa	Kilo dalton
Kiv	α-Ketoisovalerate
KR	Ketoreductase
L-Lac	L-Lactate
LB	Luria-Bertani medium
LC-MS	Liquid chromatography- mass spectrometry
MT	Methyltransferase (domain)
m/z	Mass-to-charge ratio

NRP	Nonribosomal peptide
NRPS	Nonribosomal peptide synthetase
OD	Optical density
ori	Origin of replication
PCP	Peptidyl carrier protein
PCR	Polymerase chain reaction
PFR	Plug flow reactor
PK	Polyketide
PKS	Polyketide synthase
4'-PP	4'-Phosphopantetheine
PPTase	Phosphopantetheinyl transferase
RBS	Ribosome-binding site
RNA	Ribonucleic acid
ROP	Repressor of primer
SDS-PAGE	Sodium dodecyl sulfate polyacrylamide gel electrophoresis
Sfp	Surfactin phosphopantetheinyl transferase
SOC	Super optimal broth with catabolite repression
STR	Stirred tank reactor
T	Thiolation (domain)
TB	Terrific Broth
TCR	Two-compartment reactor
TE	Thioesterase (domain)
TEII	Type II thioesterase
T_m	Melting temperature
μ	Specific growth rate
U	Unit(s)
UV	Ultraviolet
VlmSyn	Valinomycin synthetase

1. Introduction

1.1. Background of natural products

Natural products (also known as secondary metabolites), a huge family of relatively low molecular weight organic compounds, have been utilized as sources by humans for thousands of years to search for potent drugs for the treatment of human diseases (Dias et al. 2012; Ji et al. 2009). These valuable products originate from a broad and diverse range of living organisms including microorganisms (Chin et al. 2006; Woodruff 1980), plants (Balunas and Kinghorn 2005; Kinghorn et al. 2011), animals (Chin et al. 2006; Spande et al. 1992), and marine organisms (Faulkner 2002; Haefner 2003). The first purified pharmacological active natural product was morphine from a plant *Papaver somniferum* by a young German pharmacist Friedrich Sertürner in 1805 (Hamilton and Baskett 2000). This breakthrough initiated a new era of drug discovery from natural source products. Especially, the discovery of the antibiotic penicillin by Alexander Fleming in 1928 led to the "golden era" of the development of novel antibiotics between the 1940s and 1960s (Aminov 2010). During these twenty years, several new classes of antibiotics were successfully introduced into clinical use (Table 1.1) (Conly and Johnston 2005).

Table 1.1 Introduction of new classes of antibiotics from 1935 to 1968. [a]

Year introduced	Class of drug
1935	Sulphonamides
1941	Penicillins [b]
1944	Aminoglycosides
1945	Cephalosporins
1949	Chloramphenicol
1950	Tetracyclines
1952	Macrolides/lincosamides/streptogramins
1956	Glycopeptides
1957	Rifamycins
1959	Nitroimidazoles
1962	Quinolones
1968	Trimethoprim

[a] Table is adapted from (Conly and Johnston 2005).

[b] Penicillin was discovered by A. Fleming in 1928, but the first therapeutic usage was realized by Howard W. Florey only in 1941 (American Chemical Society International Historic Chemical Landmarks. Discovery and Development of Penicillin, 1928-1945. http://portal.acs.org/portal/PublicWebSite/education/whatischemistry/landmarks/flemingpenicillin/index.htm. Accessed April 30, 2013).

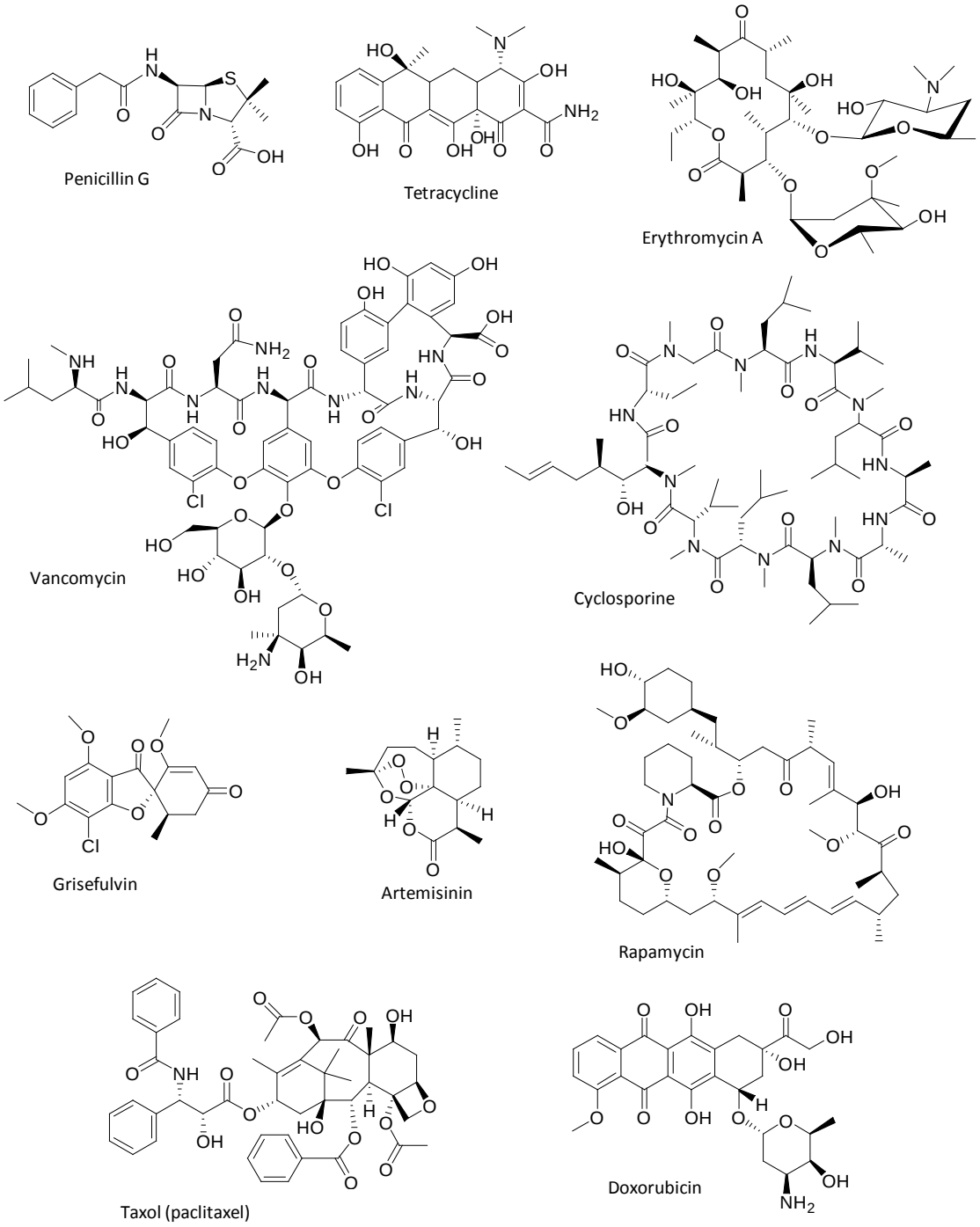

Figure 1.1 Chemical structures of therapeutically relevant natural products.

By 1990, approximately 80 % of the approved drugs were either natural products or their analogs, which included antibiotics (e.g., penicillin, tetracycline, vancomycin, erythromycin), antifungal agents (e.g., grisefulvin), immunosuppressant drugs (e.g., cyclosporine, rapamycin), antimalarial agent (e.g., artemisinin), and anticancer drugs (e.g., taxol, doxorubicin) (chemical structures see Figure 1.1) (Li and Vederas 2009).

To date, it is undoubted and clear that natural products have historically played and in the future will continue to play a significant role in novel drug discovery and development, and hence benefiting human beings. For more information, a series of reviews are recommended (Cragg et al. 1997; Newman and Cragg 2007; Newman and Cragg 2012; Newman et al. 2003).

1.2. Nonribosomal peptides

Nonribosomal peptides (NRPs), belonging to a large class of peptide natural products, are mainly produced by various microorganisms like bacteria and fungi (Caboche et al. 2010; Marahiel et al. 1997; Schwarzer et al. 2003; Stack et al. 2007). These naturally originated compounds are of great interest since they possess a broad spectrum of biological activities and are used in many pharmaceutical applications (Cane and Walsh 1999; Cane et al. 1998; Felnagle et al. 2008). Instead of the classical pathway for protein synthesis through the transcription of DNA into RNA and the translation of RNA into peptide using ribosomes, NRPs are assembled through a ribosome independent route where an mRNA template is not needed (Finking and Marahiel 2004; Fischbach and Walsh 2006; Marahiel et al. 1997). An extremely diverse group of monomers (to date more than 500 different types) have been found incorporated in NRPs including 20 proteinogenic amino acids, nonproteinogenic amino acids (e.g., D-amino acids), fatty acids, and hydroxy acids (Table 1.2) (Caboche et al. 2010; Caboche et al. 2008). Such diverse building blocks constitute NRPs (2 to ~50 residues) with great structural versatility showing linear, branched or cyclic (partially or totally) forms (Caboche et al. 2008; Marahiel et al. 1997). In addition, NRPs' structures could be further diversified by modification via acylation, glycosylation or heterocyclic ring formation (Schwarzer et al. 2003; Walsh 2004). It is believed that the enormous structural diversity and complexity of NRPs, which leads to a high density of functional groups, contributes considerably to the observed pharmacological properties (Marahiel 2009).

Table 1.2 Examples of unusual monomers in NRPs. [a]

Monomer	Structure	Abbreviation	NRP
modified proteinogenic amino acids			
N-methyl aa (e.g., *N*-methyl valine)	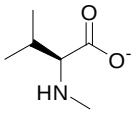	MeVal	cyclosporine enniatin
nonproteinogenic amino acids			
D-aa (e.g., D-phenylalanine)	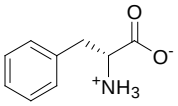	D-Phe	bacitracin gramicidin S tyrocidine
δ-(L-α-amino adipic acid)	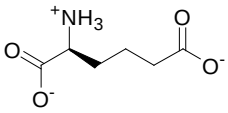	Aad	ACV-tripeptide (precursor of penicillin)
2-amino-9,10-epoxy-8-oxodecanoic acid	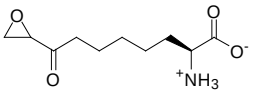	Aeo	HC-toxin
L-α-amino butyric acid	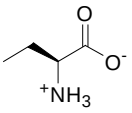	Abu	cyclosporin
(4R)-4[(E)-2-butenyl-4-methyl-L-threonine]	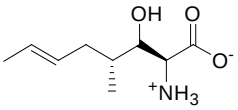	Bmt	cyclosporin
2.6-diamino-7-hydroxy-azealic acid	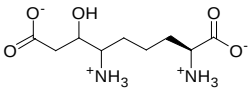	Dha	edeine
ornithine	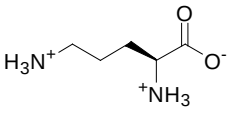	Orn	bacitracin gramicidin S tyrocidine
carboxy acids			
2,3-dihydroxy benzoic acid	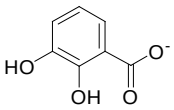	Dhb	enterobactin
D-α-hydroxyisovaleric acid	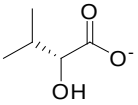	Hiv	enniatin B
amines			
spermidine	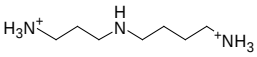	Sperm	edeine

[a] Table is adapted from (Marahiel et al. 1997).

1.3. Nonribosomal peptide biosynthesis

Naturally, NRPs are biosynthesized in native producers via assembly lines called nonribosomal peptide synthetases (NRPSs) (Finking and Marahiel 2004; Fischbach and Walsh 2006; Marahiel et al. 1997; von Döhren et al. 1997). NRPSs are multifunctional enzymes with remarkable sizes. For example, the cyclosporine NRPS in *Tolypocladium niveum* has a molecular weight of more than 1600 kDa (Weber et al. 1994). Multifunctional NRPSs are composed of several modules, where each module is responsible for incorporating one monomer residue into the final product. Usually, one classical NRPS module contains three core domains, arranged as C-A-T (Fischbach and Walsh 2006). The adenylation (A) domain is responsible for selecting and activating the substrate monomer. The thiolation (T) domain, also called peptidyl carrier protein (PCP), serves as a flexible transport unit that holds the activated substrate and moves between two adjacent catalytic positions. The third core domain, the condensation (C) domain catalyzes the peptide bond formation resulting in peptide chain elongation. The initiation module in NRPSs normally comprises two domains, A and T, allowing the subsequent elongated peptide chain that carries a free N-terminal amino group. However, in some cases, if *N*-acylated peptides are synthesized, a C domain that catalyzes *N*-acylation of the starting amino acid will be installed in the first module forming a three-domain organization (C-A-T) (Schmoock et al. 2005; Watanabe et al. 2006). The termination module commonly has a fourth C-terminal domain, a thioesterase (TE) that is responsible for the final peptide release. Alternatively, a C-terminal reductase domain (Gaitatzis et al. 2001) or a condensation-like domain (Gao et al. 2012) can also release the fully assembled peptide chain to result in the final NRP. In addition, some modifying domains, for example, epimerization (E) and *N*-methyltransferase (MT) domains, also present in some NRPSs make NRP structures considerably more versatile (Marahiel et al. 1997). A fictitious tetra-modular NRPS for initiation, elongation, modification and termination is shown in Figure 1.2.

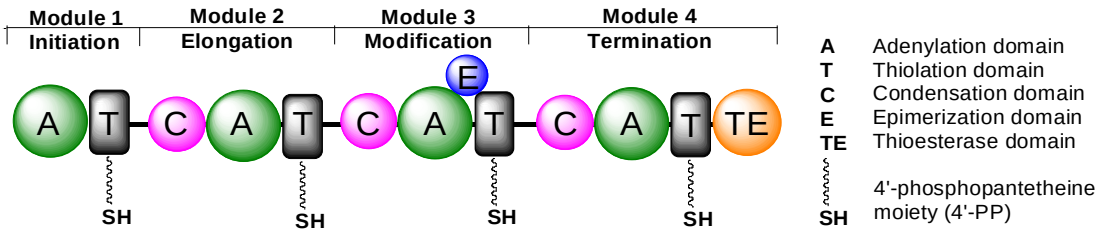

Figure 1.2 Organization of a fictitious tetra-modular NRPS.

Based on domain organization and different modes of biosynthetic logic, NRPSs are proposed to be classified into three types: linear NRPSs (Type A), iterative NRPSs (Type B), and nonlinear NRPSs (Type C) (Mootz et al. 2002). In linear NRPSs, the peptide chain will be elongated depending on the number and order of the modules and each module will be used only once. Therefore, an NRPS with *n* modules generates a peptide with *n* monomer residues. One Type A example is bacitracin synthetase (Konz et al. 1997). Iterative NRPSs, in contrast, use their modules more than once to build up peptide chains with short repetitive sequences. One example of Type B is bacillibactin synthetase (May et al. 2001). While two NRPSs syringomycin synthetase (Guenzi et al. 1998) and vibriobactin synthetase (Keating et al. 2000a) with unusual domains organization are examples regarded as the third type nonlinear NRPSs.

A hypothetic NRP biosynthesis cycle is presented in Figure 1.3, illustrating the main steps involved in the synthesis of a cyclic peptide. Briefly, NRPS gene clusters are first translated into the inactive apo-NRPS. Then, the apo-NRPS will be converted into the active holo-NRPS with the help of phosphopantetheinyl transferase (PPTase) through transfer of the 4'-phosphopantetheine (4'-PP) moiety from coenzyme A (CoA) to a conserved serine residue in the T domains. This step is termed as "priming". However, "mispriming" can occur if acyl-CoAs are used as substrates by the promiscuous PPTase. Fortunately, a discrete type II thioesterase protein can hydrolyze acyl groups attached to the 4'-PP cofactors and regenerate the holo-NRPS. On the holo-NRPS the peptide chain is growing until it reaches the last termination module, where it will be released and cyclized by the TE domain. If necessary, further modifications will be involved to produce the final mature product.

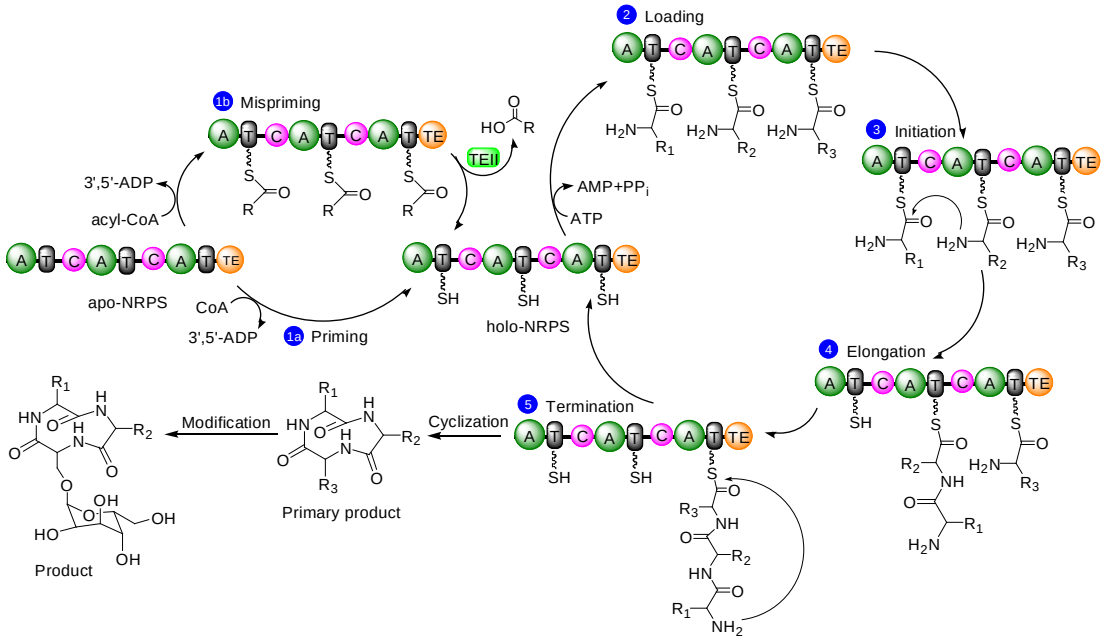

Figure 1.3 Stages of the NRP biosynthetic pathway: from inactive apo-NRPS to the final product. A= adenylation domain; T= thiolation domain; C= condensation domain; TE= thioesterase domain; TEII= type II thioesterase. Adapted from (Schwarzer et al. 2003).

1.3.1. The adenylation (A) domain

The adenylation (A) domains, key constituents of NRPSs with approximately 550 amino acids in length, are responsible for selecting and activating the building block monomers for NRP formation (Finking and Marahiel 2004). To activate the monomers, A domains catalyze a two-step reaction (Figure 1.4) (Marahiel et al. 1997). Firstly, the selected monomer is activated by the A domain generating an aminoacyl-adenylate intermediate with ATP and Mg^{2+} present. Secondly, the reactive intermediate is attached to the 4'-PP cofactor of a T domain, which is located downstream of the A domain in the same module and will be discussed in section 1.3.2.

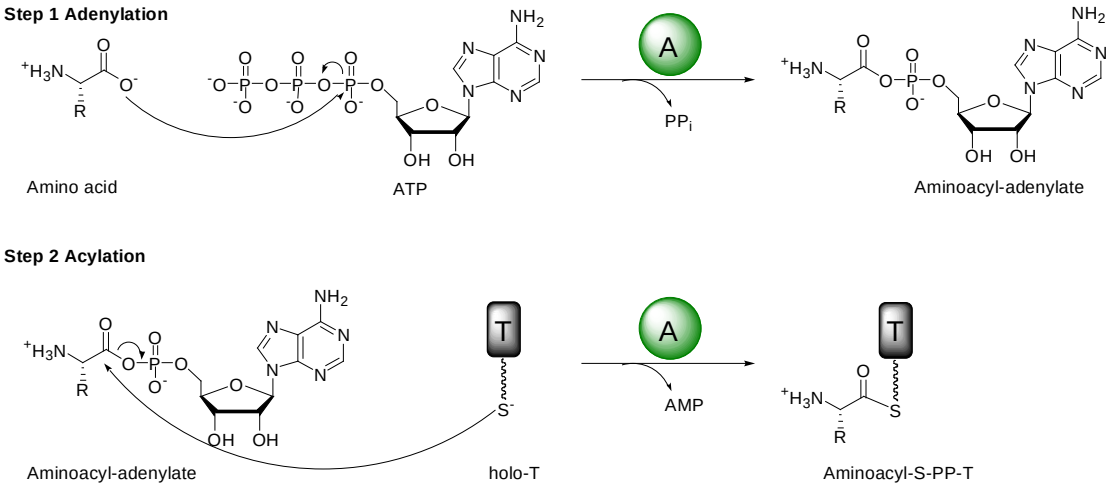

Figure 1.4 Amino acid activation and aminoacyl thioester formation catalyzed by the NRPS A domain.

The working mechanism for specific substrate recognition by the A domain was rationally illuminated when the crystal structure of the phenylalanine-activating A domain of the gramicidin S synthetase 1 (PheA) was solved together with phenylalanine and AMP (Conti et al. 1997). PheA is composed of two compact domains (Figure 1.5), a large N-terminal domain of ~400 residues (in blue) and a small 100-residue C-terminal domain (in green). Through analysis of the substrate binding pocket, ten residues lying in a 100-residue stretch of the larger N-terminal domain are the major determinants of the substrate specificity of A domains. These residues are considered as the specificity-conferring code in NRPSs, which could be used to predict the specificity of uncharacterized A domains (Challis et al. 2000; Stachelhaus et al. 1999). In addition, the relevant codes can be rationally altered by site-directed mutagenesis changing the substrate specificity of A domains and allowing the synthesis of novel NRPs (Crusemann et al. 2013; Evans et al. 2011; Stachelhaus et al. 1999).

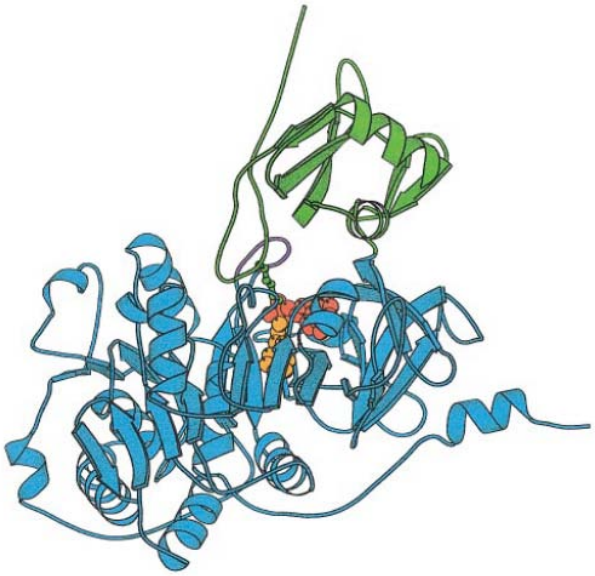

Figure 1.5 Ribbon diagram of the PheA of gramicidin synthetase 1 with phenylalanine and AMP. Blue= the large N-terminal domain; Green= the small C-terminal domain; Orange= phenylalanine; Red= AMP. Adapted from (Conti et al. 1997).

1.3.2. The thiolation (T) domain

The thiolation (T) domains (~80-100 aa), also known as peptidyl carrier proteins (PCP), play a central role in the NRPS assembly lines since they have to interact not only with A domains for aminoacyl thioester formation (Figure 1.4), but also with other catalytic domains involved in peptide bond formation, substrate modification, or product release (Fischbach and Walsh 2006). To enact these functions, T domains have to be modified in advance by transferring 4'-PP cofactor from CoA to a conserved serine residue of the T domains with the help of PPTase (Lambalot et al. 1996), thus yielding active holo-T (Figure 1.6). Then, activated substrates can be covalently bound as thioesters to the free thiol group of the flexible 4'-PP arm.

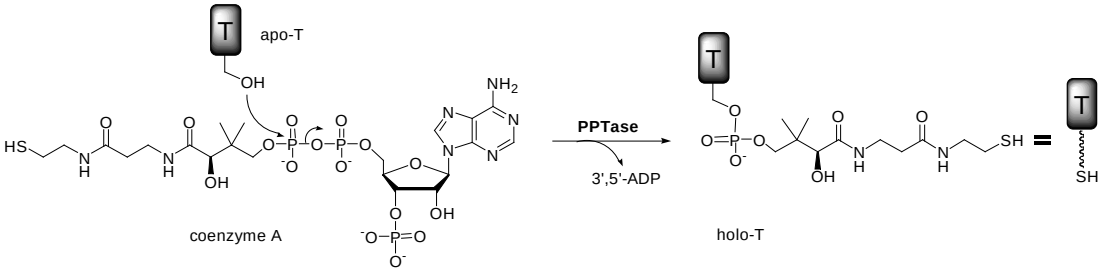

Figure 1.6 Posttranslational modification of T domain by phosphopantetheinyl transferase (PPTase).

A solution structure of the T domain of the *Bacillus brevis* tyrocidine synthetase 3 (TycC3-T) has been solved by NMR spectroscopy, showing a four-helix bundle fold with a long loop between the first two helices (Weber et al. 2000). In general, TycC3-T has a similar topological structure to the other carrier protein members: acyl carrier protein (ACP) of fatty acid synthase in *Escherichia coli* (Holak et al. 1988) and ACP of actinorhodin polyketide synthase in *Streptomyces coelicolor* A3 (Crump et al. 1997). The conserved serine residue, the binding site of 4'-PP cofactor in the three carrier proteins, is located at the same interface between the long loop and the second helix, which can be seen from Figure 1.7.

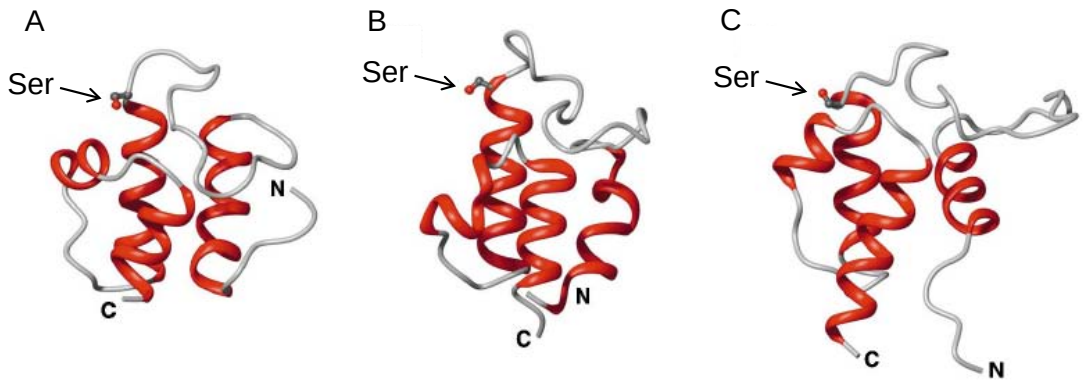

Figure 1.7 Ribbon diagrams of (A) the NRPS T domain, (B) the fatty acid synthase ACP, and (C) the actinorhodin polyketide synthase ACP. The conserved serine residues are highlighted in ball-and-stick format (indication by an arrow). The similarity of the overall fold as well as differences in lengths and relative orientations of the helices between these members of the same protein family are apparent. Adapted from (Weber and Marahiel 2001).

1.3.3. The condensation (C) domain

The condensation (C) domains (~450 aa) are peptide bond formation sites, which catalyze the reaction between the electrophilic upstream peptidyl-S-T donor and the nucleophilic downstream aminoacyl-S-T acceptor resulting in the elongation of the growing peptide chain (Figure 1.8) (Fischbach and Walsh 2006). Since the C domain catalyzes the C-N bond formation between a donor and an acceptor, it is proposed that two distinct substrate-binding sites exist in the domain. Interestingly, donor site and acceptor site also possess the function of substrate selectivity (especially stereoselectivity) rather than only passive acceptance of substrates (Belshaw et al.

1999). Of the two sites, the acceptor site appears to be more selective than the donor site. The reason why C domains act as a second “filter” for substrate selectivity in NRP synthesis is unknown, since A domains can already confer the accurate recognition of target monomers. One possible explanation could be that C domains work as the final proof-reading detector before formation of a new peptide bond by itself, thus ensuring the accuracy of the peptide and efficiency of the NRPS.

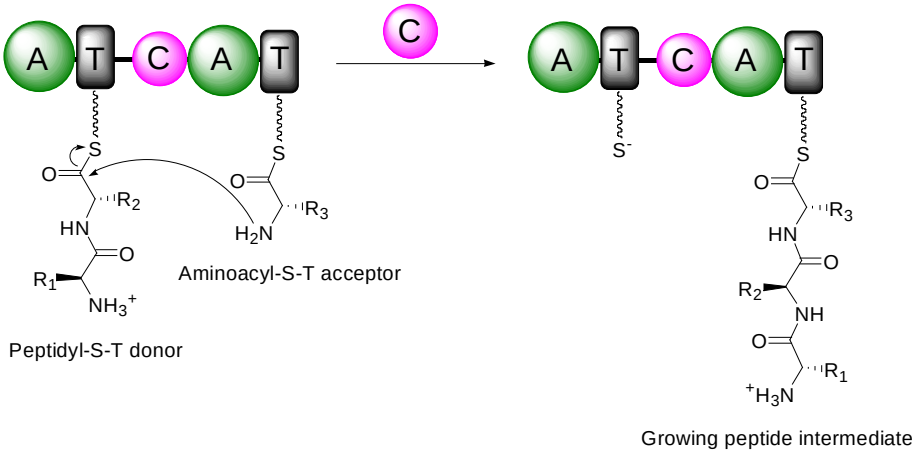

Figure 1.8 Peptide bond formation catalyzed by NRPS C domain.

Crystal structures of two C domains, the free-standing C domain (VibH) from *Vibrio cholerae* vibriobactin synthetase (Keating et al. 2002) and the TycC5-6 T-C bidomain from *Bacillus brevis* tyrocidine synthetase (Samel et al. 2007), have been solved. Both structures show two large N- and C-terminal subdomains, which are arranged in a V-shaped structure with the active site located at the junction of these two subdomains (Figure 1.9). The canyon-like active site contains a conserved amino acid motif (HHXXXDG), which is essential for the condensation activity during NRP synthesis (Bergendahl et al. 2002; Marahiel et al. 1997; Stachelhaus et al. 1998). It must be noted that, initially, the second histidine in the conserved motif (HHXXXDG) was considered to deprotonate the α-ammonium group of the acceptor substrate in order to attack the electrophilic carboxyl-thioester group of the donor substrate (Bergendahl et al. 2002). However, according to the mutational data and pKa value analysis of the active site residues, it is revealed that peptide bond formation in C domains depends mainly on electrostatic interactions rather than on general

acid-base catalysis (Samel et al. 2007).

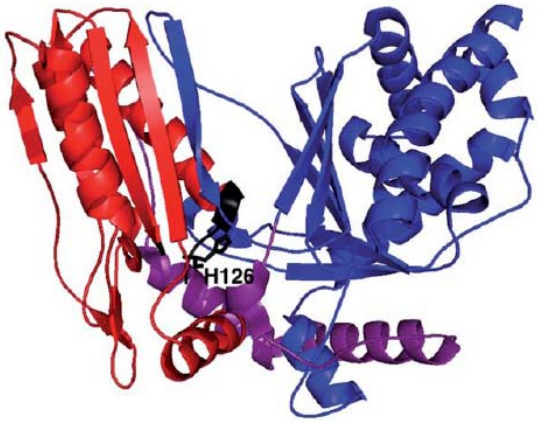

Figure 1.9 Crystal structure of the stand-alone C domain (VibH) from *Vibrio cholerae* vibriobactin synthetase. The N-terminal (red) and C-terminal (blue) subdomains are connected by a linker region (purple), forming a V-shaped canyon. The His-motif (black), containing the catalytic residue H126, marks the active site, which is located at the junction of these two subdomains. Adapted from (Hur et al. 2012).

1.3.4. The thioesterase (TE) domain

The thioesterase (TE) domain (~280 aa), typically located at the C-terminal end of the final NRPS termination module (Figure 1.2), catalyzes full-length peptide release rendering the NRPS machinery to be ready for the next synthesis cycle (Du and Lou 2010; Keating et al. 2001). The TE-mediated product liberation mainly consists of two step reactions (Figure 1.10). In the first step, the full-length assembled peptide chain is transferred from the terminal T domain to the active site of the TE domain by formation of an acyl-O-TE intermediate. Then, in the second step, the peptide chain undergoes either hydrolysis by an attack of an external nucleophile, typically water, to generate a linear peptide, or macrocyclization by an attack of a peptide-internal nucleophile, typically a hydroxyl or an amino group on the acyl-O-TE intermediate, to form a macrocyclic product (macrolactone or macrolactam) (Finking and Marahiel 2004). Beside the typical TE domain mediated peptide release routes, many other atypical release mechanisms, for example, reductase domain and C domain mediated release, also exist in the NRPS assembly lines. For more details see the following reviews (Du and Lou 2010; Keating et al. 2001).

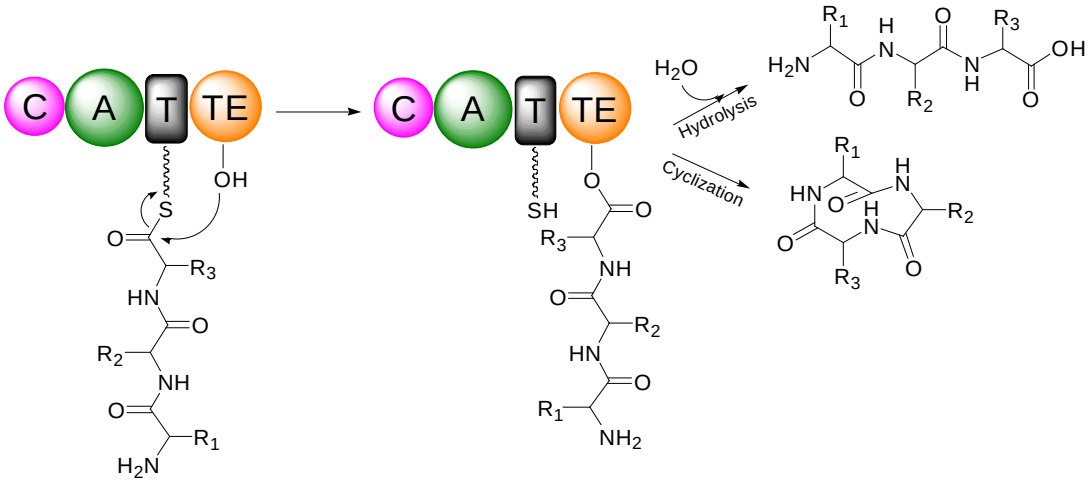

Figure 1.10 Peptide release (hydrolysis or cyclization) catalyzed by the NRPS TE domain.

Several crystal structures of dissected TE domains have been solved including SrfTE of surfactin synthetase from *Bacillus subtilis* JH642 (Bruner et al. 2002) and FenTE of fengycin synthetase from *Bacillus subtilis* F29-3 (Samel et al. 2006). Moreover, SrfTE was also co-crystallized with the terminal A, C and T domains in the last termination module from *Bacillus subtilis* ATCC 21332 (Tanovic et al. 2008). The structure data indicate that these TE domains are similar globular monomer proteins, belonging to the superfamily of α/β-hydrolases, such as lipases, esterases and proteases. They all have a conserved catalytic triad of Ser, His and Asp in the active site. Taken the excised SrfTE as an example (Figure 1.11), two independent monomers are observed in the SrfTE crystal structure (Bruner et al. 2002). The main difference between the two monomers is the so-called “lid” region, consisting primarily of three α-helices, which covers the active site catalytic triad (Ser80, His207 and Asp107). In the open (‘O’) monomer, the lid is folded back allowing substrate access to the active site, whereas in the closed (‘C’) monomer, the lid is closed, which may exclude water from the active site facilitating cyclization catalysis rather than the hydrolysis reaction.

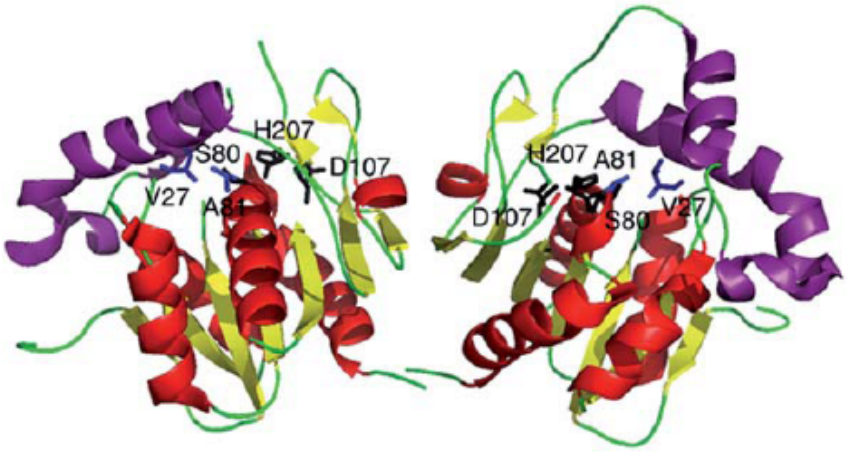

Figure 1.11 Crystal structure of the surfactin TE domain (SfrTE). The left monomer is in the closed ('C') conformation with the lid region (purple) covering the active site while the right monomer represents the open ('O') conformation with the lid folded back. Catalytic triad (Ser80, His207 and Asp107) is shown in black. Adapted from (Hur et al. 2012).

1.3.5. Creation of structural diversity of NRPs by tailoring enzymes

Although NRPSs themselves could harness more than 500 types of monomer substrates to make diverse structures of NRPs (2 to ~50 residues in length) (Caboche et al. 2010; Konz and Marahiel 1999), further modifications by tailoring enzymes heavily amplify the compound structures with numerous modified functional groups (Samel et al. 2008; Walsh 2004; Walsh et al. 2001). Overall, based on the modes of tailoring reactions, these tailoring enzymes can be grouped into two categories: some are integrated in the NRPS modules and modify the growing peptide chains *in cis* while they are still covalently tethered as peptidyl-S-T intermediates, such as epimerization (E) domains (L- to D-form amino acid) and *N*-methyltransferase (MT) domains, whereas others are distinct enzymes acting *in trans* to generate functional mature NRPs, for instance, glycosyltransferases, hydroxylases and halogenases. Normally, the genes encoding these distinct enzymes are also part of the whole NRPS gene cluster. Taken together, the various dedicated tailoring enzymes modify NRPs creating tremendously versatile and complex natural compounds. Examples of NRPs modified by tailoring enzymes can be seen in Figure 1.12.

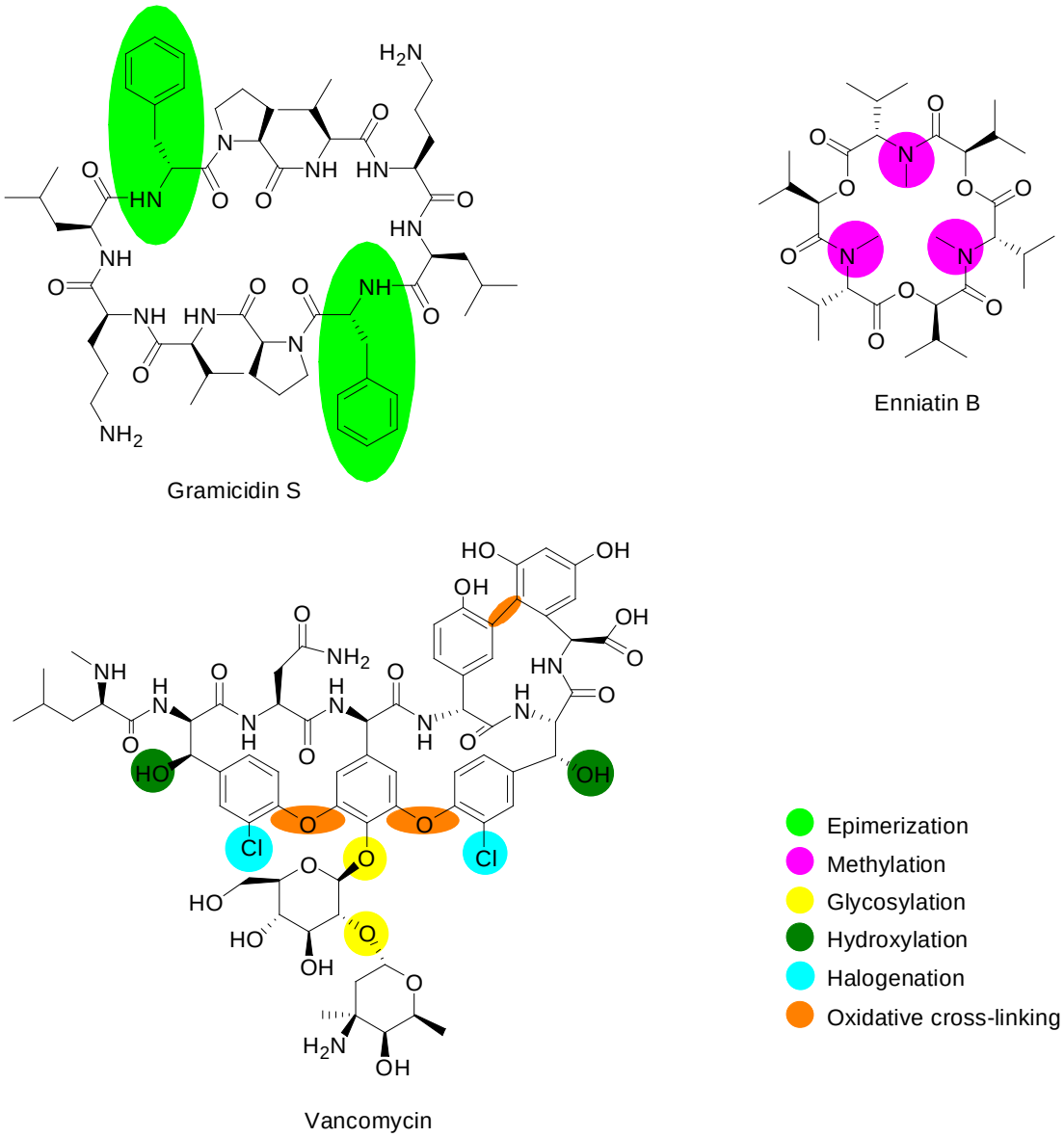

Figure 1.12 NRPs modified by tailoring enzymes. The modified sites are highlighted with different colors.

1.3.6. Regeneration of the functionality of NRPSs by a type II thioesterase

As mentioned in section 1.3.2, the nascent NRPS has to be posttranslationally modified by PPTase generating active holo-NRPS (Walsh et al. 1997). To afford the 4'-PP moiety, CoA serves as the donor substrate for PPTases to realize the apo- to holo-T conversion (Lambalot et al. 1996). However, the promiscuous PPTases use not only the presumed natural substrate CoA, but also various acyl-CoAs as 4'-PP donors, since a large fraction (~80 %) of CoAs appear acylated in bacterial cells (Quadri et al.

1998). Therefore, mispriming of T domains occurs frequently (Figure 1.3, step 1b), leading to inactive NRPS and blocking of the NRP assembly. In order to regenerate the misprimed NRPS, a discrete protein, called type II thioesterase (TEII), could serve as a repair enzyme to hydrolyze the misacylated thiol groups of 4'-PP cofactors of the T domains restoring active holo-NRPS (Schwarzer et al. 2002). Occasionally, incorrect amino acid monomers can also be activated by A domain and tethered to T domain (Keating et al. 2000b; Luo et al. 2001; Schwarzer et al. 2001). However, these non-cognate amino acids usually will not be accepted by the relevant C domains preventing peptide bond formation and peptide chain growing, thus, also blocking the NRPS machinery (Belshaw et al. 1999). In this case, TEII can remove the incorrect amino acids from T domains through hydrolysis and render the NRPSs active again (Yeh et al. 2004).

The NMR three-dimensional structure of the TEII of surfactin synthetase from *Bacillus subtilis* has been reported in a free form and in a complex form with a T domain (Koglin et al. 2008). SrfTEII exhibits the typical α/β-hydrolase fold with a central seven-stranded β-sheet surrounded by eight helices. Such structures give valuable insights into the working mechanism of TEII. SrfTEII exists in two distinct conformations, while only one form is used to interact with its native substrate -- the incorrect holo-T domain with short acyl groups attached to the 4'-PP thiol. In addition, the incorrectly loaded amino acids may be recognized and hydrolyzed by TEII through protein-protein interactions according to the increased half-life of these unprocessed aminoacyl-S-T intermediates (Yeh et al. 2004). Regeneration of the functionality of NRPSs by TEII is illustrated in Figure 1.13.

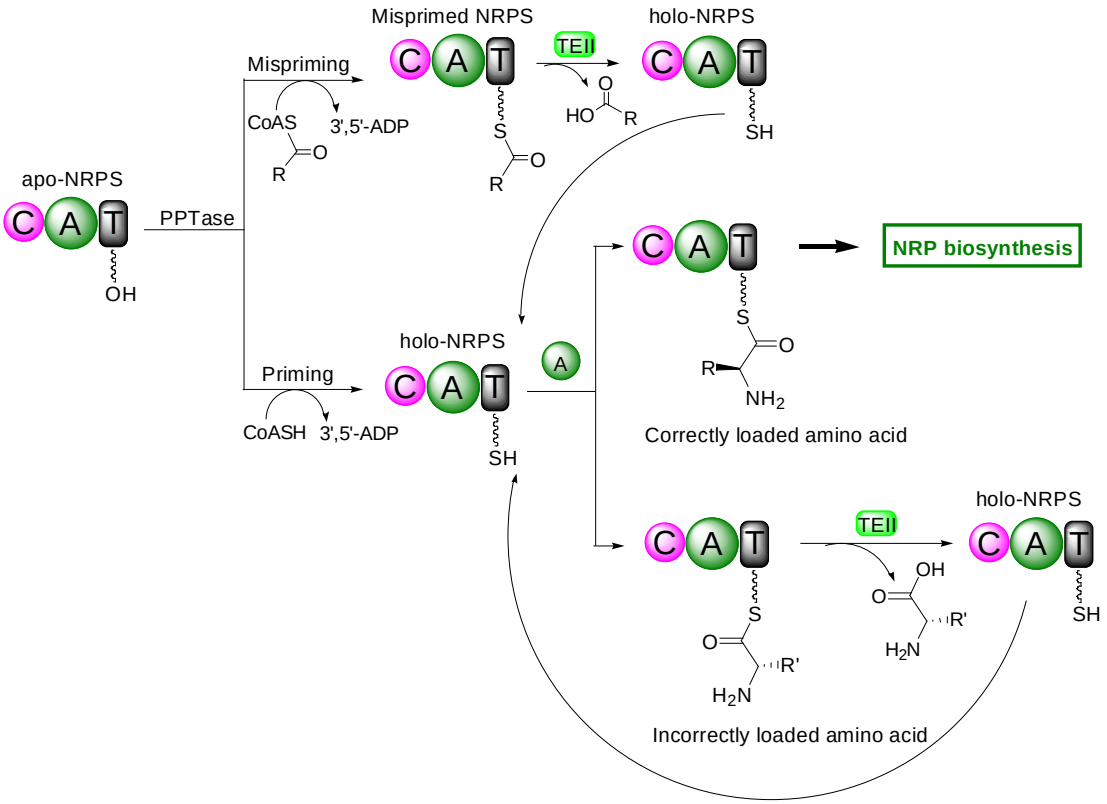

Figure 1.13 Regeneration of the functionality of NRPS catalyzed by TEII.

1.4. Valinomycin

1.4.1. Bioactivities of valinomycin

The isolation and characterization of valinomycin as an antibiotic compound from *Streptomyces fulvissimus* was first reported in 1955 (Brockmann and Schmidt-Kastner 1955). Brockmann et al. proposed the structure of valinomycin as cyclo-(D-α-hydroxyisovaleryl-D-valyl-L-lactyl-L-valyl)$_2$ (Brockmann and Geeren 1957). However, subsequent work indicated that the correct chemical structure of valinomycin was a cyclododecadepsipeptide consisting of a triple repeating unit of D-α-hydroxyisovaleryl-D-valyl-L-lactyl-L-valyl with a molecular weight of 1111.3 g mol^{-1} (Shemyakin et al. 1963a). The structural formula is shown in Figure 1.14A. This structure conformation forms a hydrophobic surface and a polar cavity in which K^+ can be coordinated with the six oxygen atoms of the interior ester carbonyls, forming the valinomycin-K^+ complex (Asher et al. 1974; Halsey et al. 2012). This allows the transportation of K^+ via the carrier through the bilayer membrane

destroying the normal K^+ gradient across the membrane, and therefore killing the cells (Altendorf et al. 1986; Andreoli et al. 1967; Junge and Schmid 1971; Moore and Pressman 1964). The cyclic 12-residue peptide confers valinomycin with significant bioactivities, since altering its structure by changing the ring size or amino acid residues would greatly reduce the capacity to form a stable valinomycin-K^+ complex and, accordingly, its antibiotic activity (Pressman 1965; Shemyakin et al. 1963b; Shemyakin et al. 1973). The working mechanism of valinomycin as a K^+-specific ionophore is illustrated in Figure 1.14B.

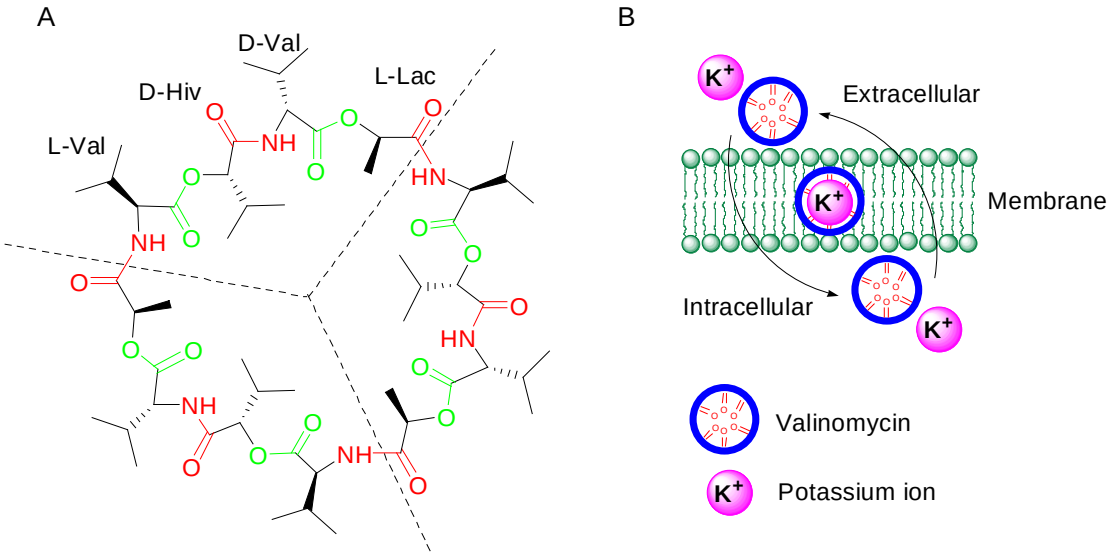

Figure 1.14 Chemical structure of valinomycin ($C_{54}H_{90}N_6O_{18}$) (A) and its potassium-specific ionophoric function (B). The structure (A) is composed via alternating peptide (in red) and ester linkages (in green).

Valinomycin possesses a broad spectrum of antimicrobial activities. A series of Gram-positive bacteria, e.g., *Staphylococcus aureus*, *Bacillus subtilis*, *Streptococcus pyogenes*, *Clostridium sporogenes*, *Listeria innocua*, *Enterococcus faecalis*, and *Micrococcus luteus*, and Gram-negative bacteria, e.g., *Escherichia coli*, *Enterobacter cloacae*, *Stenotrophomonas maltophilia*, and *Salmonella enterica*, have been tested (Pettit et al. 1999; Ryabova et al. 1975; Seshachalam et al. 1973; Tempelaars et al. 2011). These investigations indicated that all the tested Gram-positive bacteria show growth inhibition by valinomycin, albeit to different extents, whereas none of the tested Gram-negative bacteria were inhibited. The antimicrobial activity of

valinomycin is found to be related to the medium pH value and K^+ concentration depending on the type of bacteria (Ryabova et al. 1975; Seshachalam et al. 1973; Tempelaars et al. 2011). The lack of susceptibility of Gram-negative bacteria is attributed to their outer membrane of the cell wall which can prevent access of valinomycin to the inner membrane. Valinomycin also has potent antifungal activities to *Botrytis cinerea*, *Magnaporthe grisea*, *Candida albicans*, and *Aspergillus niger* (Ladeuze et al. 2011; Park et al. 2008; Pettit et al. 1999). In addition, valinomycin shows lethal properties on insects including the larvae of *Bombyx mori* (Angus 1968), *Musca domestica* (Pansa et al. 1973), and mosquito larvae (Heisey et al. 1988), and anti-parasitic activities against *Babesia gibsoni* (Yamasaki et al. 2009), *Leishmania major* and *Trypanosoma brucei* (Pimentel-Elardo et al. 2010). Furthermore, valinomycin shows antiviral activities. Addition of 10 µM valinomycin to infected Vero cells can significantly inhibit the replication of vesicular stomatitis virus (VSV) and higher concentrations of valinomycin can result in an even greater reduction in viral titer (Pettit et al. 1999). Valinomycin was also reported to be the most potent agent among more than 10,000 tested compounds against severe acute respiratory syndrome human coronavirus (SARS-CoV) in infected Vero E6 cells with an EC_{50} of 0.85 µM (Wu et al. 2004). In another antiviral study, from a 502 compounds library, valinomycin was found to be the most potent agent (IC_{50} = 24 nM) again inhibiting the replication of porcine reproductive and respiratory syndrome virus (PRRSV) in infected MARC-145 cells (Karuppannan et al. 2012).

Valinomycin also exhibits antitumor activities against several tumor cell lines (Daoud and Forde 1991; Daoud and Juliano 1986; Inai et al. 1997; Pettit et al. 1999; Ryoo et al. 2006; Smith and Blaylock 2007). Valinomycin exerts antitumor function mainly based on the induction of cell apoptosis through different mechanisms, such as depolarization of mitochondria and activation of caspase-3-like proteases against rat ascites hepatoma cells (AH-130) (Inai et al. 1997), down-regulation of the glucose-regulated protein (GRP) 78 against human colon carcinoma cells (HT-29) (Ryoo et al. 2006), and dissipation of mitochondrial membrane potential with enhanced

^{18}F-fluorodeoxyglucose (^{18}F-FDG) incorporation against breast tumor cells (MCF-7) (Smith and Blaylock 2007). Additionally, valinomycin can induce apoptosis of several other mammalian cells including murine thymocytes (Deckers et al. 1993), murine haematopoietic cells (Furlong et al. 1998), and Chinese hamster ovary (CHO) cells (Abdalah et al. 2006). However, the apoptotic capacity of valinomycin towards human natural killer (NK) cells makes it potentially toxic causing human immune suppression (Paananen et al. 2005; Paananen et al. 2000). Therefore, the toxicity of valinomycin limits its clinical use. However, interestingly, earlier studies indicated that the host toxicity of valinomycin can be considerably reduced and its antitumor efficacy can be maintained or even enhanced by incorporation of the drug into liposomes (Daoud and Juliano 1986). In addition, the low toxic liposomal valinomycin displayed synergistic cytotoxicity when used in combination with the anticancer agents doxorubicin (Daoud and Juliano 1989) and cisplatin (Daoud and Forde 1991). In order to develop valinomycin to be a potential clinical drug, more work still has to be done to reduce toxicity and enhance specific delivery using modern technologies.

1.4.2. Biosynthesis of valinomycin

Naturally, valinomycin is produced by several *Streptomyces* strains (Anke and Lipmann 1977; Brockmann and Schmidt-Kastner 1955; Heisey et al. 1988; MacDonald 1960; Park et al. 2008; Pettit et al. 1999; Pimentel-Elardo et al. 2010) with different yield levels (Table 1.3). Moreover, some *Bacillus* species were also found to produce valinomycin (Wulff et al. 2002).

Table 1.3 Production levels of valinomycin from eight *Streptomyces* strains. [a]

Strains	**Yield (mg L^{-1})**
Streptomyces tsusimaensis (ATCC 15141)	8.45
Streptomyces sp. PRL 1642 (ATCC 23836)	23.19
Streptomyces anulatus (Montana)	24.68
Streptomyces anulatus (Malaysia)	25.22
Streptomyces exfoliatus (Malaysia)	32.78
Streptomyces fulvissimus (DSM 40767)	4.25
Streptomyces griseus 1/k (DSM 41748)	10.19
Streptomyces griseus 10/ppi (DSM 41751)	22.08

[a] Table is adapted from (Matter et al. 2009).

After valinomycin was discovered in 1955, MacDonald first reported the studies of the biogenesis of valinomycin (MacDonald 1960). L-Valine-1-^{14}C rather than D-valine-1-^{14}C was found to be incorporated into the D-valyl, L-valyl, and D-α-hydroxyisovaleryl portions of valinomycin. However, no tested amino acids were incorporated into the L-lactyl portion. Later, MacDonald and Slater further reported that D-α-hydroxyisovaleric-1-^{14}C acid was incorporated largely into the corresponding portion of valinomycin (MacDonald and Slater 1968). They also discussed that free α-ketoisovaleric acid is not an obligatory precursor, however, may be converted to D-α-hydroxyisovaleric acid for the following incorporation. In order to further clarify the possible precursors of valinomycin, the responsible biosynthesizing enzyme was partially purified for synthesis *in vitro* (Anke and Lipmann 1977; Ristow et al. 1974). Ristow et al. (1974) found that the purified enzyme complex is capable of synthesizing the complete molecule of valinomycin from the precursors L-valine, and L-threonine or L-alanine which can be converted into lactic acid. By contrast, Anke et al. (1977) used lactic acid directly in their synthesis system instead of L-threonine or L-alanine and found that lactic acid can be easily incorporated into the L-lactyl moieties of valinomycin. However, both Ristow and Anke showed that pyruvate is not activated in the ATP-$^{32}PP_i$ exchange reaction using their own purified enzyme complex. While both of them proposed that the enzyme responsible for valinomycin biosynthesis is a nonribosomal peptide synthetase (Anke and Lipmann 1977; Ristow et al. 1974). The possible reason for the difference could be the isolated enzyme complex still contains some other relevant enzymes that can catalyze or convert the tested substrates into the possible precursors of valinomycin, but themselves are not the direct substrates (precursors) of valinomycin synthesizing enzyme.

In 1990, the genes from *Streptomyces levoris* A-9 involved in the biosynthesis of valinomycin were identified, however, the exact boundaries of all the necessary genes were not determined (Perkins et al. 1990). The complete gene cluster for valinomycin biosynthesis (*vlm*) from *Streptomyces tsusimaensis* ATCC 15141 was cloned, sequenced, and partially characterized by Cheng in 2006 (Cheng 2006). The

vlm gene cluster consists of two distinct biosynthetic genes, *vlm*1 and *vlm*2, together with five other ORFs. These two genes (*vlm1* and *vlm2*) encode two distinct NRPSs Vlm1 and Vlm2, which can be classified into the type B iterative NRPSs. Cheng (2006) proposed a 4-module model of valinomycin synthetase (VlmSyn) with 16 distinctive domains. Shortly after, the proposed model was rationally modified by a comparison study between two similar NRPSs valinomycin synthetase and cereulide synthetase (Magarvey et al. 2006). Two ketoreductase (KR) domains, which usually exist in another type of multimodular enzymes, polyketide synthases (PKSs) (Fischbach and Walsh 2006), were deduced to be integrated in the VlmSyn module 1 and module 3 being responsible for reduction of α-ketoisovalerate (Kiv) to D-α-hydroxyisovalerate (D-Hiv) and pyruvate to L-lactate, respectively. However, no further experiments were carried out to prove this deduction.

Recently, we confirmed the correctness of the proposed VlmSyn model (Jaitzig 2013). The VlmSyn, Vlm1 and Vlm2, was heterologously expressed in the host *Escherichia coli* in soluble form. The purified Vlm1 showed specificity to its two substrates Kiv (module 1) and L-Val (module 2), while Vlm2 exhibited specificity to pyruvate (module 3) and L-Val (module 4). Therefore, the direct precursors of valinomycin are concluded to be Kiv, pyruvate and L-Val. The proposed domain organization of VlmSyn and valinomycin biosynthesis are illustrated in Figure 1.15.

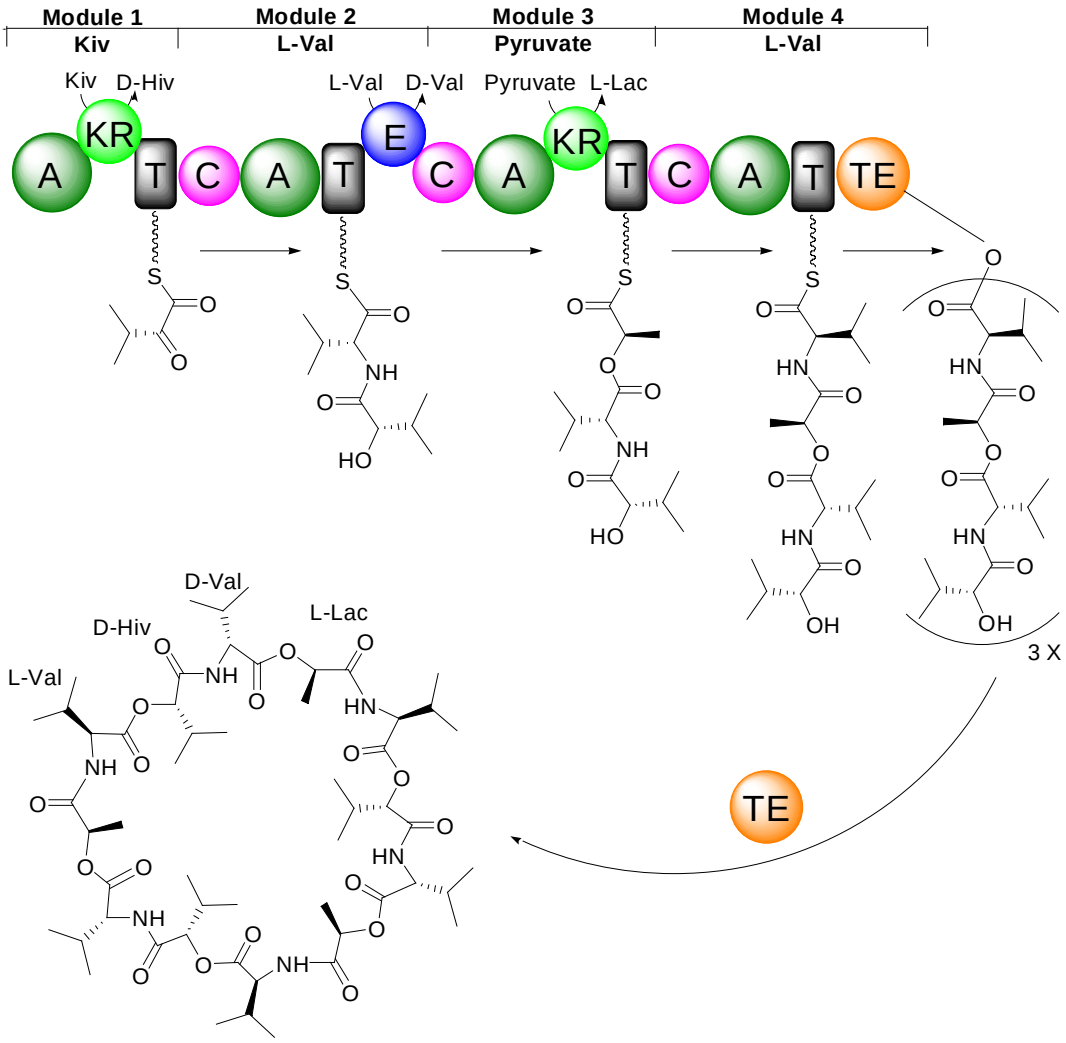

Figure 1.15 Proposed domain organization of VlmSyn and valinomycin biosynthesis. The ketoreductase (KR) domain in module 1 reduces Kiv to D-Hiv. Epimerization (E) domain in module 2 transfers L-Val to D-Val. The KR domain in module 3 reduces pyruvate to L-lac.

1.5. *E. coli*, a robust cell factory for heterologous production of NRPs, PKs and NRP/PK hybrids

Escherichia coli is a robust cell factory for heterologous production of numerous natural products originating from plants, fungi and bacteria (Zhang et al. 2011; Zhang et al. 2008a). *E. coli* is chosen as a surrogate host for the reconstitution, manipulation and optimization of natural product production due to its unquestioned advantages: (1) simple cultivation conditions and rapid growth rate; (2) knowledge of the entire genome and versatile genetic manipulation tools; (3) multiple expression strains and tolerance to foreign proteins; (4) well-understood metabolic pathways; and (5) easily scalable fermentation processes. However, *E. coli* as a host for recombinant

metabolite production also has its own disadvantages, for example, codon usage bias, incorrect folding of exogenous proteins, lack of posttranslational modification enzymes, and unavailability of necessary precursors. Nevertheless, *E. coli* has been successfully used to produce a number of natural products including NRPs, polyketides (PKs) and NRP/PK hybrids, which will be discussed in detail below.

Table 1.4 Examples of NRPs, PKs and NRP/PK hybrids heterologously produced in *E. coli*.

Compound	Titer (mg L^{-1})	Note	Reference
NRPs			
D-Phe-Pro-DKP	9	Shake-flask	(Gruenewald et al. 2004)
Echinomycin	0.3	3 L fed-batch bioreactor	(Watanabe et al. 2006)
Triostin A	13	Shake-flask	(Praseuth et al. 2008)
Ecolimycin C [a]	0.6	Shake-flask	(Watanabe et al. 2009a)
TANDEM [a]	0.2	4 L batch bioreactor	(Watanabe et al. 2009b)
Aureusimine A and B	6 and 14	96-well plate	(Wyatt and Magarvey 2013)
PKs			
6-dEB	20	Shake-flask	(Pfeifer et al. 2001)
6-dEB	1100	5 L fed-batch bioreactor	(Lau et al. 2004)
Erythromycin C and D	0.4 and 0.5	Shake-flask	(Peirú et al. 2005)
Erythromycin A	4	3 L batch bioreactor	(Zhang et al. 2012)
Anthraquinone	3	2 L fed-batch bioreactor	(Zhang et al. 2008b)
NRP/PK hybrids			
Epothilone C and D	<0.001 (both)	Shake-flask	(Mutka et al. 2006)
Yersiniabactin	67	3 L fed- batch bioreactor	(Pfeifer et al. 2003)

[a] Unnatural NRP.

As mentioned in section 1.3, NRPs are biosynthesized by the large multifunctional NRPSs. Similarly, PKs are also assembled via multimodular megaenzymes, called polyketide synthases (PKSs), and accordingly, NRP/PK hybrids are synthesized by mixed NRPS/PKSs consisting of NRPS modules as well as PKS modules (Fischbach and Walsh 2006). In order to realize heterologous production of NRPs, PKs and NRP/PK hybrids, the relevant biosynthetic enzymes have to be functionally expressed in *E. coli*. The prerequisite is posttranslational modification of the apo-T domains of NRPS

and apo-acyl carrier proteins (ACPs) of PKS by a PPTase (Lambalot et al. 1996). The enzyme Sfp, which is required for surfactin production in *Bacillus subtilis*, is found to be the most tolerant PPTase to a variety of substrates to date, and therefore widely coexpressed with NRPS and PKS genes to generate holo-enzymes (Quadri et al. 1998). Coexpression of Sfp can be achieved through either genomic integration (Pfeifer et al. 2001) or plasmid-borne means (Watanabe et al. 2006). Some examples of NRPs, PKs and NRP/PK hybrids produced in the heterologous host *E. coli* are shown in Table 1.4.

1.5.1. Production of NRPs

A few NRPs have been heterologously produced in *E. coli* either partially or completely (Gruenewald et al. 2004; Watanabe et al. 2006). As a model NRPS, the first two modules (TycA/TycB1) of the tyrocidine biosynthetic system from *Bacillus brevis* was actively expressed in *E. coli* giving rise to the expected final cyclic product D-Phe-Pro-diketopiperazine (D-Phe-Pro-DKP) (Gruenewald et al. 2004). To express TycA and TycB1, three strategies were carried out: a one-plasmid system (TycA and TycB1 were inserted into the expression plasmid as their natural locus), a two-plasmid system (TycA and TycB1 were inserted into two separate plasmids) and a fusion system (C terminus of TycA was directly joined to the N terminus of TycB1 and expressed in one plasmid). The results indicated that the two-plasmid system was the most productive one with the following order: two plasmid > one plasmid > fusion, under almost all the tested conditions. By using M9 medium supplemented with 0.1 % Casamino Acids in a batch fermentation, the final yield of D-Phe-Pro-DKP reached around 9 mg L^{-1}.

Watanabe et al. reported for the first time the total biosynthesis of the antitumor NRP echinomycin in *E. coli* (Watanabe et al. 2006). The genes for the two NRPSs Ecm6 and Ecm7, together with genes for 13 other tailoring enzymes and Sfp, were inserted into three separate plasmids, with each gene carrying its own T7 promoter, ribosome-binding site (RBS) and T7 terminator. Thereafter, *E. coli* cell harboring the three compatible plasmids was cultivated to produce echinomycin via 8 day

fed-batch fermentation in M9 minimal medium yielding 0.3 mg L^{-1} of final product. By removing the gene *ecm18* encoding Ecm 18 (an enzyme that is highly homologous to *S*-adenosyl-L-methionine dependent methyltransferases) from the plasmid, triostin A, the immature intermediate of echinomycin, can also be produced with a final yield of 0.6 mg L^{-1} using fed-batch fermentation. Subsequently, only 0.1 mg L^{-1} of triostin A was achieved when the production was performed in the shake flask. However, the titer of triostin A was markedly improved up to 13 mg L^{-1} through daily feeding of the precursor quinoxaline-2-carboxylic acid (QXC) into the shake flask culture for eight days (Praseuth et al. 2008). Based on the flexible and feasible *E. coli* platform, two echinomycin analogs were produced accordingly. One analog is ecolimycin C with a final titer of 0.6 mg L^{-1} after a 7-day-long shake-flask cultivation in M9 minimal medium (Watanabe et al. 2009a). While the other analog, des-*N*-tetramethyl triostin A called TANDEM, only reached 0.2 mg L^{-1} with fed-batch incubation in M9 minimal medium for 14 days (Watanabe et al. 2009b).

Very recently, a dimodular NRPS was also heterologously expressed in *E. coli* for the production of aureusimine (Wyatt and Magarvey 2013). By investigation of IPTG concentration, postinduction temperature and precursor supplementation, the final maximum titers of aureusimine A and B reached 6.16 mg L^{-1} and 14.34 mg L^{-1}, respectively. Interestingly, using this dimodular NRPS system, three new pyrazine products were also produced, which are either not produced or are undetectable in the native organism suggesting the potential utility of heterologously expressed NRPSs to generate novel products.

1.5.2. Production of PKs

6-Deoxyerythronolide B (6-dEB, precursor of the antibiotic erythromycin), is the most successful case by using *E. coli* as a heterologous host for polyketide production (Pfeifer et al. 2001). The three deoxyerythronolide B synthase (DEBS) genes were transferred from the soil-dwelling bacterium *Saccharopolyspora erythraea* into the expression plasmids (pBP130 and pBP144) for expression of the large enzymes DEBS1

(370 kDa), DEBS2 (380 kDa) and DEBS3 (332 kDa). By transformation of the two expression vectors into an engineered *E. coli* strain BAP1 with the genomically integrated *sfp* gene, 6-dEB was successfully produced with a final titer of 20 mg L^{-1}. After that, intensive investigations were carried out to improve the yield of 6-dEB through metabolic and bioprocess engineering (Lau et al. 2004; Murli et al. 2003; Pfeifer et al. 2002; Pistorino and Pfeifer 2009; Wang et al. 2007). 6-dEB reached 100 mg L^{-1} via a high cell density fed-batch fermentation process. Coexpression of TEII, a repairing enzyme from *S. erythraea*, further increased the final yield of 6-dEB to 180 mg L^{-1} under the same fed-batch cultivation mode (Pfeifer et al. 2002). Murli et al. created a new production strain *E. coli* K207-3 through chromosomal integration of the propionyl-CoA carboxylase (PCC) genes *accA1* and *pccB* into the strain BAP1. Besides, a new plasmid pKOS207-129, which is compatible with pBP130/DEBS2+DEBS3, was constructed to express DEBS1 (Murli et al. 2003). Thereafter, based on the stable system *E. coli* K207-3/pKOS207-129+pBP130, a high cell density fed-batch bioprocess was developed to produce 6-dEB with a maximum titer of 1.1 g L^{-1} on day 12 (Lau et al. 2004). Coexpression of an *S*-adenosylmethionine synthetase gene (*metK*) in BAP1/pBP130+pBP144 notably increased the specific yield of 6-dEB from 10.86 to 20.08 mg L^{-1} OD_{600}^{-1}, which is attributed by the authors to the involvement of the native AI-2 signaling molecule pathway (Wang et al. 2007). Further metabolic engineering results indicated that deletion of *ygfH* gene, encoding the propionyl-CoA : succinate CoA transferase, led to a 2-fold increase (from 65 to 129 mg L^{-1}) of 6-dEB titer in shake flask production. Similarly, in the batch bioreactor cultures, the titers were improved from 206 to 527 mg L^{-1} indicating a 2.5-fold increase (Zhang et al. 2010a). If *ygfH* gene deletion is combined with the overexpression of the *atoC* gene, encoding an transcriptional activator of *E. coli* short-chain fatty acid metabolism, the 6-dEB titer will be further improved to over 130 mg L^{-1} in a shake flask scale cultivation (Boghigian et al. 2011). Media optimization through experimental design in micro-scale cultures generated over 160 mg L^{-1} 6-dEB and it was found that tryptone significantly impacted on 6-dEB production as well as improved the expression levels of DEBS proteins (Pistorino and

Pfeifer 2009). In addition to the plasmid-based production platform mentioned above, the three DEBS genes (~30 kb in length) and PCC genes (*accA1* and *pccB*) were also introduced into the BAP1 chromosome creating a plasmid-free strain YW9 which could produce 6-dEB as well (Wang and Pfeifer 2008). The product yields for YW9 were 0.47 (22 °C), 0.52 (30 °C), and 0.11 (37 °C) mg L^{-1}, which were much lower than the plasmid-based production system since plasmid-borne gene expression could produce more enzyme capable of synthesizing 6-dEB.

Having realized 6-dEB production, further efforts were aimed at the heterologous biosynthesis of complete erythromycin in *E. coli*. Peirú et al. reported total production of erythromycin C (an intermediate of erythromycin A) using the 6-dEB producer strain *E. coli* K207-3/pKOS207-129+pBP130 through coexpression of sixteen genes from the megalomicin gene cluster that encode tailoring enzymes necessary to convert 6-dEB to erythromycin C and one host self-resistance gene *ermE* which encodes a rRNA methyltransferase (Peirú et al. 2005). The resulting strain finally produced two erythromycin analogs erythromycin C at a titer of 0.4 mg L^{-1} and erythromycin D at that of 0.5 mg L^{-1}. Full biosynthesis of the final form of erythromycin, erythromycin A, in *E. coli* was accomplished in 2010 (Zhang et al. 2010b). The whole gene cluster (55 kb) from the native producer *S. erythraea* containing three large genes *DEBS1/2/3* (each ~10 kb) and 17 additional genes responsible for tailoring and resistance were heterologously expressed in BAP1 yielding erythromycin A at 0.6 mg L^{-1}. Subsequently, this amount was increased up to 4 mg L^{-1} through a batch bioreactor cultivation using a strain named TB3, which is a derivative of BAP1 with *ygfH* deletion (Zhang et al. 2012).

Some other polyketide biosynthetic pathways were also reconstituted in the host *E. coli* for heterologous production of the target compounds. For example, the fungal polyketide 6-methylsalicylic acid was produced with a yield of 75 mg L^{-1} after 24 h incubation (Kealey et al. 1998). In addition, the bacterial aromatic polyketide anthraquinone was produced in *E. coli* as well, giving rise to a final titer of 3 mg L^{-1}

via a bioreactor fed-batch fermentation (Zhang et al. 2008b).

1.5.3. Production of NRP/PK hybrids

Since multimodular NRPS and PKS have similar working mechanisms, hybridization of them naturally occurs forming mixed NRPS/PKS assembly lines that can biosynthesize NRP/PK hybrids (Fischbach and Walsh 2006). One example is the anticancer agent epothilone. Epothilones are produced by the myxobacterium *Sorangium cellulosum* via a hybrid NRPS/PKS pathway, which consists of one NRPS module and nine PKS modules (Julien et al. 2000). The first attempt to produce epothilone in *E. coli* was reported by Boddy et al. based on a precursor-directed method (Boddy et al. 2004). Instead of reconstitution of the entire epothilone biosynthetic pathway in *E. coli*, the authors cloned partial genes, *epoD-M6* (module 6), *epoE* (modules 7 and 8) and *epoF* (module 9), into three expression plasmids. Production of epothilone C was achieved by exogenous feeding of a chemically synthetic substrate *N*-acetylcysteamine (SNAC) thioester, which can be recognized and accepted by module 6. The final yield of epothilone C was quantified to be 0.7 mg L^{-1}, which is comparable to the yield of the native producer.

Subsequently, the full-length (~55 kb) epothilone gene cluster was introduced into *E. coli* allowing protein expression and products formation (Mutka et al. 2006). To overcome low expression levels and limited solubility of all the proteins, several strategies were employed including low-temperature expression, codon optimization, promoter engineering, and chaperone coexpression. Especially, to express the largest protein EpoD (765 KDa) in an active soluble form, the *epoD* gene was divided into two fragments allowing expression of two smaller polypeptides EpoD34 (modules 3 and 4) and EpoD56 (modules 5 and 6). While compatible linker pairs *stiB* and *stiC* were added to the C terminus of EpoD34 and N terminus of EpoD56, respectively, to facilitate the functional interaction between EpoD modules 4 and 5. Finally, complete biosynthesis of epothilones C and D was accomplished in *E. coli*, however, with a very low yield of less than 1 μg L^{-1}.

The NRP/PK hybrid yersiniabactin, a siderophore naturally produced by *Yersinia pestis*, is another example that was heterologously produced in *E. coli* (Pfeifer et al. 2003). Yersiniabactin synthetase consists of three NRPS modules and one PKS module that are organized in two parts, HMWP1 (350 kDa) and HMWP2 (230 kDa). These two large proteins were functionally coexpressed in *E. coli* cells generating the product yersiniabactin. The final titer reached 67 mg L^{-1} through high cell density fed-batch fermentation in a bioreactor.

1.6. Research motivation and objectives

NRPs, a large group of microbial secondary metabolites, are mainly produced by soil-dwelling or marine microorganisms. They have a wide spectrum of important pharmacological activities making them valuable for the treatment of human diseases. However, these native producers normally have limited productivity in the laboratory, which hampers clinical trials and commercial use. In addition, chemical synthesis of such complex NRPs is infeasible due to drawbacks, such as expensive cost, harmful by-products and environmental pollution. In recent years, heterologous host systems have been used as an effective alternative to produce natural products including NRPs, PKs and NRP/PK hybrids. In this process, the full biosynthetic pathway for the production of a target compound is first identified and isolated from the native producer, and then reconstituted in a well-characterized and easily culturable heterologous producer such as *E. coli*. Although the gene clusters of NRPSs have been increasingly sequenced and identified, they were mainly expressed and dedicated to investigate enzyme mechanisms. Only a few of them were expressed heterologously in *E. coli* for the total biosynthesis of relevant NRP molecules. In addition, there is still a lack of information concerning bioprocess optimization for NRPs production.

Recently, we used the NRPS valinomycin synthetase as a model system and have successfully reconstituted the NRPS genes from *Streptomyces tsusimaensis* in an engineered *E. coli* host for valinomycin production (Jaitzig 2013). In order to improve

the valinomycin yield in *E. coli* and offer a reasonable route for other NRPs production, we attempted to enhance valinomycin production through multiple approaches including strain improvement and bioprocess optimization. Therefore, the principal objectives of this project were:

1) Construction of various compatible expression vectors for coexpression of valinomycin synthetase, Vlm1 and Vlm2.
2) Screening for the optimal vector combination for valinomycin production.
3) Batch and fed-batch cultivations for valinomycin production.
4) Design of experiments (DoE) based optimization of valinomycin production in milliliter scale.
5) High cell density fed-batch production of valinomycin in shake flasks.
6) Bioreactor fed-batch fermentations for valinomycin production.
7) Coexpression of type II thioesterase (TEII) for improvement of valinomycin production.

2. Experimental

2.1. Materials

2.1.1. Chemical materials

Unless otherwise mentioned, all the major chemicals and reagents were purchased from Sigma-Aldrich (St. Louis, USA) or Carl Roth (Karlsruhe, Germany).

2.1.2. Biological materials

Enzymes and markers	Source
Benzonase	Merck, Darmstadt, Germany
DreamTaq Green DNA Polymerase	Thermo Scientific, Waltham, USA
FastDigest Restriction Enzymes	Thermo Scientific, Waltham, USA
FastAP Thermosensitive Alkaline Phosphatase	Thermo Scientific, Waltham, USA
Gateway LR Clonase II Mix	Invitrogen, Karlsruhe, Germany
GeneRuler 100 bp Plus DNA Ladder	Thermo Scientific, Waltham, USA
GeneRuler 1 kb Plus DNA Ladder	Thermo Scientific, Waltham, USA
Lambda Mix Marker, 19	Thermo Scientific, Waltham, USA
Lysozyme	Sigma-Aldrich, St. Louis, USA
Phusion DNA Polymerase	Thermo Scientific, Waltham, USA
ProSieve QuadColor Protein Marker	Lonza, Basel, Switzerland
Spectra Multicolor Broad Range Protein Ladder	Thermo Scientific, Waltham, USA
T4 DNA Ligase	Roche, Mannheim, Germany

Nucleic acid stains	Source
GelRed Nucleic Acid Gel Stain	Biotium, Hayward, USA
SYBR Safe DNA Gel Stain	Invitrogen, Darmstadt, Germany

Kits	Source
HiYield PCR Clean-up/Gel Extraction Kit	Süd-Laborbedarf, Gauting, Germany
innuPREP Bacteria DNA kit	Analytikjena, Jena, Germany
Invisorb Spin Plasmid Mini Two Kit	Stratec, Berlin, Germany

2.2. Bacterial strains and cultivation media

2.2.1. Bacterial strains

Strains used in this study are listed in Table 2.1. *E. coli* strains were used to clone genes, maintain plasmids, express proteins and produce valinomycin according to different purposes. *Streptomyces tsusimaensis* provided the genome for amplifying type II thioesterase (TEII) gene fragment. For storage of *E. coli* strains, they were cultivated overnight at 30 °C on an LB agar plate supplemented with the appropriate antibiotics. Then the colonies were washed off with fresh LB medium and stored in ready-to-use Roti-Store cryo vials (Carl Roth GmbH, Germany) at -80 °C.

Table 2.1 Overview of used bacterial strains.

Strain	Genotype	Origin
E. coli BJJ01	F$^-$ *omp*T *hsd*S(r_B^- m_B^-) *dcm*$^+$ (Tet^R) *gal end*A Hte *Δxyl*A*::sfp*$_{wt}$	(Jaitzig 2013)
E. coli BL21Gold	F$^-$ *omp*T *hsd*S(r_B^- m_B^-) *dcm*$^+$ (Tet^R) *gal end*A Hte	Agilent Technologies
E. coli BL21 (DE3)pLysS	F$^-$ *omp*T *hsd*S$_B$(r_B^- m_B^-) *gal dcm* (DE3) pLysS (Cam^R)	Novagen
*E. coli ccd*B$^+$	F$^-$*mcr*A Δ(*mrr-hsd*RMS-*mcr*BC) *φ*80*lac*ZΔM15 Δ*lac*X74 *rec*A1 *ara*Δ139 Δ(*ara-leu*)7697 *gal*U *gal*K *rps*L(Str^R) *end*A1 *nup*G *fhu*A::*IS2*	Invitrogen
E. coli TOP10	F$^-$*mcr*A Δ(*mrr-hsd*RMS-*mcr*BC) *φ*80*lac*ZΔM15 Δ*lac*X74 *rec*A1 *ara*D139 Δ*(ara-leu)*7697 *gal*U *gal*K *rps*L(Str^R) *end*A1 *nup*G λ$^-$	Invitrogen
S. tsusimaensis ATCC 15141	wild-type	Keller group, TU Berlin

2.2.2. Cultivation media

Laboratory made media were prepared according the following recipes, followed by a 121 °C sterilization for 20 min. The enzyme-based glucose delivery EnBase medium was obtained from Biosilta (Oulu, Finland). Two different types were used, the liquid-based EnBase Flo and the tablet-based EnBase EnPresso. EnBase medium was used for fed-batch cultivation as described in previous reports (Krause et al. 2010;

Ukkonen et al. 2011). If necessary, appropriate antibiotics were added to the medium for strain cultivation.

Luria-Bertani (LB) medium	
Tryptone	10 g L^{-1}
Yeast extract	5 g L^{-1}
NaCl	10 g L^{-1}
pH	7.0

For agar plates add 20 g agar per 1 L medium.

Terrific Broth (TB) medium	
Tryptone	12 g L^{-1}
Yeast extract	24 g L^{-1}
Glycerol	0.4 %
KH_2PO_4	2.31 g L^{-1}
K_2HPO_4	12.54 g L^{-1}

SOC medium	
Tryptone	2 % (w/v)
Yeast extract	0.5 % (w/v)
NaCl	10 mM
KCl	2.5 mM
$MgCl_2$	10 mM
$MgSO_4$	10 mM
Glucose	20 mM
pH	7.0

GYM medium	
Glucose	4 g L^{-1}
Yeast extract	4 g L^{-1}
Malt extract	10 g L^{-1}
pH	7.2

2.3. Molecular cloning techniques

2.3.1. Genomic DNA isolation of *S. tsusimaensis*

S. tsusimaensis ATCC 15141 was grown at 30 °C and 250 rpm for 24 h in GYM medium supplemented with 0.5 % (w/v) glycine. Cell pellets were harvested by centrifugation (12,000 g, 4 °C, 5 min) from a 3 mL culture. The genomic DNA was isolated using the innuPREP Bacteria DNA kit (Analytikjena) according to the manufacturer's manual.

2.3.2. Plasmid DNA preparation

E. coli harboring plasmid was grown overnight at 30 °C in LB medium. Cell pellets were harvested by centrifugation (12,000 g, 4 °C, 5 min) from a 3 mL overnight culture. The plasmid DNA was extracted using the Invisorb Spin Plasmid Mini Two Kit (Stratec) according to the manufacturer's protocol. Isolated plasmid concentrations were quantified using the Nanodrop ND-1000 spectrophotometer at 260 nm (PeQlab, Erlangen, Germany). The plasmid was stored at 4 °C until further use.

2.3.3. Oligonucleotide primer design

Oligonucleotide primers for PCR amplification or plasmid DNA sequencing were designed with the help of the software Vector NTI Advance 11.0 (Invitrogen). All the primers were chemically synthesized and obtained from TIB Molbiol GmbH (Berlin, Germany). Details of the primers used in this work are listed in Table 2.2.

Table 2.2 Primers used in this study.

Fragment	Primer [a] (5' → 3')	Restriction enzyme
p15A	F: TG**CCTGAGG**GCTCTAGCGGAGTGTATACTG	*Bsu*36I
	R: C**ACTAGT**ACAACTTATATCGTATGGGGCTG	*Spe*I
λ t0 terminator [b]	F: GGT**AAGCTT**TGGACTCCTGTTGATAGATCC	*Hind*III
	R: CC**CACTACGTG**TCTAGCTTGGATTCTCACC	*Dra*III
λ t0 terminator [c]	F: GGT**AAGCTT**TGGACTCCTGTTGATAGATCC	*Hind*III
	R: CCTTTCTCCTTGCTGATGTTGTCTAGCTTGGATTCTCACC	
*par*B+ampicillin	F: GGTGAGAATCCAAGCTAGACAACATCAGCAAGGAGAAAGG	
	R: CGGAGACGGTCACAGCTTGTTTGCCCATGGCAATCTAAAG	
rop	F: CTTTAGATTGCCATGGGCAAACAAGCTGTGACCGTCTCCG	
	R: GG**CCTCAGG**CCTCACAACGTTCCAGTAACC	*Bsu*36I
pCU	F: GTG**TCCGGGA**CAATTAATGCATGTTAGCTCACTC	*Pfo*I
	R: AC**GGATCC**GCTTCCGCCACCGCCGTG	*Bam*HI
TEII	F: GC**GGATCC**GTGAAACTTCTCTGCTTGCC	*Bam*HI
	R: GA**CTCGAG**TTATCATCCTTGGAAGGAGAC	*Xho*I

[a] Restriction enzyme sites are indicated by bold letters in the primers. Two underlined primers with solid lines are complementary. Two underlined primers with dashed lines are complementary. F= forward, R= reverse.

[b] This PCR amplified λ t0 terminator was directly inserted into pJL02 generating pJL03.

[c] This PCR amplified λ t0 terminator was firstly ligated to the fragments of *par*B+ampicillin and *rop* by overlap extension PCR, and then the combined fragment 5' *Hind*III-λ t0 terminator_parB+ampicillin_ ROP-*Bsu36*I 3' was introduced into pJL01 yielding pJL07 (see section 2.3.7).

2.3.4. Polymerase chain reaction (PCR)

PCR is a rapid process to exponentially amplify a specific DNA sequence, generating billions of copies of the target DNA fragment in a couple of hours. This powerful technique mainly contains three steps: denaturation of the double-stranded DNA template by raising the temperature to 94-98 °C, annealing of the oligonucleotide primers to the single-stranded DNA template by lowering the temperature to 50-65 °C, and extension of the annealed primers by a thermostable DNA polymerase (e.g., *Taq* polymerase) with a commonly used temperature of 72 °C (Sambrook and Russell 2001).

a) PCR amplification of genes of interest for cloning

To amplify a gene of interest, either isolated genomic DNA or plasmid DNA was used as a template for the PCR reactions. The high fidelity Phusion DNA Polymerase with a 3´ to 5´ proofreading function (Thermo Scientific) was employed to elongate the new DNA strand complementary to the template. In a 50 µL PCR reaction mixture, 5 ng of template DNA, 200 µM of dNTP mix, 0.3 µM of each primer, and 1 U of Phusion DNA Polymerase were contained. PCR thermal cycles were executed mainly based on the following program: 1 cycle of 98 °C for 30 s, followed by 30 cycles of 98 °C for 10 s, 60 °C for 30 s, and 72 °C for 1 min. The amplification was finalized at 72 °C for 10 min allowing completed extension of new DNA fragments. The temperature of the annealing step can be different according to the T_m of the used primers.

The accuracy and quality of the resulting PCR products were analyzed by the agarose gel electrophoresis (see section 2.3.5). If the target gene was successfully amplified, the DNA fragment was purified, either directly from the PCR reaction mixture, or by further gel purification using the HiYield PCR Clean-up/Gel Extraction Kit (Süd-Laborbedarf) according to the manufacturer´s instructions.

b) Colony PCR for screening of positive transformants

After overnight cultivation of the transformed cells on agar plates, 25 single colonies were randomly picked to prepare an index plate (see section 2.3.10). Thereafter, these colonies were screened via colony PCR for the positive transformation of the plasmids inserted with the target gene sequence. DreamTaq DNA Polymerase (Thermo Scientific) was used for colony PCR screenings according to the manufacturer's protocol. Each colony PCR reaction was performed in a 25 µL mixture containing 200 µM of dNTP mix, 0.2 µM of each primer, and 2.5 U of DreamTaq DNA Polymerase. Before the reaction start, a single colony was picked up with a plastic tip from the index plate and added to the PCR reaction mixture. PCR thermal cycles were performed based on the following program: 1 cycle of 95 °C for 5 min, followed by 25 cycles of 95 °C for 30 s, 55 °C for 30 s, and 72 °C for 1 min. The final extension

step ended with 72 °C for 10 min. The temperature of the annealing step varied according to the T_m of the used primers. The target fragment was analyzed by agarose gel electrophoresis (see section 2.3.5).

2.3.5. Agarose gel electrophoresis

Agarose gel electrophoresis was performed to analyze DNA fragments according to standard protocol (Sambrook and Russell 2001). For an analytic gel, GelRed Stain (Biotium) was added to the agarose gel (1 %) for the visualization of DNA segment bands. If the gel was used to purify DNA fragments, SYBR Safe Stain was added to the gel instead of GelRed. DNA samples were mixed with 6x DNA loading buffer (Thermo Scientific) and separated together with an appropriate DNA ladder on the gel in TAE running buffer (40 mM Tris, 20 mM acetic acid, 1 mM EDTA, pH 8.4) at 100 V for 30 min. DNA bands were visualized by UV light excitation and documented using the GenoPlex Gel Documentation and Analysis System (VRW).

2.3.6. Cloning via restriction enzyme digestion and ligation

The target PCR-amplified DNA fragments (3 µg) and vector backbones (3 µg) were digested separately with the same FastDigest Restriction Enzymes (Thermo Scientific) at 37 °C for 2 h. To prevent recircularization, 1 U of FastAP Thermosensitive Alkaline Phosphatase (Thermo Scientific) was added to the vector backbones mixture after 1.5 h digestion to dephosphorylate the terminal 5´-phosphates, followed by another 30 min incubation. Then, the digested fragments and dephosphorylated vector backbones were purified using the HiYield PCR Clean-up/Gel Extraction Kit (Süd-Laborbedarf) according to the manufacturer´s manual.

DNA ligation was performed in a 10 µL mixture containing 1 U T4 DNA ligase (Roche), 20 ng digested vector backbones and DNA inserts with a molar ratio of 1 : x (vector : insert). The amount of insert in relation to vector backbone with x-fold molar excess was calculated according to the following equation:

$$m_{insert}\ [ng] = x \cdot \frac{length_{insert}\ [bp]}{length_{vector}\ [bp]} \cdot m_{vector}\ [ng]$$

The ligation was incubated overnight at 16 °C and stopped by heat inactivation at 65 °C for 20 min. The resulting ligated products were transformed into competent *E. coli* cells (see section 2.3.10).

2.3.7. Construction of destination vectors

In order to construct expression vectors via Gateway cloning (see section 2.3.8), destination vectors have to be created in advance. The destination vector pCTUT7 was used as a parental vector, which possessed a pBR322 origin of replication (*ori*) and a mutated *lac* promoter (Kraft et al. 2007). An overview of the destination vectors is shown in Table 2.3. Vector maps of the destination vectors can be found in Appendix 6.1.

pJL01

To insert a single restriction site *Spe*I between pBR322 *ori* and *lac*I, pCTUT7 was digested with *Ear*I and the linear vector was ligated with an artificial linker which was formed by two complementary oligonucleotides F_ 5'-CCCG**ACTAGT**G-3' and R_5'-GG GC**ACTAGT**C-3' (bold sequences refer to the *Spe*I site). The resulting vector was named pJL01.

pJL02

The p15A *ori* was PCR amplified from the plasmid pLysS (Novagen) flanked by two restriction sites *Bsu*36I and *Spe*I. The PCR product was digested by *Bsu*36I and *Spe*I and inserted into pJL01 replacing pBR322 to give pJL02.

pJL03

To introduce a 3' mRNA transcription terminator into pJL02, the λ t0 terminator gene fragment was amplified from the template plasmid pTNA_mod (Jaitzig 2013). The restriction sites *Hind*III and *Dra*III flanking λ t0 terminator were digested and the product was ligated into pJL02 to yield pJL03.

pJL04

The N-terminal 6xHis tag was removed from pJL03 generating pJL04. pJL03 was digested with *Nde*I and *Nhe*I and the linear vector was ligated by an artificial linker which was formed by two complementary oligonucleotides F_5'-**TA**TCAACGACTG-3' (bold letters refer to *Nde*I sticky end) and R_5'-**CTAG**CAGTCGTTGA-3' (bold letters refer to *Nhe*I sticky end), yielding the destination vector pJL04.

pJL05

To replace the N-terminal 6xHis tag with an N-terminal Strep tag (8 amino acids: Trp-Ser-His-Pro-Gln-Phe-Glu-Lys), pJL03 was digested with *Nde*I and *Nhe*I, followed by ligation with the Strep tag which was formed by two complementary oligonucleotides F_5'-**TA**TGGCGTGGAGCCACCCGCAGTTCGAAAAATCTCTGGGTGGCCATG-3' (bold letters refer to *Nde*I sticky end) and R_5'-**CTAG**CATGGCCACCCAGAGATTTTTCGAACTGCGGGTGGCTCCACGCCA-3' (bold letters refer to *Nhe*I sticky end). The resulting ligated vector was pJL05.

pJL06

To introduce C-terminal Strep tag, pJL04 was digested with a single restriction enzyme, *Hind*III. The C-Strep tag insert was formed by two complementary oligonucleotides F_5'-**AGCT**TGCATGGCGGTCTGTCTTGGAGCCACCCGCAGTTCGAAAAATGATA-3' and R_5'-**AGCT**TATCATTTTTCGAACTGCGGGTGGCTCCAAGACAGACCGCCATGCA-3' (bold letters refer to *Hind*III sticky end). Insertion of C-Strep tag into pJL04 generated pJL06.

pJL07

pJL07 was derived from pJL01 by inserting the *rop* gene (Cesareni et al. 1982), replacing the chloramphenicol resistance marker with an ampicillin resistance marker, and introducing the plasmid stabilizing *par*B locus (Gerdes 1988). In addition, the 3' mRNA transcription λ t0 terminator was also incorporated into pJL07. The *rop* gene was amplified from a plasmid pET15b/Sfp (Jaitzig 2013). The ampicillin resistance marker and *par*B were amplified together from the plasmid pKS01 (Jaitzig 2013).

pTNA_mod was used as a template to amplify the λ t0 terminator fragment (Jaitzig 2013). Afterwards, the three DNA fragments were spliced together through overlap extension PCR (Horton et al. 1989), yielding a combined fragment 5' *Hind*III-λ t0 terminator_*par*B+ampicillin_ROP-*Bsu*36I 3'. pJL01 was digested with *Hind*III and *Bsu*36I and ligated by the combined fragment giving rise to pJL07.

pJL08

To remove the N-terminal 6xHis tag, pJL07 was digested with *Nde*I and *Nhe*I, followed by ligation of an artificial linker that was formed by two complementary oligonucleotides F_5'-**TA**TCAACGACTG-3' (bold letters refer to *Nde*I sticky end) and R_5'-**CTAG**CAGTCG TTGA-3' (bold letters refer to *Nhe*I sticky end). The resulting linked vector was pJL08.

pJL09

To introduce a C-terminal 6xHis tag, pJL08 was digested with a single restriction enzyme, *Hind*III. The C-6xHis tag, formed by two complementary oligonucleotides F_5'-**AGCT**TGAGCGGAGGCGGTGGCCACCATCACCATCACCATTGATA-3' and R_5'-**AGCT**T ATCAATGGTGATGGTGATGGTGGCCACCGCCTCCGCTCA-3' (bold letters refer to *Hind*III sticky end), was inserted into pJL08 to yield pJL09.

To screen and confirm accuracy of the constructed vector, either restriction enzyme digestion (see section 2.3.6) or colony PCR (see section 2.3.4) was performed initially. If the result of restriction digestion or colony PCR was positive with the expected size of DNA bands, the vector was sent for sequencing to verify that the target fragment was correct (LGC Genomics, Berlin, Germany).

Table 2.3 Overview of destination vectors.

Vector	*Ori*	Tag	Resistance	Reference
pCTUT7	pBR322-ROP [a]	N-His	cm	(Kraft et al. 2007)
pJL01	pBR322-ROP	N-His	cm	This work
pJL02	p15A	N-His	cm	This work
pJL03	p15A	N-His	cm	This work
pJL04	p15A	-	cm	This work
pJL05	p15A	N-Strep	cm	This work
pJL06	p15A	C-Strep	cm	This work
pJL07	pBR322+ROP [b]	N-His	amp (+parB) [c]	This work
pJL08	pBR322+ROP	-	amp (+parB)	This work
pJL09	pBR322+ROP	C-His	amp (+parB)	This work

[a] pBR322 *ori* without *rop* gene.

[b] pBR322 *ori* with *rop* gene.

[c] parB: plasmid stabilizing locus.

2.3.8. Construction of VlmSyn expression vectors

In order to construct various VlmSyn expression vectors, the Gateway Recombinational Cloning technology was carried out following the manufacturer´s manual. This technology allows transferring the gene of interest from an entry clone to numerous destination vectors without using restriction enzymes and ligase (Hartley et al. 2000; Walhout et al. 2000). Two entry clones pENTR-Vlm1 and pENTR-Vlm2 had been created in our previous work (Jaitzig 2013). In this study, pENTR-Vlm1 and pENTR-Vlm2 were modified by removing stop codons from the C-terminus of the genes *vlm*1 and *vlm*2 if a C-terminal 6xHis or Strep tag was to be linked to the proteins Vlm1 and Vlm2. All the destination vectors constructed can be found in section 2.3.7. With the help of the LR recombination reaction (LR Clonase II enzyme mix, Invitrogen), various Vlm1 and Vlm2 expression vectors were created (for details see Table 3.1). The resulting expression vectors have been transformed into competent *E. coli* cells (see section 2.3.10).

2.3.9. Construction of type II thioesterase (TEII) expression vector

A discrete TEII protein serves as a repair enzyme to regenerate misprimed thiolation domains of NRPSs for intermediate peptidyl transfer (Schwarzer et al. 2002). In order to coexpress TEII and VlmSyn, a compatible vector pJL10 was constructed by

modification of pRSF-1b (Novagen) which carries a RSF *ori* and a kanamycin antibiotic resistance marker. The strong T7 promoter in pRSF-1b was replaced by a lower strength pCU promoter which is mutated from the wild type *lac* promoter (Kraft et al. 2007). Genomic DNA from *S. tsusimaensis* ATCC 15141 was used as a template for PCR amplification of the TEII gene fragment. After digestion with *Bam*HI and *Xho*I, the PCR product was inserted into pJL10 generating the expression vector pJL10-TEII (see the vector map in Appendix 6.1).

2.3.10. Electrotransformation of competent *E. coli* cells

Electrocompetent *E. coli* cells were prepared and stored at -80 °C according to a standard protocol (Sambrook and Russell 2001). For the electrotransformation, a 50 µL aliquot of frozen cells was thawed on ice, followed by gently mixing with 1 µL of plasmid (~100 ng), ligation product, or LR reaction product. After incubation on ice for 1 min, the mixture was transferred into a pre-cooled 1 mm electroporation cuvette (VWR). Then, the electrotransformation was executed with a pulsed voltage value of 1800 V in the electroporator 2510 (Eppendorf). The transformed cells were immediately washed out with 450 µL pre-heated SOC medium (37 °C), followed by 1 h shaking incubation at 37 °C. Thereafter, the cells were spread on LB agar plates containing appropriate antibiotics. After overnight incubation at 30 °C, single colonies were randomly picked to prepare an index plate for the following screening for positives through colony PCR (see section 2.3.4) or restriction digestion (see section 2.3.6).

2.4. Protein expression and analysis

2.4.1. Protein expression in TB medium

E. coli BJJ01 harboring different expression vectors was precultured on LB agar plates containing appropriate antibiotics at 30 °C overnight. Cultivation was performed in a 125 mL baffled Ultra Yield Flask (Thomson Instrument Company, USA) containing 25 mL TB medium, which was sealed by an air-permeable membrane, AirOtop Enhanced Seals (Thomson Instrument Company, USA). After inoculation with an

initial OD_{600} of 0.1, the culture was incubated on an orbital shaker (Infors HT, Switzerland) with a speed of 200 rpm at 30 °C. When the OD_{600} reached 0.6-0.8, protein expression was induced with 20 µM IPTG followed by further 5 h cultivation. In the end, the final OD_{600} was measured and cells were harvested by centrifugation (12,000 g, 4 °C, 5 min). Supernatant was discarded and the pellets were stored at -20 °C for the following SDS-PAGE analysis (see section 2.4.4).

2.4.2. Protein expression in EnBase medium

EnBase medium (BioSilta), containing liquid-based Flo and tablet-based EnPresso, was used for VlmSyn expression according to the previous reports with slight modifications (Krause et al. 2010; Ukkonen et al. 2011).

For Flo medium, cells were cultivated in 50 mL Flo in a 250 mL Ultra Yield Flask covered by the AirOtop Enhanced Seals. To initiate the cultivation, the medium was inoculated with a starting OD_{600} of 0.1 and 0.6 U L^{-1} enzyme, 0.1 mL thiamine and 0.1 mL magnesium were added. In addition, 5 µL antifoam 204 was added to the culture to prevent foam formation. After overnight cultivation at 30 °C and 200 rpm, the culture was boosted with 5 mL complex additives solution as well as additional 1.5 U L^{-1} enzyme was added. At the point of boosting, either 20 µM IPTG or no IPTG was added into the culture to induce protein expression. Then, the cultivation was continued for 24 h at 30 °C and 200 rpm. At the end, the final OD_{600} was measured and cells were harvested by centrifugation (12,000 g, 4 °C, 5 min). Supernatant was discarded and the pellets were stored at -20 °C for the following SDS-PAGE analysis (see section 2.4.4).

For EnPresso medium, two tablets were dissolved in 50 mL of sterile water in a 250 mL Ultra Yield Flask supplemented with 5 µL antifoam 204. Then, the enzyme was added to a concentration of 0.3 U L^{-1} shortly before inoculation with an OD_{600} of 0.1. Afterwards, the flask was sealed by the AirOtop Seals and the cultivation was initiated in a shaker at 200 rpm and 30 °C. After overnight cultivation, one EnPresso

nutrients boosting tablet and another dose of the enzyme (0.6 U L^{-1}) were added to the culture for further 24 h cultivation. At the boosting point, either 20 µM IPTG or no IPTG was added into the culture to induce protein expression. At the end, the final OD_{600} was measured and cells were harvested by centrifugation (12,000 g, 4 °C, 5 min). Supernatant was discarded and the pellets were stored at -20 °C for the following SDS-PAGE analysis (see section 2.4.4).

2.4.3. Cell disruption

Frozen cell pellets were directly resuspended in BugBuster Protein Extraction reagent (Merck) by gently pipetting up and down. For 1 mL of BugBuster reagent, 1 µL Benzonase nuclease (25 U) and 1 µL lysozyme (50 mg mL^{-1}) were added. The cell suspension was incubated on a shaking platform with a slow setting for 15 min at room temperature. Then, the lysates were kept on ice before SDS-PAGE analysis. The amount of Bugbuster added per pellet was calculated according to the following equation:

$$\text{Amount Bugbuster [µL]} = 67 \cdot \frac{OD_{600}}{2} \cdot \frac{\text{culture volume [µL]}}{1000}$$

where OD_{600} is the final cell density of the culture; culture volume is the amount of culture used for cell pellets collection; 67 is the calculation factor; 2 is the sample dilution factor due to addition of 2x SDS loading buffer; and 1000 is the order of magnitude between milliliter and microliter.

2.4.4. SDS-PAGE analysis

Sodium dodecyl sulfate polyacrylamide gel electrophoresis (SDS-PAGE) was used for analysis of soluble and insoluble proteins. 5 % or 10 % separating Tris-glycine SDS-polyacrylamide gels with 4 % stacking gels were prepared following a standard protocol (Sambrook and Russell 2001) with additional 0.5 M urea. For sample preparation, 50 µL of cell lysate were mixed with 25 µL Solution A (1.5 M NaCl, 60 mM EDTA, 6 % Triton X-100, pH 7.0) followed by centrifugation (16,000 g, 30 min,

4 °C). The supernatant was transferred into a fresh 1.5 mL tube (soluble protein fraction). The insoluble protein fraction and cell debris were resuspended in 75 µL Solution B (0.1 M Tris-HCl pH 8.0, 8 M urea, 100 mM DTT, 1 mM EDTA). Afterwards, both soluble and insoluble fractions were mixed 1:1 with 2x SDS loading buffer (100 mM Tris-HCl pH 6.8, 200 mM DTT, 4 % SDS, 0.2 % bromophenol blue, 20 % glycerol). The samples were incubated at 95 °C for 7 min and cooled to room temperature. 15 µL of each sample were applied for SDS-PAGE analysis. A protein molecular weight marker was also loaded onto the gel for reference. Gels were run in SDS running buffer (25 mM Tris-HCl pH 8.3, 192 mM glycine, 500 mM urea, 0.1 % SDS, 1 mM EDTA) at 64 V for ~20 min until samples line had passed the boundary of stacking gel, followed by 90 min running at 120 V. Then, on a shaking platform, gels were washed thrice for 5 min in water and stained for 1 h in Coomassie staining solution (80 mg L^{-1} Brilliant Blue G-250, 35 mM HCl). Finally, the gels were destained in water until the color background was reduced sufficiently.

2.5. *E. coli* BJJ01 resistance to valinomycin

2.5.1. Effect of external valinomycin on cell growth

E. coli BJJ01 (for details see Table 2.1) with chromosomally integrated *sfp* gene from *Bacillus subtilis* for posttranslational phosphopantetheinylation was used to produce the antibiotic valinomycin (Jaitzig 2013). Therefore, it is essential to test the inhibiting effect of valinomycin on BJJ01 growth. EnBase Flo medium was used in this experiment. 50 mL of Flo medium in a 250 mL Ultra Yield Flask were inoculated with an initial OD_{600} of 0.1, followed by cultivation at 30 °C and 250 rpm for 2 h. Then, 5 mL boosting solution were added to the culture. Afterwards, 2.7 mL of the culture were distributed into each well of a 24-deep well plate (Ritter, Schwabmünchen, Germany) and commercial valinomycin standard was added to the culture at final concentrations of 10, 30, 50 and 100 mg L^{-1}. Since the commercial ready-to-use valinomycin (1 mg mL^{-1} solution) was stored in DMSO, if 100 mg L^{-1} of valinomycin were added, the final concentration of DMSO in the culture would be 10 % (v/v).

Therefore, for the cultures supplemented with less valinomycin, additional pure DMSO was added to get the concentration of 10 % (v/v). For cell growth comparison, two negative controls supplemented with ddH_2O (10 %, v/v) and DMSO (10 %, v/v) were cultivated in parallel. The final culture volume per well was 3 mL and the 24-deep well plate was covered by Breathable Film (Starlab, Hamburg, Germany) during the cultivation. OD_{600} values were measured at the time points of 2, 4, 8, 12, 24, 32 and 48 h.

2.5.2. Effect of internal valinomycin on cell growth

In order to evaluate an inhibiting effect of internal valinomycin on cell growth, three strains were grown in EnBase EnPresso medium. BJJ01 was cultivated as a negative control. The second control was BL21Gold/pCTUT7-Vlm1+pKS01-Vlm2 which only expresses inactive apo-VlmSyn but does not produce valinomycin. BJJ01/pCTUT7-Vlm1+pKS01-Vlm2 could produce active holo-VlmSyn as well as the antibiotic valinomycin. Each strain was cultivated in 50 mL medium in a 250 mL Ultra Yield Flask at 30 °C and 200 rpm. After boosting, cultivations were continued for 48 h allowing valinomycin formation in the cells. OD_{600} values were measured after 6, 12, 24, 36 and 48 h. At the end, valinomycin was extracted from the culture for quantification (see section 2.7).

2.6. Multiple strategies for valinomycin production

2.6.1. Inoculum preparation

The frozen cells of *E. coli* BJJ01/pCTUT7-Vlm1+pKS01-Vlm2 were precultured on LB agar plate supplemented with 34 mg L^{-1} chloramphenicol and 100 mg L^{-1} ampicillin. The plate was incubated overnight at 30 °C. Before inoculation, the cells were washed from the agar plate with fresh cultivation medium. For each cultivation the culture was inoculated with an initial OD_{600} of 0.1.

2.6.2. Cell growth determination

To monitor cell growth in shake flasks or bioreactors, OD_{600} values were measured with a 1 cm path length cuvette at different time points during the cultivation using a UV/Visible spectrophotometer (Ultrospec 3300, Amersham Biosciences, Germany). For 24-well plate samples, an automatic measurement of OD_{600} was performed using a robotic platform (Hamilton Robotics, Switzerland). 5 µL culture of each well were mixed with 145 µL of 0.9 % NaCl resulting in a 30-fold dilution in a new flat bottom 96-microwell plate (Corning Incorporated, USA). Then the values were measured by the Synergy Mx microplate reader (BioTek Instruments, USA) at 600 nm. Finally, these plate reading values ($OD_{600\text{-microplate reader}}$) were calculated to OD_{600} with a 1 cm path length cuvette using the equation below, which is obtained from a calibration curve:

$$OD_{600} = (OD_{600\text{-microplate reader}} - 0.037) \times 30 \times 3.003$$

where 0.037 is the 0.9 % NaCl blank value; 30 is the dilution factor; and 3.003 is the calibration factor. All measurements were determined in triplicate.

2.6.3. TB batch cultivation

Valinomycin production through batch cultivation mode was performed in a 500 mL Ultra Yield Flask containing 100 mL TB medium. After inoculation, the culture was incubated on an orbital shaker (Infors HT, Switzerland) with a speed of 200 rpm at 30 °C. When the OD_{600} reached 0.6-0.8, VlmSyn expression was induced by addition of 20 µM IPTG followed by 36 h cultivation for valinomycin production. Samples were taken out for valinomycin quantification at different time intervals during the cultivation (see section 2.7).

2.6.4. EnBase fed-batch cultivation

Valinomycin production through fed-batch mode was carried out using the enzyme-based glucose delivery EnBase cultivation system. Cultivation procedures with Flo or EnPresso were similar to the VlmSyn expression experiments as described in section 2.4.2, however, without IPTG induction. After boosting, the cultivation was continued

for additional 96 h for valinomycin production. Samples were taken out for valinomycin quantification at different time intervals during the cultivation (see section 2.7).

2.6.5. Optimization for valinomycin production by DoE*

The design of experiments (DoE) guided optimization was conducted in parallel 24-well plates (total volume per well: 3.3 mL, PreSens-Precision Sensing GmbH, Germany) using EnBase EnPresso fed-batch medium. The PreSens 24-well plate system allows non-invasive online measurement of oxygen (OxoDish OD24) and pH (HydroDish HD24) during the cultivation process. Three key parameters, nutrients boosting (Yes/No), enzyme concentration relating to glucose releasing rate (0-6 U L^{-1}) and culture volume correlating to oxygen transfer rate (0.5-1.5 mL), were investigated and optimized in relation to the product titer based on the DoE D-Optimal design created with the software MODDE 8.0.2 (Umetrics) (for details see Table 3.2 in section 3.5).

These DoE generated 20 experimental runs were carried out as follows. Overnight cultivation procedures were the same as described above in section 2.4.2. The overnight culture was divided into two portions (50 mL of each). One of them was boosted by one EnPresso nutrients tablet. The other 50 mL culture were not boosted. Then two groups of the culture were distributed into the 24-well plates. For each well, the second enzyme dose and culture volume were executed according to Table 3.2 (see section 3.5). Afterwards, the 24-well plate was covered by a so-called "System Duetz" sandwich cover and fixed on the clamp systems (Enzyscreen, Netherlands). The following cultivation lasted for 48 h at 250 rpm under 30 °C and, meanwhile, online oxygen and pH values were acquired accordingly with the SensorDish Reader system (PreSens). OD_{600} was measured using a 96-microwell plate as described in section 2.6.2. At the end, valinomycin was extracted from each well for the following determination (see section 2.7).

* The optimization for valinomycin production by design of experiments (DoE) was performed in cooperation with Jennifer Jaitzig (PhD student, Neubauer group, TU Berlin).

2.6.6. Effect of enzyme concentration on valinomycin production

In the enzyme-based glucose delivery EnBase cultivation system, glucose feeding rate is mediated by the applied enzyme concentration in the medium. In order to obtain the optimal enzyme dosage, a high throughput screening was conducted in the PseSens 24-well plate with EnBase Flo medium. Overnight cultivation in a shake flask was performed as described above in section 2.4.2. After nutrients boosting, the culture was distributed into the 24-well plates with 1 mL per well. Then, different amounts of enzyme were added per well with 1.5, 3, 9, 15, 20, 25, 30, 35, 40, 50, 70, or 90 U L^{-1}. The cultivations without nutrients boosting were also tested with the same amounts of enzyme concentrations. The subsequent cultivation was continued for 48 h at 30 °C and 250 rpm. Simultaneously, online oxygen and pH values were recorded by the SensorDish Reader system (PreSens). OD_{600} values were measured using a 96-microwell plate as described in section 2.6.2. At the end, valinomycin was extracted from each well for the following determination (see section 2.7).

2.6.7. Glucose polymer feeding for valinomycin production

In the EnBase medium, glucose is released from a certain amount of a soluble glucose polymer. If the polymer is depleted and glucose is not available, the cells will starve and stop to grow. However, if additional polymer is added to the medium, glucose will be offered again for cells growth. In this polymer feeding experiment, EnBase Flo was used as an initial growth medium and overnight pre-cultivation was performed as mentioned in section 2.4.2. At the boosting point, additional enzyme (9 U L^{-1}) was added to the culture. Then, 12.5 mL culture were transferred into a 125 mL baffled shake flask (PreSens), which allows online non-invasive measurement of DO and pH. One flask worked as a control without glucose polymer feeding. The second flask was fed with 30 g L^{-1} polymer after 12 h. The third flask was fed twice with 30 g L^{-1} polymer after 12 h and 24 h, respectively. OD_{600} values were measured as described in section 2.6.2. At the end of the cultivation, valinomycin was extracted from each culture for subsequent quantification (see section 2.7).

2.6.8. Bioreactor fed-batch fermentation*

A high cell density fed-batch bioprocess for valinomycin production was performed in a 3.7 L bench-top bioreactor (KLF2000, Bioengineering, Switzerland). The cultivation comprised two phases: i) an EnBase Flo cultivation and ii) a fed-batch cultivation with external glucose feeding. 2 L Flo medium were prepared without complex additives and autoclaved in the bioreactor at 121 °C for 20 min. 3 U L^{-1} enzyme were added to the medium shortly before inoculation with an initial OD_{600} of 0.1. Cells were grown at 30 °C and the pH was maintained at 7.0 with 25 % NH_4OH and 10 % H_3PO_4. The level of DO was maintained above 20 % (air saturation) through adjustment of the stirrer rate and air flow rate during the fermentation. Foaming was controlled by adding 2 mL antifoam (PPG2000) per time manually.

When the polymer releasing glucose in the Flo medium was depleted 16-18 h after inoculation (as indicated by continuous increase of oxygen content), glucose feeding was initiated at a rate of 0.07 mL min^{-1}, which is calculated according to the following equation:

$$F_0 = \frac{\mu \; X_0 \, V_0}{S_f \, Y_{X/S}}$$

where X_0 and V_0 are the cell dry weight (g L^{-1}) and culture volume (L) at the time of feeding start, μ is the specific growth rate – 0.2 h^{-1}, S_f is the glucose concentration in the feeding solution – 400 g L^{-1}, and $Y_{X/S}$ is the yield coefficient – 0.4 g g^{-1} (biomass produced per glucose for *E. coli*).

The subsequent exponential feeding process was continued for 12 h with a specific growth rate (μ) of ~0.2 h^{-1} and the feeding profile was calculated according to the following equation:

$$\mathrm{F}(t) = F_0 \cdot e^{\mu \cdot t}$$

* The bioreactor fed-batch fermentation was performed in cooperation with Jennifer Jaitzig (PhD student, Neubauer group, TU Berlin).

where F_0 is the initial feeding rate (L h^{-1}), μ is the specific growth rate (h^{-1}) to be maintained, and *t* is the time (h) after feeding start.

Afterwards, glucose feeding rate was gradually decreased from 0.85 to 0.45 mL min^{-1} in 6 h, followed by constant feeding at 0.45 mL min^{-1} until the end of the fermentation. During the whole fed-batch phase, when OD_{600} increased by ~20, a mixture of 2 mL $MgSO_4$ (1.5 M), 2 mL trace elements (per L: 0.5 g $CaCl_2 \cdot 2H_2O$, 0.18 g $ZnSO_4 \cdot 7H_2O$, 0.10 g $MnSO_4 \cdot H_2O$, 20.1 g Na_2-EDTA, 16.70 g $FeCl_3 \cdot 6H_2O$, 0.16 g $CuSO_4 \cdot 5H_2O$ and 0.18 g $CoCl_2 \cdot 6H_2O$, 0.132 g $Na_2SeO_3 \cdot 5H_2O$, 0.12 g $Na_2MoO_4 \cdot 2H_2O$, and 0.725 g $Ni(NO_3)_2 \cdot 6H_2O$), and 2 mL thiamine (50 g L^{-1}) was added aseptically to the bioreactor containing 2 L culture. Samples were drawn from the bioreactor for OD_{600} measurement (see section 2.6.2) and valinomycin quantification (see section 2.7).

2.6.9. Coexpression of VlmSyn and TEII for valinomycin production

E. coli BJJ01 harboring pJL03-Vlm1, pJL07-Vlm2 and pJL10-TEII was used to coexpress VlmSyn and TEII as well for valinomycin production. Cultivations were carried out in EnBase media Flo and EnPresso without IPTG induction (see section 2.4.2). After nutrient boosting, the cultures were incubated for further 48 h for valinomycin formation. For comparison, *E. coli* BJJ01/pJL03-Vlm1+pJL07-Vlm2 was cultivated in parallel. OD_{600} values were measured as described in section 2.6.2. At the end of the cultivation, valinomycin was extracted from each culture for quantification (see section 2.7).

2.6.10. Two-compartment bioreactor fermentation

To investigate valinomycin production under oscillating conditions, a scale-down two-compartment reactor (TCR) system, which consists of a 15 L standard stirred tank reactor (STR) (B. Braun+Diessel Biotech GmbH, Germany) and a 1.2 L plug flow reactor (PFR) equipped with static mixers, was used for the fermentation (see Appendix 6.4). The strain *E. coli* BJJ01/pJL03-Vlm1+pJL07-Vlm2+pJL10-TEII was used

in this experiment. One reference fermentation was performed in the STR without PFR. In the STR fed-batch fermentation, 10 L EnBase Flo were used for the initial cultivation followed by a glucose fed-batch cultivation. The exponential feeding was continued for 8 h with a specific growth rate (μ) of 0.2 h^{-1}. In the TCR (STR+PFR) fed-batch fermentation, glucose was fed at the inlet of the PFR with the μ of 0.22 h^{-1} for 8 h. The culture was circulated between the STR and the PFR by a pump with a residence time of 1 min in the PFR. The inoculation, cultivation temperature, DO, pH and other additives were kept the same as described in section 2.6.8. All the samples were drawn from the STR for OD_{600} measurement (see section 2.6.2) and valinomycin quantification (see section 2.7).

2.7. Valinomycin extraction and quantification

2.7.1. Valinomycin extraction

One milliliter of the culture was centrifuged at 16,000 g and 4 °C for 5 min. The medium supernatant was transferred into a 15 mL tube and extracted with 2 mL ethyl acetate. 2 mL methanol were added to the pellets, followed by sonication for 3 min (30 s on/off). After centrifugation (16,000 g, 15 min), the organic fractions from the medium and pellet extractions were combined and dried by vacuum rotary evaporation. The residue was resuspended in 1 mL of methanol for the following valinomycin determination.

2.7.2. Valinomycin quantification

One microliter of each sample was injected into the Agilent 6460 Triple Quadrupole LC/MS System equipped with an Eclipse Plus C18 column (RRHD 1.8 µm, 2.1 × 50 mm) for valinomycin detection. The buffers A (H_2O + 0.1 % formic acid) and B (acetonitrile + 0.1 % formic acid) were used to elute analytes with a flow rate of 0.3 mL min^{-1} through a linear gradient elution from 5 to 100 % B over 2.5 min, followed by a 100 % B wash for 7.5 min and finishing with a linear gradient back to 5 % B over 2 min. Mass spectra collected in the Multiple Reaction Monitoring (MRM) mode were obtained by monitoring three characteristic mass transitions of the parent ion $[M+NH_4]^+$ (m/z

1128.6): m/z 1128.6 → 343.3, m/z 1128.6 → 713.4, and m/z 1128.6 → 1083.6. The product ion m/z 1083.6 served as quantifier, while the product ions m/z 713.4 and m/z 343.3 served as qualifiers for identification. Before every experimental analysis, a calibration curve was generated from a series of valinomycin standards with concentrations of 10, 100, 1000, 2000, and 4000 µg L^{-1}. All measurements were determined at least in duplicate. Data analysis was conducted using the Agilent MassHunter Workstation Software for Qualitative Analysis (version B.04.00).

3. Results

3.1. Construction of expression vectors and VlmSyn expression

3.1.1. Features of original VlmSyn expression vectors

The large NRPS VlmSyn is composed of the two proteins Vlm1 (370 kDa) and Vlm2 (284 kDa). In order to actively express VlmSyn in *E. coli*, we had previously constructed two expression vectors pCTUT7-Vlm1 and pKS01-Vlm2 to express Vlm1 and Vlm2, respectively (Jaitzig 2013). The main features of the two vectors can be seen in Figure 3.1. Both vectors have the same origin of replication (*ori*) pBR322 and the same promoter pCTU which is mutated from the native *lac* promoter (Kraft et al. 2007). To keep the two plasmids stable in the cell, the chloramphenicol (cmR) and ampicillin (ampR) resistance cassettes are inserted into pCTUT7-Vlm1 and pKS01-Vlm2, respectively. In addition, the stability of pKS01-Vlm2 is further strengthened through the incorporation of the plasmid stabilizing *parB* locus (Gerdes 1988).

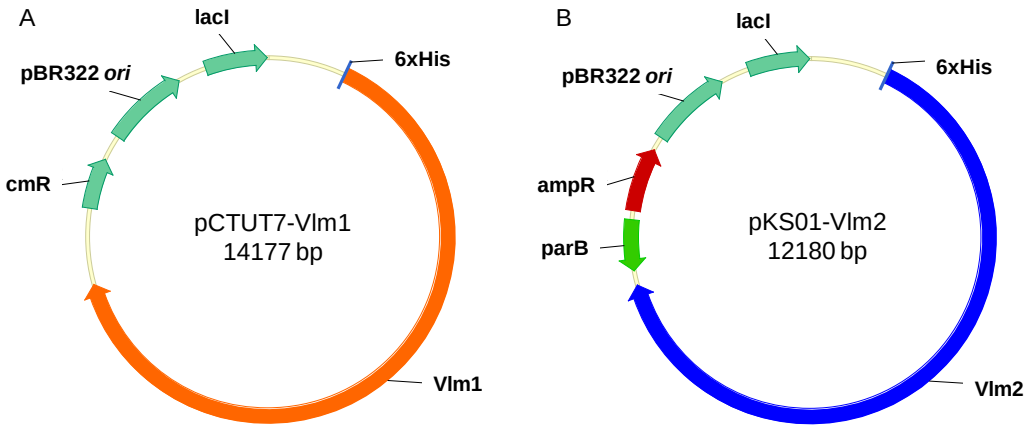

Figure 3.1 Vector maps of the VlmSyn expression vectors pCTUT7-Vlm1 (A) and pKS01-Vlm2 (B).

3.1.2. Construction of new VlmSyn expression vectors

To realize heterologous production of valinomycin, the two proteins Vlm1 and Vlm2 have to be coexpressed in *E. coli*. When coexpressing multiple proteins in one cell, it is common to use several plasmids that possess compatible *ori*s and different antibiotic resistance genes for maintenance (Tolia and Joshua-Tor 2006). However, our original dual expression vectors have the same pBR322 *ori* (Figure 3.1), which may inhibit the replication of each plasmid and cause plasmid segregation or loss within different generations. We therefore attempted to create new compatible plasmids for Vlm1 and Vlm2 coexpression, even though our initial incompatible plasmids pCTUT7-Vlm1 and pKS01-Vlm2 show a reasonable VlmSyn expression level. Like this, we were able to screen for the best plasmid combination based on the VlmSyn expression as well as valinomycin productivity.

The VlmSyn expression vectors were created with the Gateway Cloning technology through the LR recombination reaction between an Entry Clone carrying the gene of interest (*vlm1* or *vlm2*) and a Destination Vector offering essential plasmid components (Hartley et al. 2000; Walhout et al. 2000). The destination vector pCTUT7 was used as a parent to generate nine new vectors (Figure 3.2). Two compatible *ori*s pBR322 and p15A were put into the parallel vectors for stable coexpression. In order to replace pBR322 by p15A, a single restriction site *Spe*I was inserted between pBR322 *ori* and *lac*I in pCTUT7 generating pJL01. All the plasmid maps are displayed in Appendix 6.1.

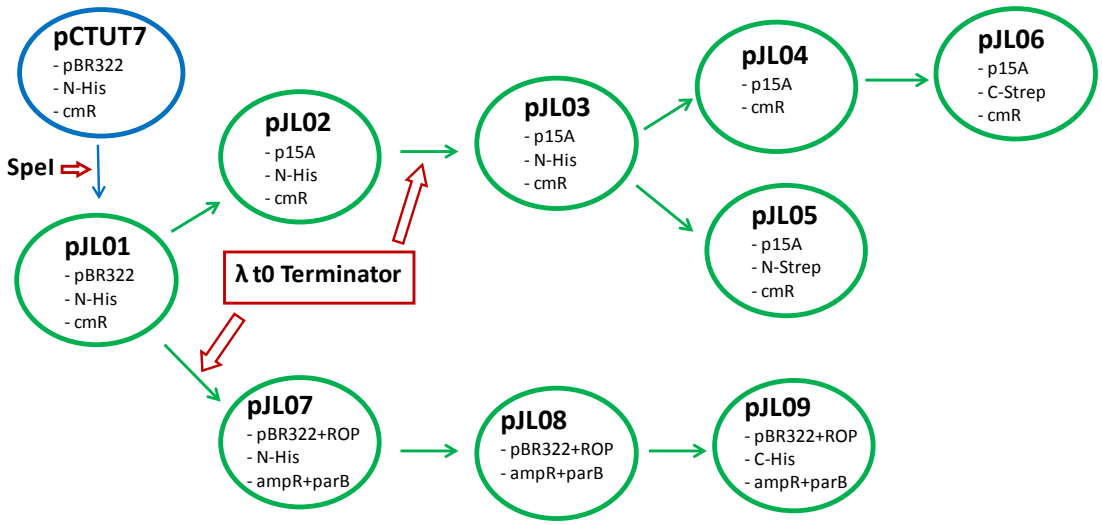

Figure 3.2 Overview of the nine constructed destination vectors. For more details of the destination vector construction see section 2.3.7. Vector maps can be found in Appendix 6.1.

Table 3.1 Overview of the expression vectors.

Plasmid	*ori*	Copy number	Tag	Resistance	Expression	Reference
pCTUT7	pBR322-ROP [a]	45-60	N-His	cm	Vlm1	(Jaitzig 2013)
pKS01	pBR322-ROP	45-60	N-His	amp (+parB) [c]	Vlm2	(Jaitzig 2013)
pJL01	pBR322-ROP	45-60	N-His	cm	-	This work
pJL02	p15A	10-12	N-His	cm	-	This work
pJL03	p15A	10-12	N-His	cm	Vlm1	This work
pJL04	p15A	10-12	-	cm	Vlm1	This work
pJL05	p15A	10-12	N-Strep	cm	Vlm1	This work
pJL06	p15A	10-12	C-Strep	cm	Vlm1	This work
pJL07	pBR322+ROP [b]	15-20	N-His	amp (+parB)	Vlm2	This work
pJL08	pBR322+ROP	15-20	-	amp (+parB)	Vlm2	This work
pJL09	pBR322+ROP	15-20	C-His	amp (+parB)	Vlm2	This work

[a] pBR322 *ori* without *rop* gene.

[b] pBR322 *ori* with *rop* gene.

[c] parB: plasmid stabilizing locus.

The main features of the expression plasmids are listed in Table 3.1. To express Vlm1 and Vlm2 equally, the copy number of the two expression plasmids should be comparable. Therefore, the plasmids with p15A (copy number 10-12) *ori* instead of pBR322 were used to express Vlm1. While Vlm2 was expressed by the plasmids with pBR322 *ori* plus the *rop* gene (copy number 15-20). The *rop* gene, which encodes the ROP protein (repressor of primer), can reduce copy number 1.5 to 3-fold in pBR322

plasmids (Som and Tomizawa 1983; Twigg and Sherratt 1980). In addition, we used an N-/C-terminal Strep tag (8 amino acids: Trp-Ser-His-Pro-Gln-Phe-Glu-Lys) linked to Vlm1 that could facilitate the subsequent co-purification with N-/C-terminal 6xHis-tagged Vlm2.

3.1.3. Effect of different vectors on VlmSyn expression

Vlm1 or Vlm2 expression vectors were first transformed separately into the host strain *E. coli* BJJ01. For comparison and screening, all the expressions were executed in parallel in TB medium at 30 °C for 5 h after 20 µM IPTG induction. Surprisingly, the final OD_{600} values varied significantly between the different expression strains. In the group of Vlm1 expression (Figure 3.3A), the lowest OD_{600} of 2.7 was observed in the original strain BJJ01/pCTUT7-Vlm1, while the other four strains reached higher cell density that could be attributed to the lower copy number plasmid in the cells alleviating the plasmid-mediated metabolic burden. The results suggested that a fusion tag could also impact the cell growth. The strain harboring the plasmid pJL04-Vlm1 without any tag reached a final OD_{600} of 9.5, which is 2-fold higher than the pJL03-Vlm1 strain with N-terminal His tag. When the strains harbored the plasmid with N-/C-terminal Strep tag, they resulted in a similar cell density (~7). For Vlm2 expression (Figure 3.3B), the final OD_{600} ranged from 1.7 in BJJ01/pJL07- Vlm2 to 9.5 in BJJ01/pJL08-Vlm2. Similar to the Vlm1 expression *E. coli* containing a Vlm2 expression plasmid without any tag could reach the highest cell density compared to the other expression plasmids. Insertion of the *rop* gene into pKS01-Vlm2 obviously inhibited cell growth as can be seen from the strain BJJ01/pJL07-Vlm2. Interestingly, OD_{600} increased again up to 3.7-fold when the His tag was moved from the N-terminus in pJL07-Vlm2 to the C-terminus in pJL09-Vlm2.

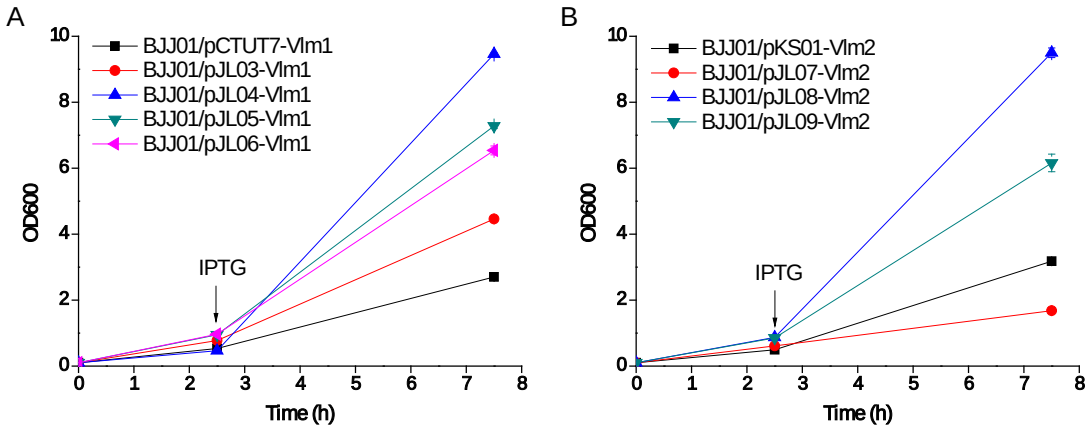

Figure 3.3 Growth curves of BJJ01 with a single Vlm1 (A) or Vlm2 (B) expression vector.

While different expression vectors had a considerable impact on cell growth, expression levels of Vlm1 and Vlm2 were also diverse as confirmed by SDS-PAGE analysis (Figure 3.4). Compared to the original plasmid pCTUT7-Vlm1, Vlm1 was expressed to a comparable level with pJL03-Vlm1 in *E. coli* BJJ01, even though this plasmid has a lower copy number than pCTUT7-Vlm1. However, Vlm1 expression levels were much lower with the other three plasmids which, in fact, could be reflected by the cell growth behavior. With a lower protein expression level and also lower metabolic burden, a higher cell density was reached in the end. Apparently, in our case the 6 amino acids His tag or 8 amino acids Strep tag significantly influenced Vlm1 expression levels. The reason is not clear, but we could assume that the secondary 5' mRNA structures are changed due to the alteration of N-terminal base pairs resulting in a different efficiency of protein translation (Szeker et al. 2011). In general, Vlm2 expression levels with the new vectors were comparable, albeit slightly lower than with the original vector pKS01-Vlm2. It has to be noted that almost half of the amount of the total Vlm2 was expressed in insoluble form with the vector pJL07-Vlm2, inhibiting obviously cell growth (Figure 3.3B).

Overall, the large proteins Vlm1 and Vlm2 were successfully expressed with all the new constructed vectors, however, at different quantities (total expression level) and qualities (soluble protein). Although the expression levels of the new vectors were not obviously better than those of the original ones, we investigated the

coexpression of Vlm1 and Vlm2 with several combinations from the created vector pool.

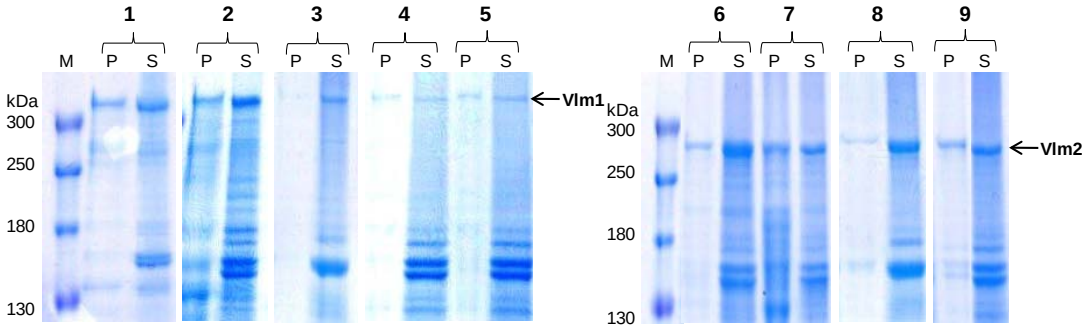

Figure 3.4 SDS-PAGE analysis of Vlm1 and Vlm2 expression with different vectors. The cultivations were performed at 30 °C in TB medium. Cells were harvested 5 h after induction with 20 µM IPTG. Protein samples were separated on a 5 % polyacrylamide gel. 1, BJJ01/pCTUT7-Vlm1; 2, BJJ01/pJL03-Vlm1; 3, BJJ01/pJL04-Vlm1; 4, BJJ01/pJL05-Vlm1; 5, BJJ01/pJL06-Vlm1; 6, BJJ01/pKS01-Vlm2; 7, BJJ01/pJL07- Vlm2; 8, BJJ01/pJL08-Vlm2; 9, BJJ01/pJL09-Vlm2. Vlm1 (370 kDa) and Vlm2 (284 kDa) are indicated by arrows. P= insoluble protein; S= soluble protein; M= protein molecular weight marker.

3.1.4. Coexpression of Vlm1 and Vlm2 with compatible vectors

Seven combinations of compatible vectors were transformed into *E. coli* strain BJJ01 for coexpressing Vlm1 and Vlm2. *E. coli* BJJ01 was cultivated in TB medium at 30 °C and protein expression was induced by addition of 20 µM IPTG. Meanwhile, *E. coli* BJJ01 harboring the original vector constructs pCTUT7-Vlm1 and pKS01-Vlm2 was also cultivated under the same conditions as a reference. The final OD_{600} values with the different expression vector combinations can be seen in Figure 3.5. Compared to the reference vector combination (OD_{600} ~6), three combinations led to higher OD_{600} valuses around 7, whereas the other four combinations led to very low cell densities. Especially *E. coli* BJJ01 with combinations of vector pJL07-Vlm2 did almost not grow at all during the 5 h cultivation after induction with final low OD_{600} values around 1. The possible reason would be that pJL07-Vlm2 severely impeded cell growth which is in agreement with the single expression of Vlm2 using pJL07-Vlm2 vector (Figure 3.3B).

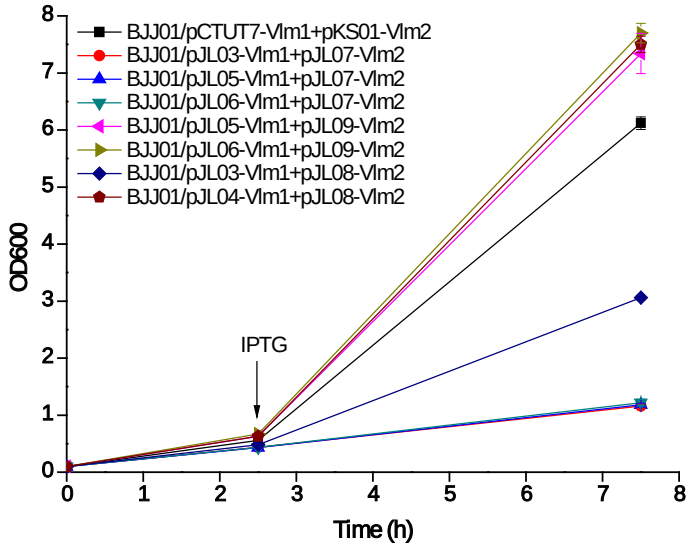

Figure 3.5 Growth curves of BJJ01 with Vlm1 and Vlm2 expression vector combinations.

As shown in Figure 3.6, in all the compatible vector combinations tested, Vlm1 expression levels were much lower than Vlm2, except with the combination of pJL03-Vlm1 and pJL08-Vlm2, which showed an equal expression level of the two proteins like we expected initially. However, the OD_{600} of BJJ01/pJL03-Vlm1+pJL08-Vlm2 was only half of the value (~6) obtained with the reference constructs (Figure 3.5). Therefore, the original strain BJJ01/pCTUT7-Vlm1+pKS01-Vlm2, which showed reasonable growth rate and proteins expression levels, was considered as a satisfactory candidate for the following investigation of valinomycin production.

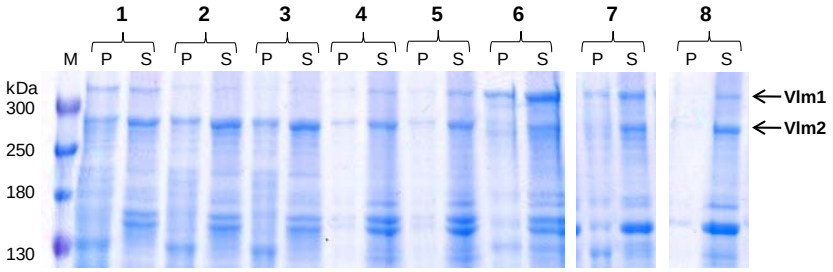

Figure 3.6 SDS-PAGE analysis of Vlm1 and Vlm2 coexpression with different vector combinations. The cultivations were performed at 30 °C in TB medium. Cells were harvested 5 h after induction with 20 µM IPTG. Protein samples were separated on a 5 % polyacrylamide gel. 1, BJJ01/pJL03-Vlm1+pJL07-Vlm2; 2, BJJ01/pJL05-Vlm1+pJL07-Vlm2; 3, BJJ01/pJL06-Vlm1+pJL07-Vlm2; 4, BJJ01/pJL05-Vlm1+pJL09-Vlm2; 5, BJJ01/pJL06-Vlm1+pJL09-Vlm2; 6, BJJ01/pCTUT7-Vlm1+pKS01-Vlm2; 7, BJJ01/pJL03-Vlm1+pJL08-Vlm2; 8, BJJ01/pJL04-Vlm1+pJL08-Vlm2. Vlm1 (370 kDa) and Vlm2 (284 kDa) are indicated by arrows. P= insoluble protein; S= soluble protein; M= protein molecular weight marker.

3.2. *E. coli* BJJ01 resistance to valinomycin

3.2.1. Effect of external valinomycin on *E. coli* BJJ01 growth

E. coli BJJ01 is the host strain used for valinomycin production. It is thus necessary to test the inhibiting effect of the antibiotic valinomycin on BJJ01 growth. BJJ01 was grown in EnBase Flo medium supplemented with valinomycin at final concentrations of 10, 30, 50 and 100 mg L^{-1}. Since the commercial valinomycin (1 mg mL^{-1} solution) was dissolved in DMSO, if we add valinomycin to a concentration of 100 mg L^{-1} to the culture, the final amount of DMSO in the culture would be 10 % (v/v). For cultures supplemented with 10, 30 and 50 mg L^{-1} valinomycin, additional DMSO was added equal the amount to 10 % (v/v) as well. Therefore, two negative controls supplemented with H_2O (10 %, v/v) and DMSO (10 %, v/v) were cultivated in parallel for comparison. OD_{600} values were measured at different time intervals during the 48 h cultivation. As shown in Figure 3.7, during the whole course of cultivation, OD_{600} values of the negative DMSO control and all the cultures with externally applied valinomycin reached a very similar level. However, cell growth was significantly inhibited in these cultures causing a drop of 64 % of the final OD_{600} values compared to the negative H_2O control culture. We conclude that the inhibiting effect on cell growth was only caused by DMSO rather than valinomycin because there was no cell density drop if the valinomycin concentration increased from 10 to 100 mg L^{-1}. Our results are supported by two previous findings: 1) the organic solvent DMSO can markedly inhibit *E. coli* cell growth if its concentration in the medium is 10 % (v/v) (Fowler and Zabin 1966); 2) *E. coli* as a Gram-negative bacterium has an additional outer membrane that can prevent access of valinomycin to the inside of the cell (Ryabova et al. 1975; Tempelaars et al. 2011).

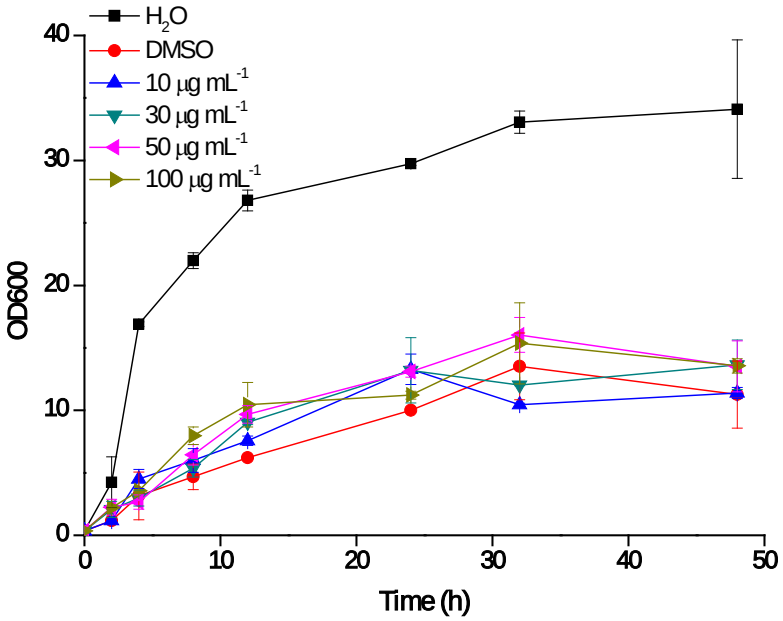

Figure 3.7 Growth curves of BJJ01 supplemented with external valinomycin.

3.2.2. Effect of internal valinomycin on *E. coli* BJJ01 growth

In order to assay the tolerance of BJJ01 to valinomycin from inside of the cell, the valinomycin-producing strain BJJ01/pCTUT7-Vlm1+pKS01-Vlm2 was grown in EnBase EnPresso medium. *E. coli* BJJ01 without Vlm1 and Vlm2 experssion plasmids and BL21Gold/pCTUT7-Vlm1+pKS01-Vlm2 were cultivated as two controls for comparison. BL21Gold/pCTUT7-Vlm1+pKS01-Vlm2 was selected as a control because this strain does not contain the genomic integration of the *sfp* gene for NRPS posttranslational modification and should therefore not be able to biosynthesize valinomycin. Figure 3.8 shows the growth curves of the three strains. OD_{600} values of BJJ01 without experssion plasmids were always >1.5-fold higher at each measurement point than those of the other two strains which had very similar cell densities during the whole cultivation. After cultivation, valinomycin was extracted and determined from the three cultures. As expected no valinomycin was detected from BJJ01. The titer from BJJ01/pCTUT7-Vlm1+pKS01-Vlm2 was determined to be 1447 µg L^{-1}. However, to our surprise, valinomycin was also detected from BL21Gold/pCTUT7-Vlm1+pKS01-Vlm2 with a titer of 722 µg L^{-1}. This is probably due to native enzymes in *E. coli* which can act as a phosphopantetheinyl transferases (PPTase) instead of Sfp to convert inactive apo-VlmSyn to active holo-VlmSyn (Quadri et al. 1998). Although BJJ01/pCTUT7-

Vlm1+pKS01-Vlm2 produced 2-fold more valinomycin than BL21Gold/pCTUT7-Vlm1+ pKS01-Vlm2, the OD_{600} values were nearly the same suggesting that at these concentrations valinomycin produced within *E. coli* had no obvious inhibiting effect on cell growth. Hence, cell growth inhibition compared to BJJ01 alone was mainly due to the metabolic burden from expression of the large VlmSyn rather than internally formed valinomycin.

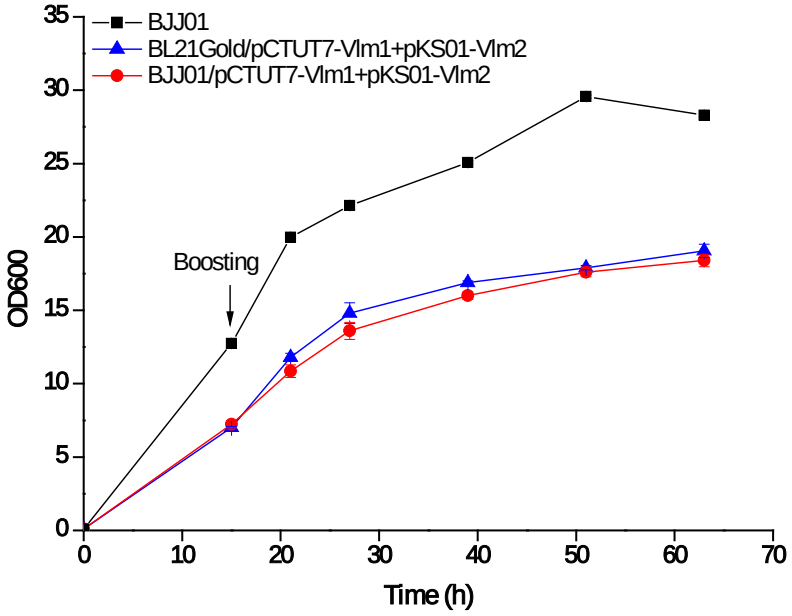

Figure 3.8 Growth curves of BJJ01 with internal produced valinomycin.

3.3. Batch cultivation for valinomycin production

3.3.1. Screening of the best vector combination

In section 3.1, we have constructed several expression vectors and investigated VlmSyn expression levels. To achieve a high valinomycin yield, the best expression vector combination of Vlm1 and Vlm2 has to be screened for the production. We anticipated that a higher producing strain should synthesize the enzyme VlmSyn with a high quantity and quality. Based on the coexpression results of Vlm1 and Vlm2 (Figure 3.6), Vlm1 was expressed in a significantly lower level in the strains BJJ01/pJL05-Vlm1+pJL07-Vlm2 and BJJ01/pJL06-Vlm1+pJL07-Vlm2 compared to the other strains. Thus, we decided to omit these two strains and screen the six best combinations from protein expression experiments.

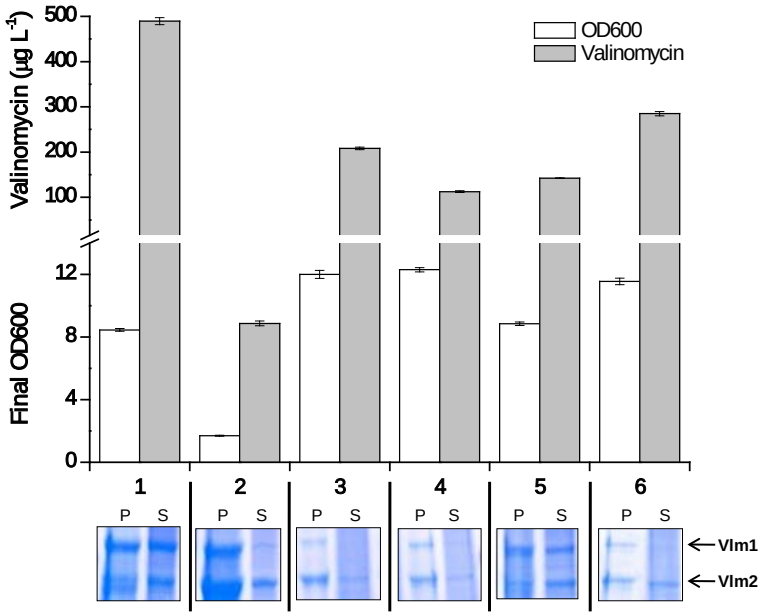

Figure 3.9 Screening of the best vector combinations for valinomycin production. 1, BJJ01/pCTUT7-Vlm1+pKS01-Vlm2; 2, BJJ01/pJL03-Vlm1+pJL07-Vlm2; 3, BJJ01/pJL05-Vlm1+pJL09-Vlm2; 4, BJJ01/pJL06-Vlm1+pJL09-Vlm2; 5, BJJ01/pJL03-Vlm1+pJL08-Vlm2; 6, BJJ01/pJL04-Vlm1+pJL08-Vlm2. Vlm1 (370 kDa) and Vlm2 (284 kDa) are indicated by arrows. P= insoluble protein; S= soluble protein.

E. coli BJJ01 with the six vector combinations was cultivated in TB medium at 30 °C. VlmSyn expression was induced by addition of 20 μM IPTG followed by 16 h of cultivation. At the end of the cultivation, OD_{600} values were measured and cells were collected for protein expression analysis. Valinomycin was extracted from each culture for the following LC-MS measurement. As shown in Figure 3.9, the highest valinomycin titer (489 μg L^{-1}) was obtained from BJJ01/pCTUT7-Vlm1+pKS01-Vlm2 with a final OD_{600} of 8.5. Both valinomycin titer (9 μg L^{-1}) and OD_{600} value (1.7) were the lowest in the culture of BJJ01/pJL03-Vlm1+pJL07-Vlm2. The other four vector combinations generated similar levels of OD_{600} and valinomycin. SDS-PAGE analysis clearly revealed that total VlmSyn expression levels and soluble protein fractions are different from each other. BJJ01/pCTUT7-Vlm1+pKS01-Vlm2 showed the highest yield of soluble VlmSyn in the cells. An equal expression of Vlm1 and Vlm2 in the soluble fraction was observed in BJJ01/pJL03-Vlm1+pJL08-Vlm2. But it only produced a modest yield of valinomycin (142 μg L^{-1}). BJJ01/pJL03-Vlm1+pJL07-Vlm2 expressed a great quantity of VlmSyn, however, most of it was insoluble. After 16 h cultivation,

almost no soluble VlmSyn can be seen from the other three vector combinations and their total expression levels were rather low. Finally, based on the results of cell density, VlmSyn expression levels and valinomycin titer, we chose BJJ01/pCTUT7-Vlm1+pKS01-Vlm2 as our working strain to further investigate valinomycin production.

3.3.2. Batch cultivation

The main aim of this work is to enhance valinomycin production through multiple approaches, one of which is bioprocess engineering. According to the previous screening (section 3.3.1), the strain BJJ01/pCTUT7-Vlm1+pKS01-Vlm2 was initially investigated in a batch cultivation process in shake flasks for valinomycin production. The batch cultivation was performed in TB medium at 30 °C. IPTG was added to induce Vlm1 and Vlm2 expression when the OD_{600} reached 0.6-0.8 followed by 36 h of cultivation for valinomycin formation. As shown in Figure 3.10, the cells keep growing exponentially for ~4 h after induction until an OD_{600} of ~7 was reached. Afterwards cells entered the stationary phase after 8 h at an OD_{600} of ~8.5. After 24 h, cells started to die and lyse and the OD_{600} values dropped remarkably. The final volumetric valinomycin titer reached 300 µg L^{-1}, while most of the product (~225 µg L^{-1}) was produced within the initial 4 h period, which is consistent with the exponential growth phase. Only 25 % of the total valinomycin was accumulated in the subsequent 32 h presumably due to decreased cell growth and thus precursor limitation. This inspired us to find a way that can prolong the exponential growth phase to obtain high cell densities and, hopefully, also resulting in higher valinomycin yields. Therefore, the first choice would be fed-batch cultivation.

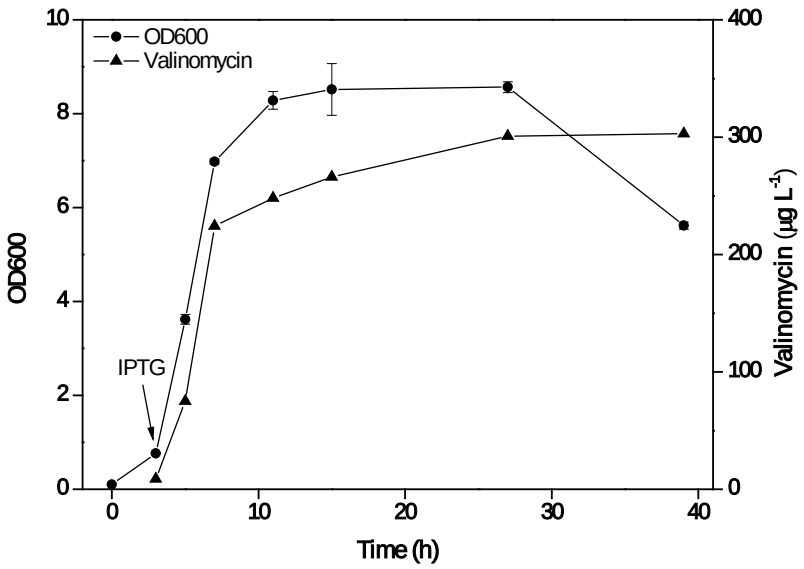

Figure 3.10 Time courses for cell growth and valinomycin production in a batch cultivation in shake flask.

3.4. Fed-batch cultivation for valinomycin production

To prolong cell growth and obtain high cell densities, the enzyme-based glucose delivery EnBase system, which allows fed-batch cultivation in small-scale vessels such as shake flasks, was used. This system has been reported to produce high cell densities and significantly improve expression yields of recombinant proteins compared to the typical TB medium (Krause et al. 2010; Ukkonen et al. 2011). There are, in general, two phases during the EnBase fed-batch cultivation. Phase 1 is a controlled cultivation process in a mineral salt medium that is supplemented with certain amount of complex additives, trace elements and a soluble starch-based polymer. The second phase following phase 1 is initiated by addition of complex boosting nutrients and if necessary the protein expression inducer (e.g., IPTG). After boosting, cells grow more rapidly but still controlled by enzyme-based glucose release and recombinant protein synthesis is promoted since rich nutrients, for example, amino acids and cofactors, are available in the medium.

Two types of EnBase medium were employed in our work, the liquid-based EnBase Flo and the tablet-based EnBase EnPresso. Valinomycin production using EnBase Flo and EnPresso was primarily carried out in shake flasks. Our results suggested that the

two large proteins, Vlm1 and Vlm2, were highly expressed together in both EnBase media without IPTG induction (data not shown), probably because the *lac* promoter-derived expression plasmids used in our system were leaky (Kraft et al. 2007). No IPTG needed for induction in the cultivation would be very economical in large scale production. As can be seen from Figure 3.11, OD_{600} of the culture reached 9 in EnPresso and 7.6 in Flo at the end of overnight cultivation (15 h, phase 1). However, OD_{600} did not increase further in 2 h after boosting mainly because cells have to adapt to the "new" medium environment inhibiting cells growth. Then, cells kept continuously growing for 46 h up to an OD_{600} of approximately 20 from both Flo and EnPresso, which is 2.4-fold higher than in TB batch cultivation. Meanwhile, valinomycin formation was remarkably enhanced along with the extended cells growth period. The final titer of valinomycin (2.4 mg L^{-1}) in EnPresso indicated an 8-fold increase without any optimization compared to the titer obtained in TB batch fermentation. A similar yield of valinomycin (2.0 mg L^{-1}) was achieved in Flo medium as well, suggesting that both EnBase media are suitable for fed-batch production of valinomycin in small-scale shake flasks.

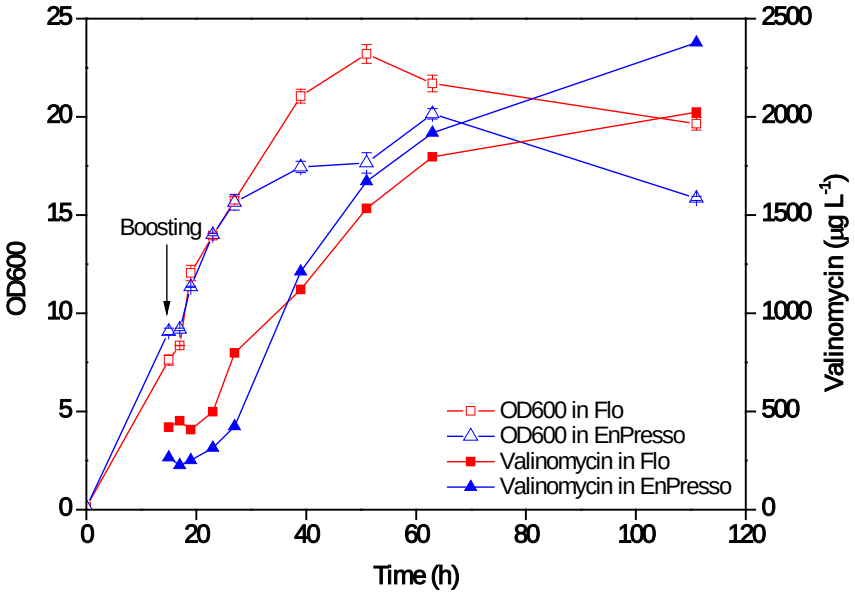

Figure 3.11 Time courses for cell growth and valinomycin production with EnBase Flo and EnBase EnPresso fed-batch cultivations in shake flask.

3.5. DoE optimization of valinomycin production in milliliter scale

One principle of the EnBase fed-batch cultivation is that glucose is gradually released by the enzyme from the starch-based polymer and then consumed by the cells. If the enzyme concentration is too low, cells starve for glucose resulting in low cell densities. If the enzyme concentration is too high, high metabolic activites and overflow metabolism may lead to oxygen limitation and medium acidification, which deteriorates the cultivation. Therefore, the enzyme concentration corresponding to the glucose-release rate was optimized for valinomycin production. Oxygen content and pH were monitored and evaluated as key parameters during the cultivation, because of their influence on cell growth and recombinant protein expression in *E. coli* (Ukkonen et al. 2011).

The fed-batch EnBase EnPresso medium was used in the optimization. To obtain the optimal conditions and enhance valinomycin production, three key parameters, which are nutrients boosting, enzyme concentration and culture volume correlating to dissolved oxygen content, were selected for the following optimization. In order to avoid laborious and time-consuming flask-scale optimization, a robot-assisted high-throughput screening for improved valinomycin titer conditions was established with a DoE guided optimization in milliliter-scale 24-well plates. The PreSens 24-well plate system allows online non-invasive measurement of dissolved oxygen (DO) and pH during the cultivation process. This could provide us with more information to monitor the changes of oxygen and pH in each well and to understand the relationships between the cultivation parameters and the final valinomycin yields.

Table 3.2 Design of experiments for parameters optimization and experimental results including OD_{600} and volumetric valinomycin titers as responses

Run no.	Enzyme (U L^{-1})	Volume (mL)	Boosting	OD_{600}	Valinomycin (µg L^{-1})
1	0	0.5	No	20.82±1.12	656.48±134.42
2	6	0.5	No	17.56±2.23	529.00±76.45
3	0	1.5	No	19.04±0.70	279.38±37.08
4	6	1.5	No	7.65±1.74	204.18±24.97
5	0	1.167	No	21.21±1.40	323.73±39.32
6	6	0.833	No	17.56±1.67	369.94±0.00
7	2	0.5	No	20.42±1.12	539.58±42.81
8	4	1.5	No	16.33±0.63	425.03±32.53
9	0	0.5	Yes	26.98±2.86	5345.87±603.65
10	6	0.5	Yes	27.62±0.70	6364.39±546.70
11	0	1.5	Yes	19.83±0.14	1080.51±41.57
12	6	1.5	Yes	15.44±0.21	1194.15±50.48
13	0	0.833	Yes	29.10±4.05	2912.11±109.16
14	6	1.167	Yes	19.29±1.05	1610.19±21.63
15	4	0.5	Yes	29.60±0.56	6123.16±81.03
16	2	1.5	Yes	18.10±0.07	1155.59±16.20
17	3	1	Yes	27.57±2.86	1559.51±37.65
18	3	1	Yes	25.70±1.19	1435.52±35.33
19	3	1	Yes	26.64±0.56	1469.40±4.79
20	3	1	Yes	26.00±0.07	1542.94±21.38

The experimental design, final OD_{600} values and volumetric valinomycin titers are summarized in Table 3.2. A quadratic model with interactions was fitted to the measured values. The regression coefficients for both models were high (R^2 = 0.96 for OD_{600} and R^2 = 0.97 for valomycin production, respectively) and both models were significant ($\alpha < 0.05$). It is obvious from the effect plots (Figures 3.12A and B), which result from the analysis of variance, that boosting causes the highest effect on cell growth and valinomycin production. If booster was added to the culture, both cell density and valomycin production increased. The added complex nutrient booster contains amino acids, vitamins and cofactors and thus supports the efficient synthesis of proteins (Vlm1 and Vlm2) and supplies further precursors for valinomycin biosynthesis. Culture volume caused the second highest effect on both parameters. This effect is even higher with boosting than without, which can be concluded from the high value for the interaction between both parameters (7 in Figures 3.12A and B). Since a regression analysis is difficult with qualitative factors,

boosting was eliminated from the model and a quadratic model is established using the results of the experiments with boosting. The stepwise elimination of the insignificant effects led to a reduced quadratic model, which only contained the culture volume as an influencing factor. The two models have again a good regression coefficient (R^2 = 0.84 for OD_{600} and R^2 = 0.98 for valinomycin production) and both models are significant. The *lack of fit* is not significant for the OD_{600}, but for the valinomycin production, which is caused by the high reproducibility in the center points of the experimental plan (Table 3.2). The variety is probably higher with other settings of the experimental plan, which results in the mentioned *lack of fit*. The effect of the culture volume, which is related to the oxygen transfer rate, on cell growth and valinomycin production is shown in Figures 3.12C and D, suggesting the lower culture volume was better. The effect of the enzyme concentration might be judged as insignificant, because of the small range which has been investigated. Therefore the range was increased in the next optimization step (see section 3.6.1). The parity plots of cell density and valinomycin revealed a satisfactory correlation between the observed values and the predicted values (Figure 3.13).

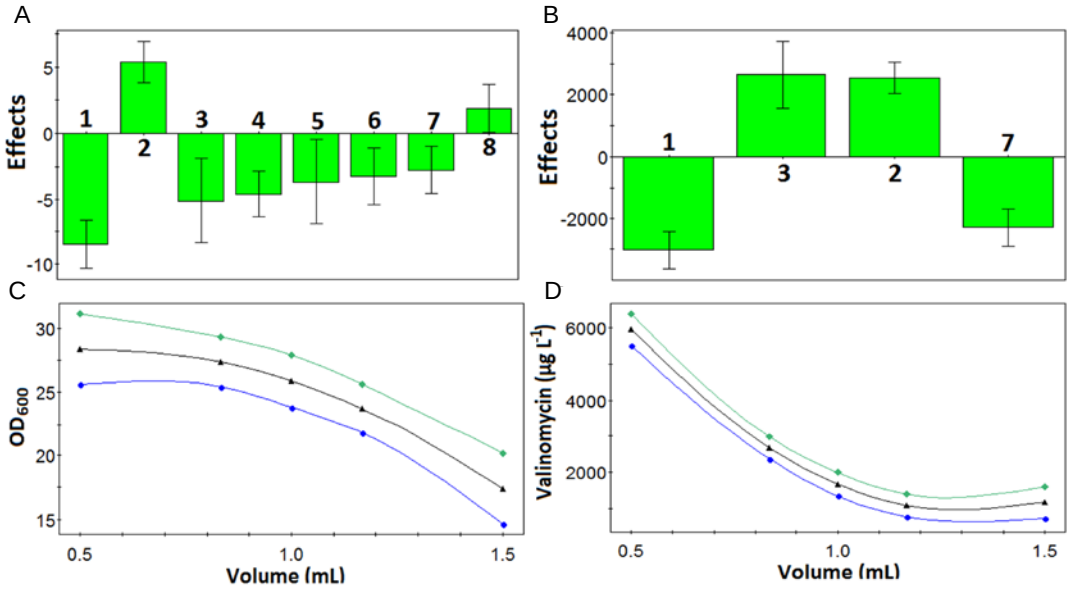

Figure 3.12 Results of the design of experiments. Top: Effect plots for the influence of 1, volume; 2, boosting; 3, (volume)²; 4, enzyme; 5, (enzyme)²; 6, (enzyme × volume); 7, (boosting × volume); 8, (enzyme × boosting) on (A) OD_{600} (R^2 = 0.96) and (B) valinomycin titer (µg L^{-1}) (R^2 = 0.95). Bottom: Response prediction plot with 95 % confidence interval for the reduced quadratic model fitted to the results obtained with boosting for (C) OD_{600} (model equation: OD_{600} = 24.9 + 13.0 × volume – 12.0 × (volume)², R^2 = 0.84) and (D) valinomycin titer (µg L^{-1}) (model equation: valinomycin = 13988 – 19866 × volume + 7548 × (volume)², R^2 = 0.98). All models are significant ($\alpha < 0.05$) and the models for OD_{600} have no significant *lack of fit* ($\alpha > 0.05$).

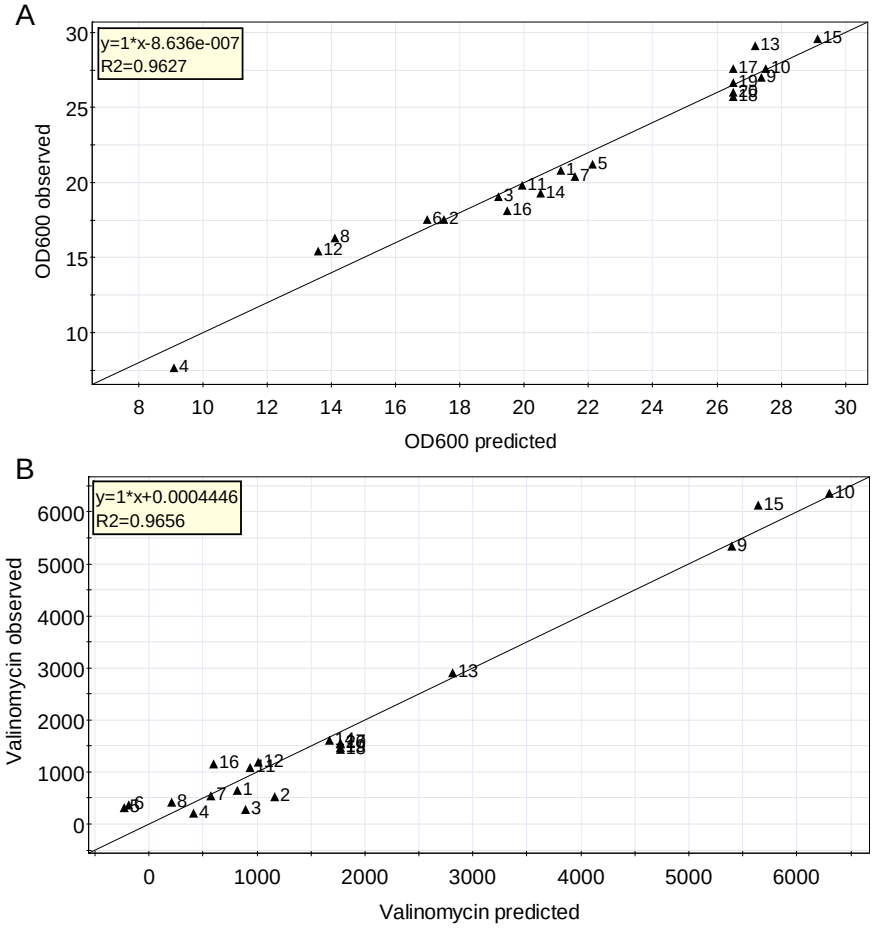

Figure 3.13 Parity plot of observed *vs*. predicted values of cell density (A) and valinomycin titer (B).

The stability of the pH was obviously not influenced by boosting. The online data showed that a very stable pH level is maintained in the EnBase medium, although in general the values (~7.0-7.5) with boosting are a little higher compared to those without boosting (~6.5-7.0) (Appendix 6.2). These pH values are very close to the optimal pH of 7.0 for *E. coli* growth, demonstrating the fed-batch-like medium could buffer the culture system well without external pH control. In contrast, pH gradually increased from initial 7.0 to final 8.5 in TB batch cultivations, which is beyond the optimal pH range of *E. coli* growth (data not shown).

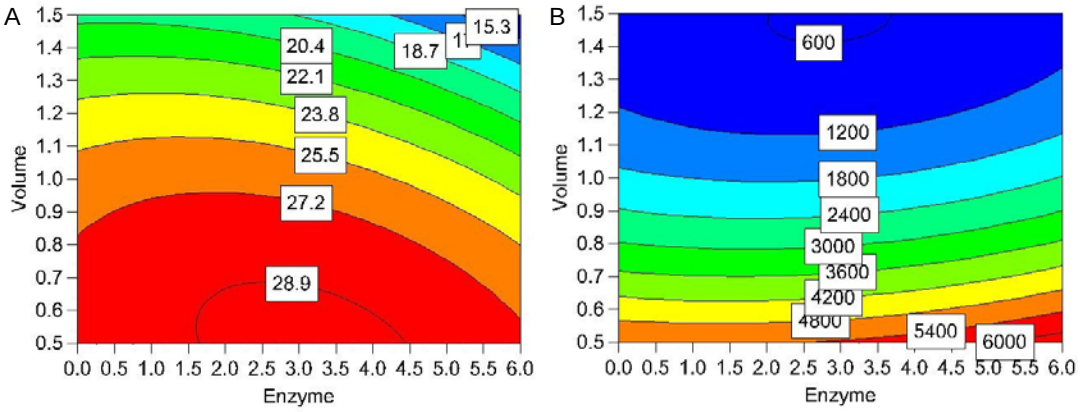

Figure 3.14 Contour plot of cell density (A) and valinomycin titer (B) *vs*. enzyme and volume with boosting.

In the EnBase fed-batch cultivation process, the glucose-releasing enzyme was added twice to the culture to maximize the controlled feeding of glucose. At the inoculation point, enzyme was added to get the concentration of 0.3 U L^{-1}. The initial low amount of enzyme could provide a consistent cultivation environment with slowly released glucose for the cells to reach a reasonable density before the following nutrients boosting and production phase. To optimize the enzyme concentration, the second addition was investigated in a range from 0 to 6 U L^{-1}. Our results revealed that higher enzyme concentrations correlate with higher valinomycin titers, while there was no obvious influence on cell density (Figure 3.14).

The total volume of a well in the 24-well plate was 3.3 mL and working volumes from 0.5 to 1.5 mL were tested. According to the online data (Appendix 6.2) in the boosting group, the change of the DO content with the same culture volume was similar. Along with an increase of the culture volume from 0.5 to 1.5 mL, a prolonged period of oxygen limitation appeared. This underlines the big influence of the culture volume, i.e. a good oxygen supply, on cell growth and valinomycin production found with the experimental design approach. The DO increase in the late period of the cultivation is probably due to the exhaustion of the glucose polymer substrate, leading to the stop of cell growth and less oxygen being consumed. A lower culture volume and therefore a higher oxygen transfer rate led to higher cell density and valinomycin titer (Figure 3.14).

The optimized parameters determined from the DoE experiment were: addition of nutrients, an enzyme concentration of 6 U L^{-1} and a culture volume of 0.5 mL. These conditions lead to a 3-fold improvement of the final OD_{600} compared to the batch cultivation in TB medium (Figure 3.15). More important, the final volumetric valinomycin titer dramatically increased to 6.4 mg L^{-1}, which is >20-fold higher than that in the initial batch fermentation. In addition, oxygen and pH were shown to remain stable at nearly 100 % and around 7.2, respectively, during the 48 h production process (Figure 3.15).

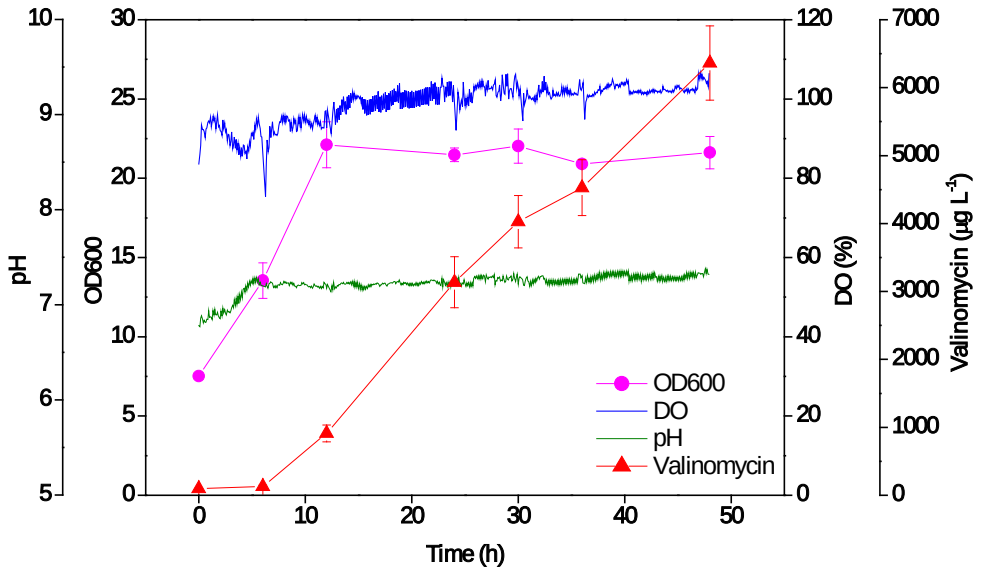

Figure 3.15 Time courses for cell growth, oxygen, pH and valinomycin production with optimal EnBase fed-batch cultivation in milliliter-scale.

3.6. High cell density fed-batch production of valinomycin in shake flasks

3.6.1. Effect of enzyme concentration on valinomycin production

Since high cell density cultivation led to more valinomycin (see sections 3.3 and 3.4), we attempted to further increase the cell density to obtain an even larger quantity of valinomycin. In the EnBase system, the glucose feeding rate is dependent on the enzyme concentration. A higher enzyme dosage in the medium should release more glucose faster to feed the cells and yield higher cell densities. According to the results from the DoE optimization (see section 3.5), higher enzyme concentration meaning

faster glucose feeding rate resulted in more valinomycin within the tested range (0 to 6 U L^{-1}). Therefore, we decided to broaden the range of tested enzyme concentrations to see whether an optimum enzyme concentration above 6 U L^{-1} for valinomycin production could be determined. For easy handling and high-throughput screening, this experiment was performed in the PreSens 24-well plate with 1 mL liquid EnBase Flo medium per well. A broad range of enzyme concentrations between 1.5 and 90 U L^{-1} (for details see section 2.6.6) was tested to see if the positive correlation between enzyme concentration and valinomycin formation could be established. Effect of enzyme concentration on valinomycin production in EnBase Flo medium without boosting was also tested. The DO, pH and cell growth of the cultivations without boosting are shown in Appendix 6.3. The following results are based on the cultivations with boosting.

Figure 3.16 shows the online DO in each well with different enzyme concentrations. In the group of enzyme concentrations ≤9 U L^{-1} DO decreased from ~80 % to ~40 % within the initial 5 h. Then, the DO remained stable at ~40 % up to 10 h (1.5 U L^{-1}), 12 h (3 U L^{-1}) or 15 h (9 U L^{-1}) followed by a continuous increase until the end of the cultivation. The enzyme concentrations ≥15 U L^{-1} resulted in a similar change of DO in the medium during the first 5 h. Afterwards, the DO in these wells immediately started to increase and kept stable until the end. The reasons for this phenomenon can be explained as follows. If a low amount of enzyme is in the medium, less glucose is released from the polymer slowly and cells can keep growing for longer period of time. Therefore, cells have to continuously uptake oxygen for their growth resulting in a longer low oxygen period. When all the glucose is consumed, cells will suffer starvation and stop fast growing. Then, the oxygen concentration in the medium will gradually increase. By contrast, a high amount of enzyme in the medium can rapidly release more glucose and all substrates will be completely depleted in a short time. Thus, cells starve and oxygen increases shortly after the cultivation.

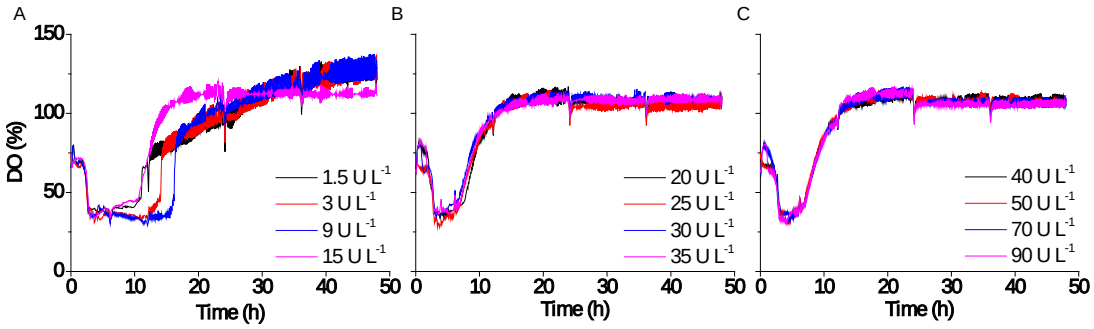

Figure 3.16 Online measurement of oxygen in the 24-well plate. The cultivations were performed at 30 °C in EnBase Flo medium with different amounts of enzyme. The culture volume in each well was 1 mL.

Online data also suggested that the pH in each well was related to the enzyme concentrations (Figure 3.17). The initial pH in all wells was around 7.2. With enzyme concentrations ≤9 U L^{-1}, pH values kept slightly increasing for ~15 h and then stayed stable to the end. With higher enzyme concentrations ≥15 U L^{-1}, the pH gradually decreased to 6.5 within 10 h and remained stable afterwards. A possible explanation would be that high enzyme concentrations cause glucose overfeeding, which results in acetate accumulation and medium acidification.

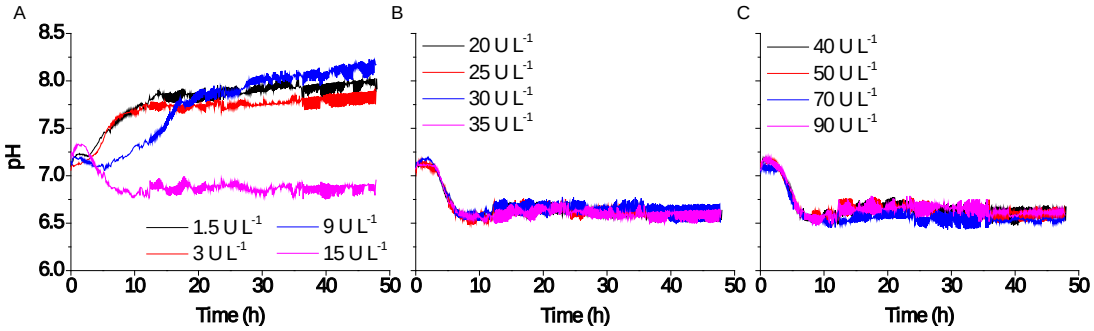

Figure 3.17 Online measurement of pH in the 24-well plate. The cultivations were performed at 30 °C in EnBase Flo medium with different amounts of enzyme. The culture volume in each well was 1 mL.

Likewise, enzyme concentrations also influenced cell growth (Figure 3.18). It is clear that low enzyme concentrations support a longer growth phase with lower growth rates and thus give rise to higher cell densities, which is well in agreement with the oxygen concentrations in the medium (Figure 3.16). With enzyme concentrations ≤3 U L^{-1} the final OD_{600} values reached around 30, which is >3-fold higher than the cultivations with enzyme concentrations ≥15 U L^{-1}.

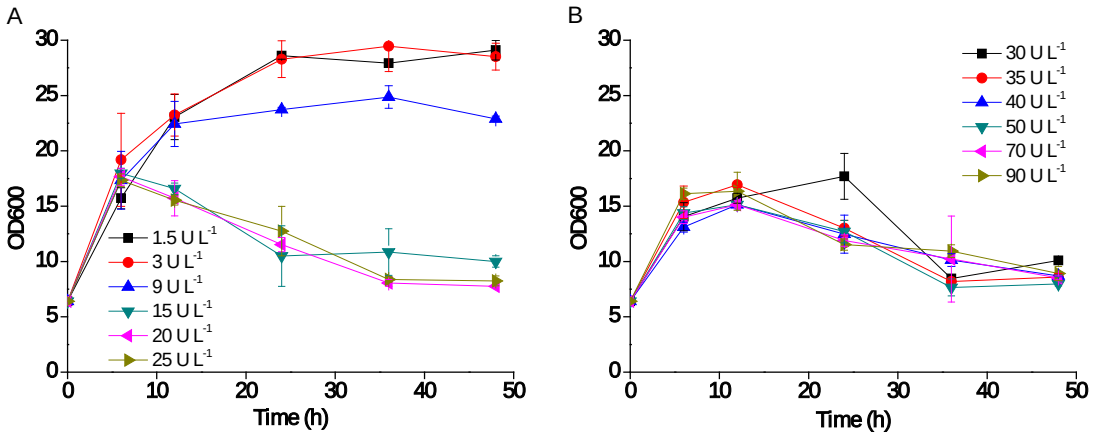

Figure 3.18 Cell growth curves with different enzyme concentrations.

The final valinomycin titers are presented in Figure 3.19. The results indicated that enzyme concentrations ≤50 U L^{-1} had no big influence on valinomycin production without boosting, while with enzyme concentrations ≥70 U L^{-1} the yields significantly decreased. In the boosting group, within the range of 1.5 to 9 U L^{-1} of enzyme, more enzyme resulted in a higher volumetric valinomycin yield. However, if the enzyme concentrations were higher than 9 U L^{-1}, the yield of valinomycin was sharply reduced 16-fold compared to the highest value of 2.4 mg L^{-1}. The enzyme concentration that resulted in the highest amount of valinomycin produced in EnBase medium in our study was 9 U L^{-1}.

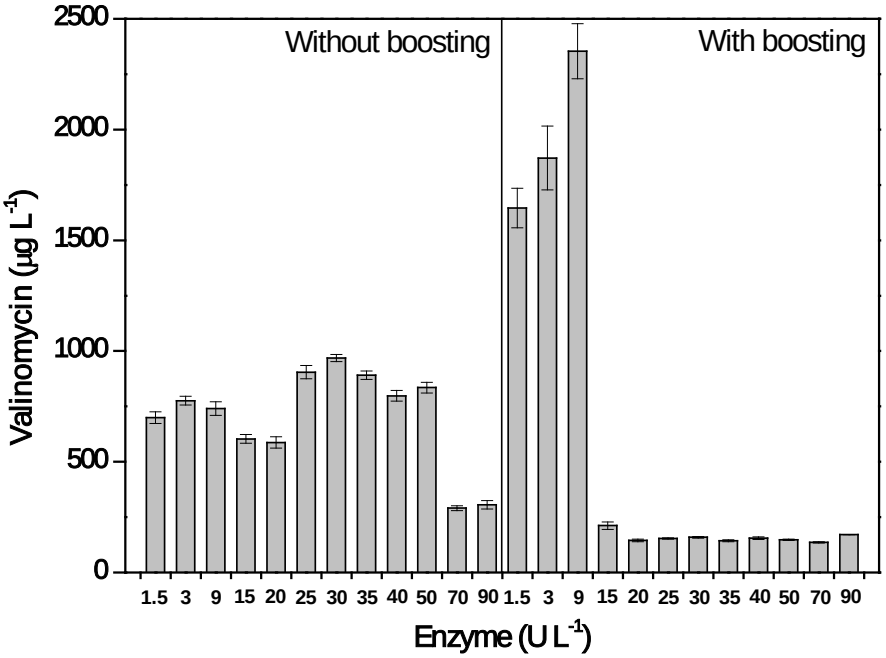

Figure 3.19 Valinomycin titers produced with different enzyme concentrations.

3.6.2. Glucose polymer feeding enhances valinomycin production

The curves for the DO (Figure 3.16A) and for the cell growth (Figure 3.18A) suggested that the carbon source polymer for glucose release was exhausted with an enzyme concentration of 9 U L^{-1} after ~15 h (DO increase and no change in cell density). Therefore, we tested if continued glucose release by supply of additional polymer to the medium, would further enhance cell growth and valinomycin formation.

EnBase Flo medium was used in this polymer feeding experiment. After overnight cultivation, boosting solution and 9 U L^{-1} enzyme were added to the main culture. Then, the culture was distributed into three baffled shake flasks (PreSens), which allow non-invasive online measurement of oxygen and pH. The first flask was a control without additional polymer feeding. The second flask was fed with 30 g L^{-1} polymer after 12 h. The third flask was fed twice with 30 g L^{-1} polymer after 12 h and 24 h, respectively.

Figure 3.20 shows the online data of oxygen and pH, cell growth curves, and final valinomycin titers. As shown in Figure 3.20A, before the first feeding point (12 h), all three cultures had the same oxygen conentratoins in the medium. The DO decreased in the initial batch phase (until 5 h) under glucose excess from 70 % to 5 %. Afterwards the DO increased to 60 % in the following 2 h indicating the transition to glucose-limited growth. In the flasks where extra polymer was added to the medium (at 12 h), the DO suddenly decreased to almost 0 %, but recovered fast to a stable level. This short disturbance in the DO is probably because the glucose polymer contains some degraded free glucose that the cells will take up immediately and the resulting fast growth leads to nearly anaerobic conditions in the medium. A comparison of the three DO profiles clearly revealed that the growth could be maintained by additional feeding of the polymer. With polymer feeding, the pH slightly decreased compared to the control but still remained close to pH 7 (Figure 3.20B). OD_{600} values indicated that polymer feeding was beneficial for cell growth as assumed (Figure 3.20C). Without polymer feeding, cells stopped growing after 12 h

with a final OD_{600} of 24. Polymer feeding at two times significantly improved cell density up to an OD_{600} of 55. In parallel, the volumetric valinomycin titer was dramatically promoted up to 10 mg L^{-1} (Figure 3.20D), which is a 33-fold increase compared to TB batch production (see section 3.3.2). In addition, the specific yield of valinomycin with twice polymer feeding reached 182 µg L^{-1} OD_{600}^{-1}, indicating a 5.2-fold improvement compared to the initial TB batch cultivation with a specific yield of 35 µg L^{-1} OD_{600}^{-1}.

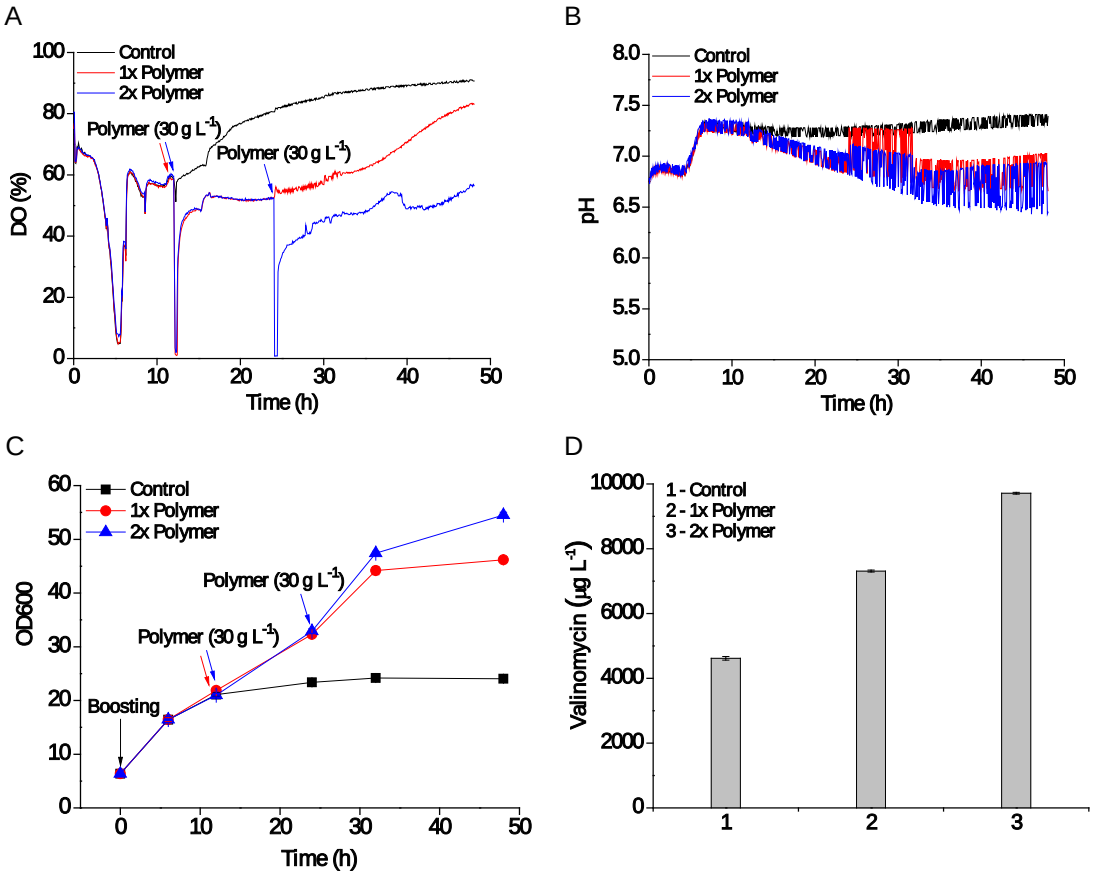

Figure 3.20 Glucose polymer feeding for valinomycin production with *E. coli* BJJ01/pCTUT7-Vlm1+ pKS01-Vlm2: online measurement of oxygen (A) and pH (B), cell growth curves (C) and valinomycin titers (D). The cultivations were performed at 30 °C in EnBase Flo medium with an enzyme concentration of 9 U L^{-1}. The culture volume in each PreSens shake flask (125 mL) was 12.5 mL.

3.7. Bioreactor fed-batch fermentation for valinomycin production

In order to scale up the high cell density fed-batch fermentation, the cultivation was performed in a 3.7 L bench-top bioreactor with 2 L culture volume. Instead of the normally used initial batch mode cultivation in the bioreactor, the fed-batch-like EnBase Flo medium was used for starter culture for the high cell density cultivation, which would confer cells with consistent intracellular physiological conditions, avoiding overflow metabolism in the initial cultivation phase (Glazyrina et al. 2012). Since modest yields of valinomycin could be reached without boosting (Figure 3.19), the bioreactor fed-batch production was performed only based on pure glucose feeding without complex nutrients boosting. The cultivation in the bioreactor was started with an OD_{600} of 0.1 after inoculation and 3 U L^{-1} enzyme were added for glucose release. During the whole fermentation (Figure 3.21C), cells were grown at 30 °C with a constant pH of 7.0 and the DO was maintained above 20 %.

After 16-18 h cultivation, the polymer releasing glucose in the Flo medium was depleted, as indicated by the continuous increase of DO (Figure 3.21C). Glucose measurement also indicated no glucose accumulation in the medium (data no shown). Then, the glucose feeding was initiated with a targeted specific growth rate (μ) of ~0.2 h^{-1}. The subsequent exponential feeding process was continued for 12 h followed by a gradual decrease to a constant feeding to the end of the fermentation (Figure 3.21A). After feeding, cells grew exponentially along with the exponential feeding period. When the feeding was adjusted to the constant rate, the specific growth rate was reduced to below 0.05 h^{-1} until the end of the cultivation with a final OD_{600} of 144 (Figure 3.21A).

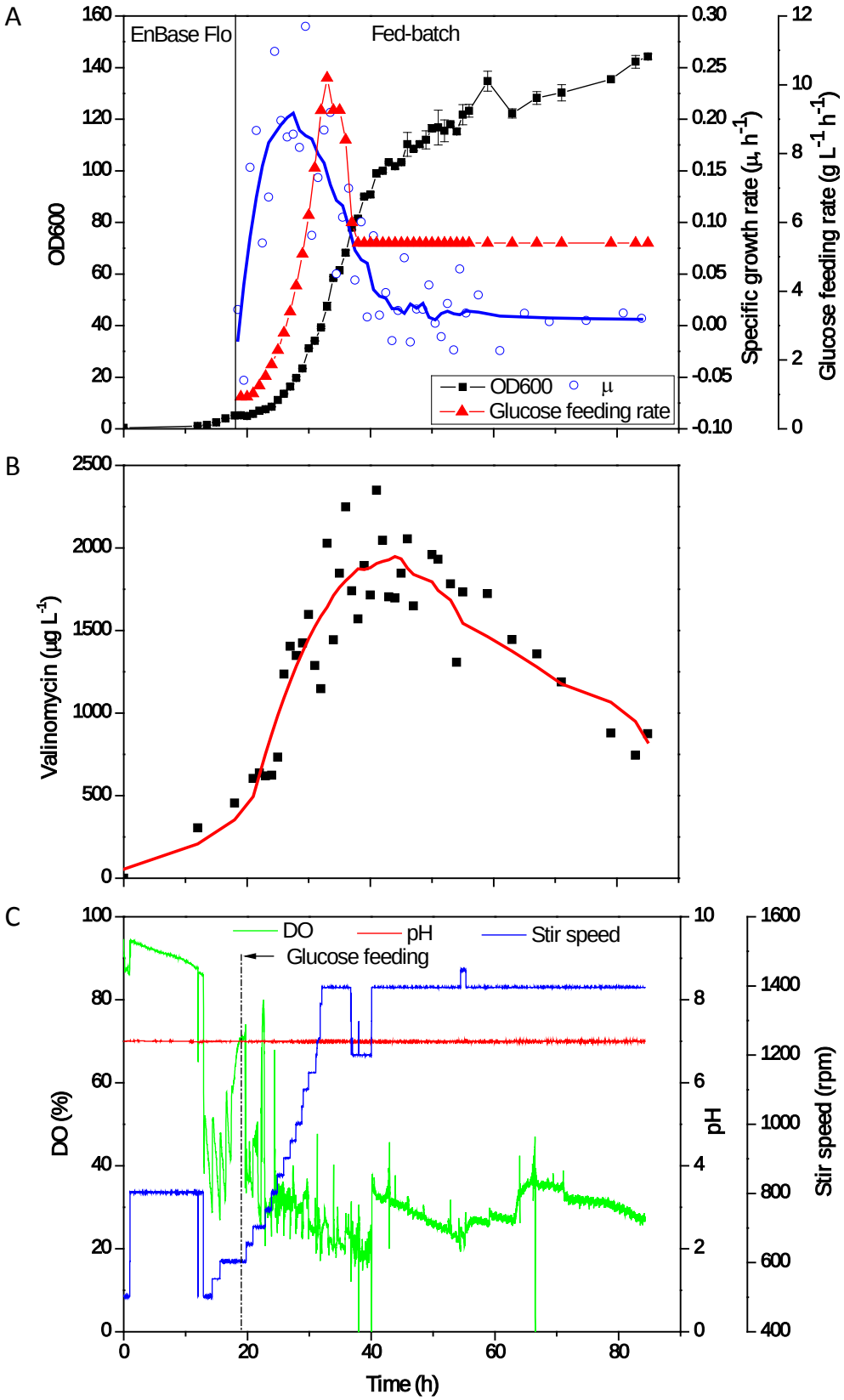

Figure 3.21 Fed-batch fermentation in the bioreactor for valinomycin production. (A) Cell growth curve, glucose feeding rate and specific growth rate. (B) Valinomycin titers. (C) Profile of online data.

Figure 3.21B shows valinomycin titers obtained from the high cell density fed-batch fermentation in the 3.7 L bioreactor. Valinomycin titers were measured every hour after starting of the glucose feeding. These yields scattered during the full fermentation, however, the trend of the titers was clear with an increase of the yield up to 2.4 mg L^{-1} after 41 h followed by a gradual decrease to around 0.9 mg L^{-1}. Unlike in the small-scale shake flasks (Figure 3.20), a high cell density cultivation in the large scale bioreactor did not further improve the valinomycin titer. The SDS-PAGE analysis indicated that Vlm1 was expressed to a high level throughout the whole fermentation, whereas Vlm2 was expressed only weakly (data not shown). The lower expression of Vlm2 is probably due to the plasmid instability within the cells, especially during the longer high cell density cultivation in large scale. Therefore, two plasmids with compatible *ori*s for Vlm1 and Vlm2 coexpression are necessarily needed in the large scale production.

3.8. Coexpression of VlmSyn and TEII for valinomycin production

3.8.1. Cloning and expression of TEII

To convert NRPS from its inactive apo-form to its active holo-form, all T domains of the NRPS need to be posttranslationally modified by a phosphopantetheinyl transferase (PPTase) (Walsh et al. 1997). This occurs by transferring a 4'-phosphopantetheine (4'-PP) moiety from coenzyme A (CoA) to a conserved serine residue in the T domains with the help of the PPTase (Lambalot et al. 1996). However, promiscuous PPTases use not only the dedicated natural substrate CoA, but also various acyl-CoA derivatives as 4'-PP donors (Quadri et al. 1998). In these cases, the acyl-4'-PP is tethered to T domains and the biosynthetic assembly line will be blocked resulting in an inactive NRPS. It was reported that, TEII, a discrete protein encoded by a gene within the NRPS gene cluster, could serve as a repair enzyme to regenerate misacylated thiol groups of 4'PP cofactors of the T domains and restore the activity of NRPS (Schwarzer et al. 2002). Reasonably, coexpression of TEII and picromycin/methymycin polyketide synthase or deoxyerythronolide B polyketide

synthase (DEBS) increased 4-7 times of the total polyketide level in the heterologous host *Streptomyces lividans*, and 2-fold of the 6-deoxyerythronolide B (6dEB) in the heterologous host *E. coli*, respectively (Pfeifer et al. 2002; Tang et al. 1999). Since TEII was also identified from the VlmSyn gene cluster (Cheng 2006), we thought to enhance valinomycin production through coexpression of VlmSyn and TEII in *E. coli*.

Genomic DNA was isolated from *S. tsusimaensis* ATCC 15141 and used as a template to amplify the TEII gene via gradient PCR (annealing temperature 55 °C±10 °C). The results indicated that complete chromosomal DNA of *S. tsusimaensis* was successfully isolated, even though a certain amount of DNA was degraded (Figure 3.22A), and the target TEII fragment (735 bp) was successfully amplified showing a correct band size on the agarose gel (Figure 3.22B). The purified PCR product was subsequently cloned into the expression vector pJL10 (see section 2.3.9).

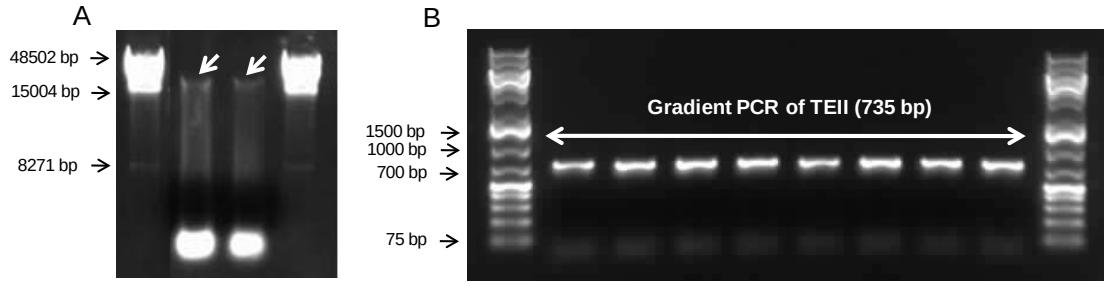

Figure 3.22 Agarose gel analysis of isolated *S. tsusimaensis* genomic DNA on a 0.5 % agarose gel (A) and gradient PCR amplified TEII fragment on a 1 % agarose gel (B).

To express TEII (27 kDa), the plasmid pJL10-TEII was transformed into *E. coli* BJJ01. The expression was initially tested by using TB medium with IPTG concentrations from 0 to 100 µM. As shown in Figure 3.23A, four cultivations had almost the same final OD_{600} values, suggesting IPTG had no impact on cell growth. With 20, 50 or 100 µM IPTG induction, TEII could be expressed in similar level, however, almost exclusively in insoluble form (Figure 3.23B). Clearly, TEII was also expressed without IPTG induction due to the leaky mutated *lac* promoter in plasmid pJL10 (see section 2.3.9). Although TEII was expressed mostly insoluble, some soluble TEII was confirmed by western blot immunodetection (data not shown). Our TEII expression results showed a similar tendency like some other TEIIs, which could only be

expressed poorly in soluble form in *E. coli* (Kotowska et al. 2009; Schwarzer et al. 2002).

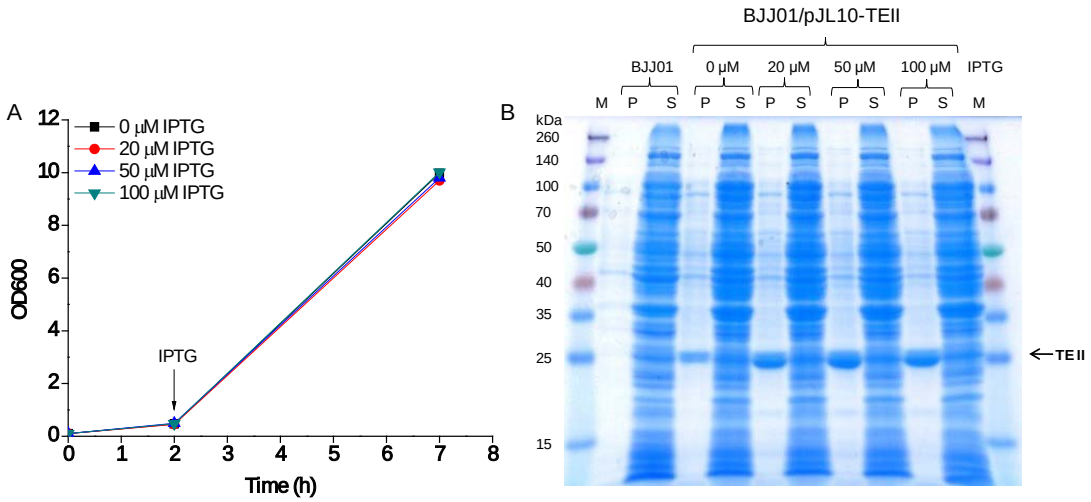

Figure 3.23 Growth curves of *E. coli* BJJ01/pJL10-TEII (A) and SDS-PAGE analysis of TEII expression (B) with different concentrations of IPTG. The cultivations were performed at 30 °C in TB medium. Cells were harvested 5 h after induction. Protein samples were separated on a 10 % polyacrylamide gel. BJJ01 is a negative control without TEII expression vector. TEII (27 kDa) is indicated by an arrow. P= insoluble protein; S= soluble protein; M= protein molecular weight marker.

Since EnBase medium could improve the yield and quality of recombinant proteins compared to TB medium (Krause et al. 2010; Ukkonen et al. 2011), we attempted to use the EnBase cultivation system to increase the expression of soluble TEII. Cells were grown in 50 mL EnBase Flo and EnPresso at 30 °C and 200 rpm. After overnight cultivation, the cultures were boosted by addition of nutrient additives and TEII expression was induced with 20 µM or without IPTG, followed by further 24 h incubation. The results clearly indicated that IPTG has no influence on cell growth neither in Flo nor in EnPresso medium (Figure 3.24A). Figure 3.24B shows the expression levels of TEII in EnBase cultivations. Total expression yields were significantly increased in EnBase medium compared to TB cultivations. However, the quality was not improved as indicated by the soluble TEII fractions. Without IPTG induction, TEII was expressed similarly to TB medium.

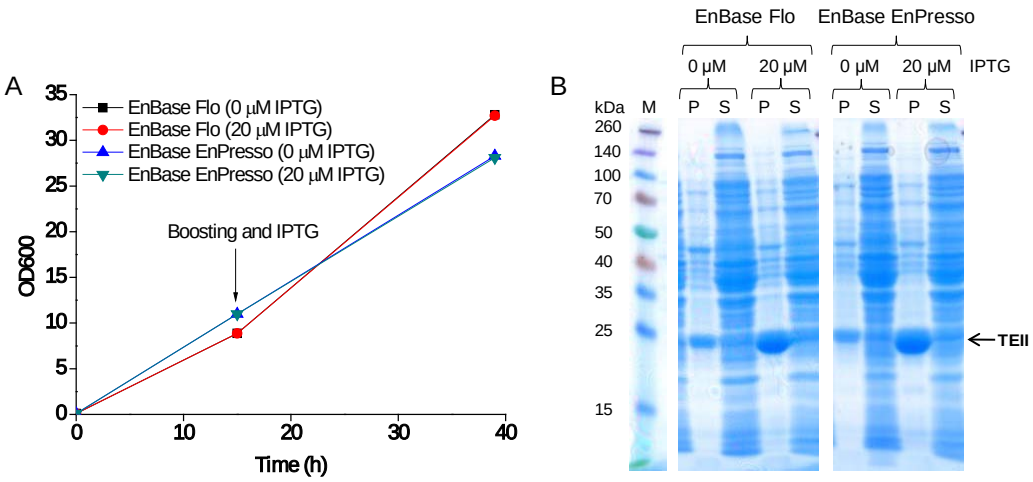

Figure 3.24 Growth curves of *E. coli* BJJ01/pJL10-TEII (A) and SDS-PAGE analysis of TEII expression (B) using EnBase media. The cultivations were performed at 30 °C in Flo and EnPresso medium. Cells were harvested 24 h after boosting and induction. Protein samples were separated on a 10 % polyacrylamide gel. TEII (27 kDa) is indicated by an arrow. P= insoluble protein; S= soluble protein; M= protein molecular weight marker.

3.8.2. Coexpression of VlmSyn and TEII

Although most TEII was expressed in insoluble form, pJL10-TEII was transformed into BJJ01/pCTUT7-Vlm1+pKS01-Vlm2 to achieve coexpression of the three proteins (Vlm1, Vlm2 and TEII) from a separate expression plasmid each. The cultivations were carried out in EnBase EnPresso medium without IPTG induction. As can be seen in Figure 3.25A, BJJ01/pCTUT7-Vlm1+pKS01-Vlm2+pJL10-TEII only reached an OD_{600} of ~2 after overnight cultivation, which was 3-fold lower than BJJ01/pCTUT7-Vlm1+ pKS01-Vlm2. However, after boosting, BJJ01/pCTUT7-Vlm1+pKS01-Vlm2+pJL10-TEII grew faster reaching a final OD_{600} of 24 compared to the control (BJJ01/pCTUT7-Vlm1+pKS01-Vlm2) with a final OD_{600} of 16. SDS-PAGE analysis revealed that, when VlmSyn (Vlm1+Vlm2) and TEII were coexpressed, Vlm1 and TEII were mostly formed insoluble, while Vlm2 was not expressed at all (Figure 3.25B). This could be explained by the VlmSyn expression vectors, pCTUT7 and pKS01, which carry the same pBR322 *ori* making them instable upon coexpression from a third expression vector pJL10 (RSF *ori*) due to the increased metabolic load. Therefore, pKS01-Vlm2 was probably lost during the cultivation, lowering the metabolic burden as indicated by the faster growth rate after boosting (Figure 3.25A).

To circumvent expression vector loss, we transformed pJL10-TEII into BJJ01/pJL03-Vlm1+pJL07-Vlm2. These three plasmids could coexist stably in a single cell, since they have compatible *ori*s, p15A (pJL03), pBR322 (pJL07) and RSF (pJL10) (Tolia and Joshua-Tor 2006). In EnBase EnPresso cultivations without IPTG induction, BJJ01/pJL03-Vlm1+pJL07-Vlm2 and BJJ01/pJL03-Vlm1+pJL07-Vlm2+pJL10-TEII showed similar growth curves (Figure 3.25A). OD_{600} in the latter culture was slightly lower than that in the former culture due to the third protein TEII being coexpressed with VlmSyn. The SDS-PAGE analysis showed that both Vlm1 and Vlm2 are expressed in soluble form, while interestingly, no obvious TEII band could be observed on the gel even in the insoluble fraction (Figure 3.25B). The reason for this remains unclear at present.

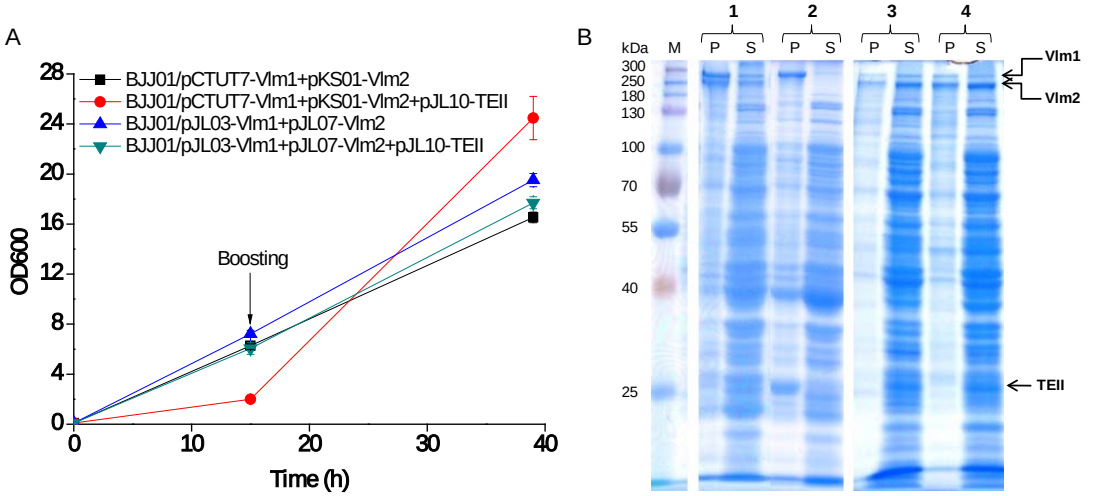

Figure 3.25 Growth curves (A) and SDS-PAGE (B) of VlmSyn and TEII coexpression. The cultivations were performed at 30 °C in EnPresso medium. Cells were harvested 24 h after boosting. Protein samples were separated on a 10 % polyacrylamide gel. 1, BJJ01/pCTUT7-Vlm1+pKS01-Vlm2; 2, BJJ01/pCTUT7-Vlm1+pKS01-Vlm2+pJL10-TEII; 3, BJJ01/pJL03-Vlm1+pJL07-Vlm2; 4, BJJ01/pJL03-Vlm1+pJL07-Vlm2+pJL10-TEII. Vlm1 (370 kDa), Vlm2 (284 kDa) and TEII (27 kDa) are indicated by arrows. P= insoluble protein; S= soluble protein; M= protein molecular weight marker.

3.8.3. Improvement of valinomycin productivity with TEII coexpression

Valinomycin production using BJJ01/pJL03-Vlm1+pJL07-Vlm2+pJL10-TEII was carried out in EnBase Flo and EnPresso media. For comparison, BJJ01/pCTUT7-Vlm1+pKS01-Vlm2 and BJJ01/pJL03-Vlm1+pJL07-Vlm2 were cultivated. After overnight cultivation,

nutrient additives were added to the cultures for boosting. No IPTG was used to induce VlmSyn or TEII expression. In EnBase Flo, BJJ01/pJL03-Vlm1+pJL07-Vlm2+ pJL10-TEII reached the highest OD_{600} value of 27 and the other two strains showed a similar final OD_{600} value of 20 (Figure 3.26A). By contrast, in EnPresso, the highest OD_{600} of 25 was found in BJJ01/pJL03-Vlm1+pJL07-Vlm2, which is higher than that of 20 obtained with the other two strains (Figure 3.26B).

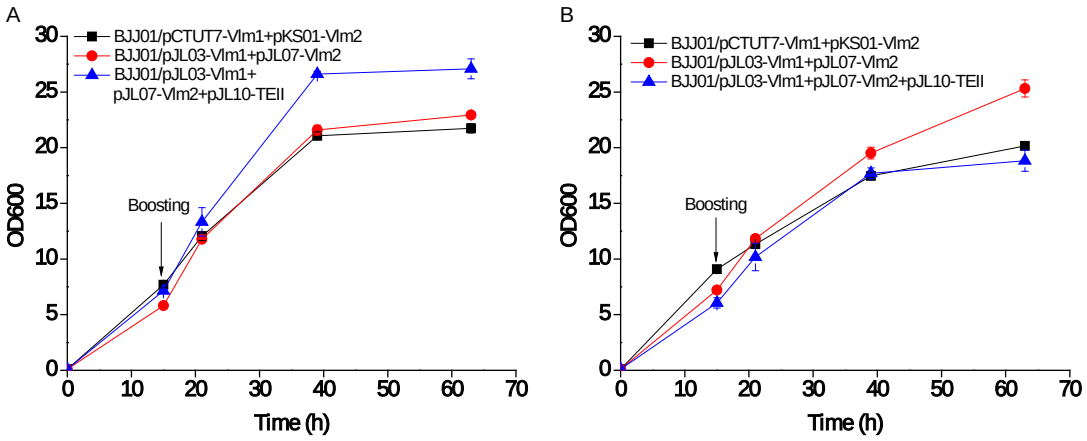

Figure 3.26 Growth curves of BJJ01/pCTUT7-Vlm1+pKS01-Vlm2, BJJ01/pJL03-Vlm1+pJL07-Vlm2 and BJJ01/pJL03-Vlm1+pJL07-Vlm2+pJL10-TEII in EnBase Flo (A) and EnPresso (B) media.

At the end of the cultivation, valinomycin was extracted and quantified. Figure 3.27 shows valinomycin titers from the cultures. In EnPresso cultures, TEII coexpression remarkably enhanced valinomycin titer up to 3.3 mg L^{-1}, which is >6.5-fold greater than that obtained in the control BJJ01/pJL03-Vlm1+pJL07-Vlm2 (0.5 mg L^{-1}) and an approximately 2-fold increase compared to BJJ01/pCTUT7-Vlm1+pKS01-Vlm2. Similar trend of the titers was also observed in EnBase Flo cultivations. Therefore, TEII coexpression could significantly improve valinomycin titers, even though soluble TEII was not readily visible on the SDS-PAGE gel (Figure 3.25B).

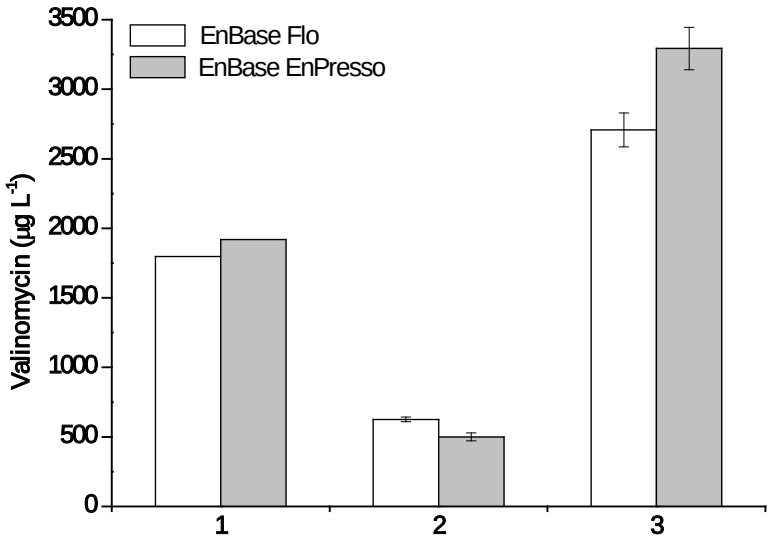

Figure 3.27 Valinomycin titers of BJJ01/pCTUT7-Vlm1+pKS01-Vlm2 (1), BJJ01/pJL03-Vlm1+pJL07-Vlm2 (2), and BJJ01/pJL03-Vlm1+pJL07-Vlm2+pJL10-TEII (3) cultivated in EnBase Flo and EnPresso media.

Glucose polymer feeding for valinomycin production was also performed with the strain BJJ01/pJL03-Vlm1+pJL07-Vlm2+pJL10-TEII. The online data of oxygen and pH are shown in Figure 3.28A and B, which were similar as described in section 3.6.2. The cell density was significantly increased with twice polymer feeding, reaching a final OD_{600} of 55 (Figure 3.28C), which is the same value as obtained with the strain BJJ01/pCTUT7-Vlm1+pKS01-Vlm2 (Figure 3.20C). The final volumetric valinomycin titer was dramatically enhanced to 13 mg L^{-1} (Figure 3.28D), which represents a 43-fold increase compared to the initial TB batch production. With twice polymer feeding both strains reached the same OD_{600} of 55 (Figures 3.20C and 3.28C), while the specific valinomycin titer of BJJ01/pJL03-Vlm1+pJL07-Vlm2+pJL10-TEII was 1.3-fold higher than BJJ01/pCTUT7-Vlm1+pKS01-Vlm2, further demonstrating the positive role TEII plays during valinomycin production *in vivo*.

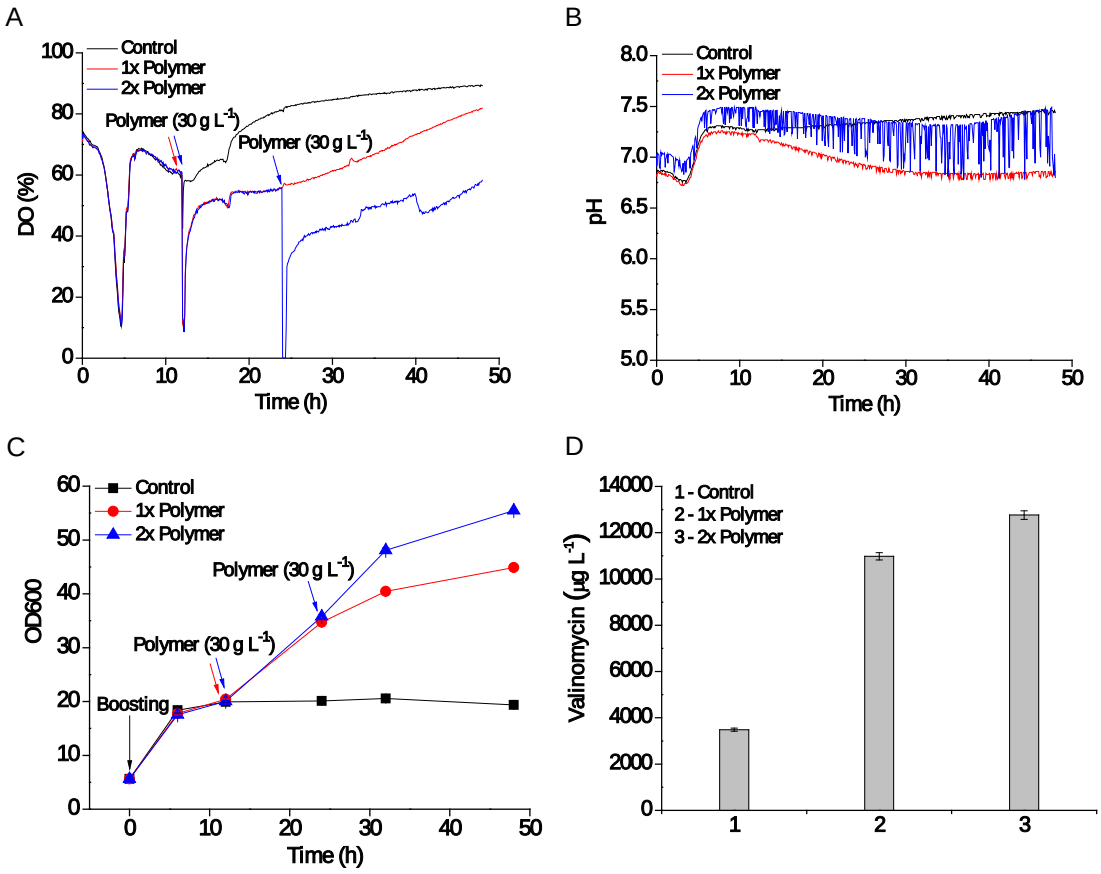

Figure 3.28 Glucose polymer feeding for valinomycin production with the strain BJJ01/pJL03-Vlm1+ pJL07-Vlm2+pJL10-TEII: online measurement of oxygen (A) and pH (B), cell growth curves (C) and valinomycin titers (D). The cultivations were performed at 30 °C in EnBase Flo medium with enzyme concentration of 9 U L^{-1}. The culture volume in each PreSens shake flask (125 mL) was 12.5 mL.

3.9. Effect of oscillating conditions for valinomycin production in a scale-down TCR

The availability of biosynthetic precursors for reconstituted biosynthesis of natural products in the heterologous host *E. coli* is a main issue that has to be resolved. Valinomycin synthetase utilizes three precursors (pyruvate, α-ketoisovalerate and L-valine) for valinomycin biosynthesis (Jaitzig 2013; Magarvey et al. 2006), which are also native metabolites of *E. coli* involved in the branched chain amino acid metabolic pathway of L-valine (Figure 4.1). Therefore, it is not necessary to feed precursors during the cultivation or engineer *E. coli* metabolic pathways to provide precursors for complete biosynthesis. We assume that valinomycin yield may be increased by improvement of the precursors in *E. coli* through bioprocess engineering. A previous

study indicated that pyruvate and L-valine can be significantly accumulated in *E. coli* after a downshift of oxygen at a high glucose concentration in a bioreactor fed-batch fermentation (Soini et al. 2008). This means under anaerobic and high glucose conditions the flux through the metabolic pathway from pyruvate to L-valine, which contains the three precursors of valinomycin, was enhanced. To simulate these conditions, we used a scale-down two-compartment reactor (TCR, see Appendix 6.4) for valinomycin production. This TCR system allows continuous circulation of the culture between a stirred tank reactor (STR) and a plug flow reactor (PFR), generating the oscillating fermentation conditions with high glucose and oxygen limitation for a short time (e.g., 1 min) in the PFR (Enfors et al. 2001; Neubauer and Junne 2010).

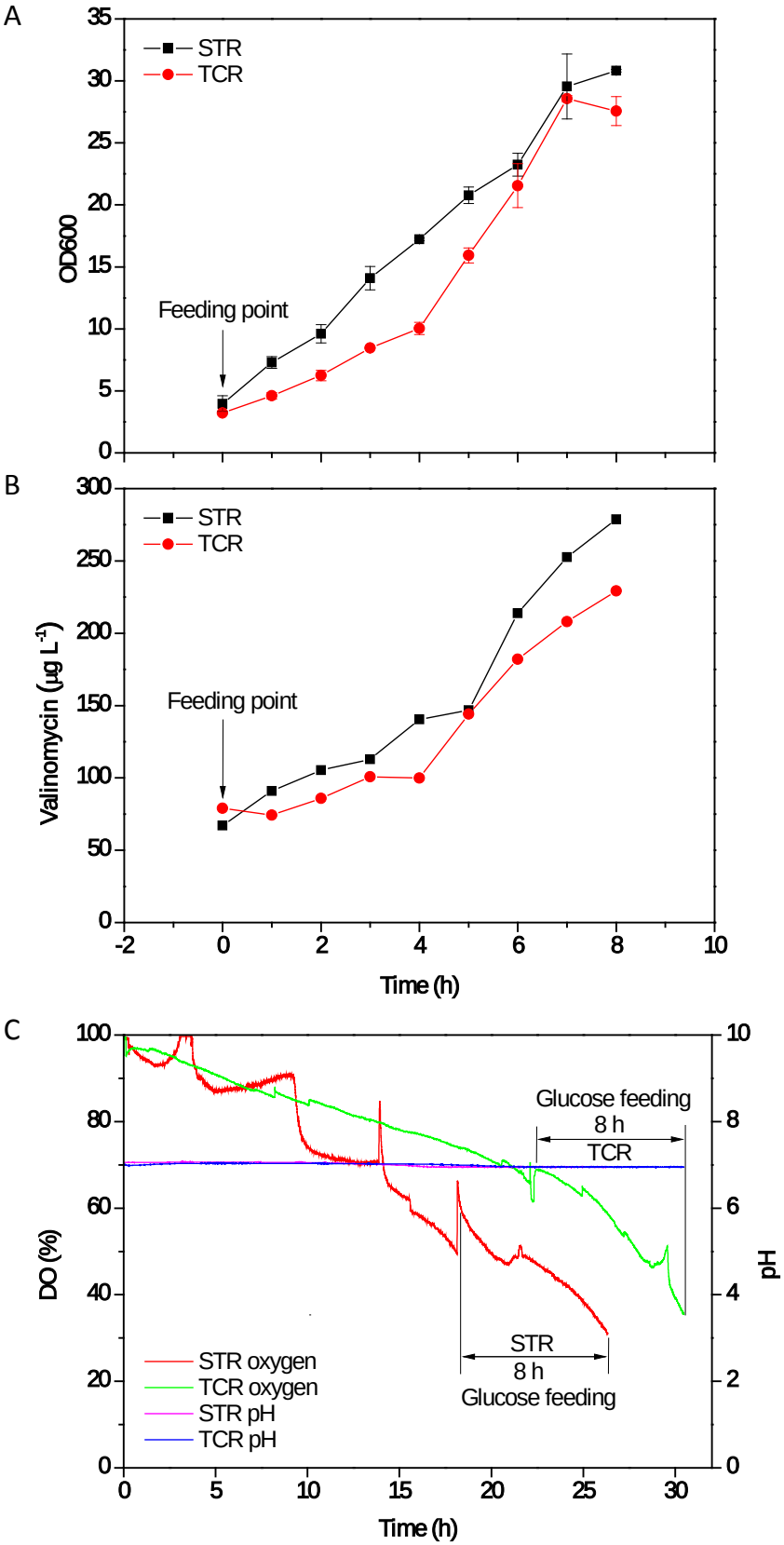

Figure 3.29 Valinomycin production under oscillating conditions in a scale-down two-compartment reactor. (A) Cell growth curves. (B) Valinomycin titers. (C) Profile of online oxygen and pH.

Figure 3.29 shows valinomycin production with the strain BJJ01/pJL03-Vlm1+pJL07-Vlm2+pJL10-TEII under oscillating conditions in the scale-down TCR (STR+PFR). The fermentation in the STR without PFR was performed as a reference. In both the STR and the TCR fermentation, glucose feeding was initiated when the oxygen increased (Figure 3.29C) at an OD_{600} of ~4 (Figure 3.29A). In the STR, glucose was directly fed into the bioreactor, while in the TCR glucose was fed at the inlet of the PFR (see Appendix 6.4), forming an anaerobic and high glucose growth environment. The feeding process was continued for 8 h and the samples were drawn from the STR each hour for the analysis. It is clear that OD_{600} values in the STR fermentation were always higher than in the TCR fermentation even though the OD_{600} values were similar at the starting point of glucose feeding (Figure 3.29A). This is because the anaerobic condition inhibits the cell growth, which is also found in other oxygen downshift fermentations (Soini et al. 2008). Likewise, the volumetric valinomycin titers in the TCR fed-batch fermentation were also lower than the reference (Figure 3.29B). The specific valinomycin titers were similar in both the STR and the TCR fermentation (data not shown). Although pyruvate and L-valine, precursors of valinomycin, can be increased under oxygen limitation and high glucose conditions (Soini et al. 2008), there is no obvious impact on valinomycin production. The reason remains unknown at present. Further work should be carried out to investigate whether the residence time of the culture in the PFR is sufficient for the cells to respond the oscillating conditions and accumulate pyruvate and L-valine. In addition, the expression level and quality of valinomycin synthetase at oscillating conditions should be also investigated since the biosynthetic enzymes and the precursors are the essential elements for heterologous biosynthesis of valinomycin in *E. coli*.

4. Discussion

4.1. Coexpression of Vlm1 and Vlm2 in *E. coli*

Valinomycin synthetase is a heterodimeric protein containing two large NRPSs, Vlm1 (370 kDa) and Vlm2 (284 kDa). In order to reconstitute the valinomycin biosynthetic pathway and realize valinomycin production in *E. coli*, the first and foremost prerequisite is active coexpression of Vlm1 and Vlm2 in the host strain. We first screened the expression vectors from an expression library and found that the pCTUT7 vector with an N-terminal 6xHis-tag is more suitable for expression of single Vlm1 or Vlm2 (Jaitzig 2013). To coexpress Vlm1 and Vlm2, a second vector pKS01 was used to express Vlm2, which is modified from pCTUT7 through replacing chloramphenicol (cmR) selective marker by ampicillin (ampR) resistance cassette and incorporating the plasmid stabilizing *parB* locus (Gerdes 1988). However, both expression vectors, pCTUT7-Vlm1 and pKS01-Vlm2, have the same origin of replication (*ori*) pBR322 (Figure 3.1). Although two incompatible plasmids carrying the same *ori* can also be stabilized by different antibiotic resistance markers (Yang et al. 2001), it can lead to plasmid instability and loss within the cells, especially during the longer high cell density cultivations in large scale (Tolia and Joshua-Tor 2006). This phenomenon of plasmid instability could be observed in our 3.7 L bioreactor under high cell density fermentation conditions even though pCTUT7-Vlm1 and pKS01-Vlm2 were both maintained well during small scale cultivations. The SDS-PAGE analysis suggested that Vlm1 was expressed to a high level throughout the whole bioreactor fermentation, whereas Vlm2 was only weakly expressed (data not shown). To alleviate the plasmid instability, two series of compatible plasmids were constructed with compatible *ori*s for coexpression of Vlm1 and Vlm2 (Table 3.1). The plasmids carrying p15A *ori* (copy number 10-12) were created for expression of Vlm1, while the ones with pBR322 *ori* plus *rop* gene (copy number 15-20) were designed to express Vlm2. Overall, the copy number of Vlm2 expression plasmids is a bit higher than that of Vlm1, which led to higher expression levels of Vlm2 than those of Vlm1 (Figure 3.6). This could even be beneficial to valinomycin formation, since Vlm2

carries the C-terminal thioesterase (TE) domain, which catalyzes the rate-limiting oligomerization and circularization during valinomycin biosynthesis. In a bimodular NRPS (TycA and TycB1) model system, increase of the ratio between the terminal module TycB1 and the first module TycA could obviously improve the final product yields *in vitro* and *in vivo*, suggesting that the protein-protein interaction between NRPSs is actually a dynamic process of fast association and disassociation rather than a commonly regarded rigid assembly line (Gruenewald et al. 2004). However, in our system, the original dual expression plasmids pCTUT7-Vlm1 and pKS01-Vlm2 generated the highest valinomycin yield compared to the other compatible plasmid combinations (Figure 3.9). This is probably because the overall expression level of VlmSyn was higher with pCTUT7-Vlm1 and pKS01-Vlm2 compared to the new constructed plasmids which have ~3 to 5-fold lower copy numbers. Therefore, the plasmid combination of pCTUT7-Vlm1 and pKS01-Vlm2 has mainly been used in this work for the investigation of valinomycin production.

Often, a strong transcriptional promoter (e.g., T7 promoter) is used for a high level of gene expression. However, to produce the sizable complex NRPSs, a strongly induced expression should be avoided since the large proteins need to be translated and folded slowly in the cells. In our expression system, a relative weak and leaky promoter pCTUT7 was used, which is derived from the wild type *lac* promoter (Kraft et al. 2007). This system could produce high levels of VlmSyn in soluble form with a very low concentration of the inducer IPTG (20 µM) or even without IPTG induction (Jaitzig 2013), which allows protein expression at a slower rate and better protein folding. No IPTG needed for induction in the cultivation would be very economical in large scale production. Similar results were also observed during the expression of other large multimodular enzyme complexes. The solubility and total expression levels of epothilone NRPS/PKS (~2 MDa) could be significantly improved when expression with the somewhat weak arabinose-induced pBAD promoter instead of the strong T7 promoter system (Mutka et al. 2006). Similarly, the first two modules of the tyrocidine NRPS, TycA and TycB1 (242 kDa), could be coexpressed from weak and

leaky promoters yielding relatively high levels of proteins without IPTG induction (Gruenewald et al. 2004).

The choice and positioning of fusion tags on VlmSyn expression was also investigated under consideration of the following aspects. If Vlm1 and Vlm2 were expressed with different affinity tags, they could be purified separately avoiding heterogeneity of the purified proteins. In addition, expression levels of Vlm1 or Vlm2 could be quantified separately by enzyme-linked immunosorbent assay (ELISA) even from crude cell lysates of coexpressed cultures. Moreover, the tag for Vlm2 was moved to its C-terminus leaving its N-terminus free to interact with the C-terminus of Vlm1, in order to not disturb the protein-protein interactions and enhance stability of the heterodimeric VlmSyn complex. Therefore, two small tags, 6xHis tag and Strep tag (8 amino acids: Trp-Ser-His-Pro-Gln-Phe-Glu-Lys), were fused to Vlm1 or Vlm2 (Table 3.1). However, our data indicated that N-/C-terminal Strep tag significantly reduces the expression levels of Vlm1 (Figure 3.4). We assume the reason might be that the secondary 5’ mRNA structures are changed due to the alteration of N-terminal base pairs making a different efficiency of protein translation (Szeker et al. 2011). While Vlm2 expression levels with N-/C-terminal 6xHis tag with the new vector constructs were similar (Figure 3.4), even though somewhat lower than the original vector pKS01-Vlm2 probably due to the lower plasmid copy numbers.

Low temperature favoring slower expression rates has previously been shown to increase soluble expression yields of large NRPS and PKS proteins in *E. coli* (Mutka et al. 2006; Pfeifer et al. 2001; Pfeifer et al. 2003). We also tested different expression temperatures on VlmSyn expression. The results revealed that expression at 20 °C could slightly increase the soluble VlmSyn yields but significantly reduced the final cell biomass compared to expression at 30 °C (data not shown). Therefore, 30 °C was used in this study for both VlmSyn expression and valinomycin production.

4.2. Usability of *E. coli* for valinomycin production

In order to utilize *E. coli* as a vehicle to produce bioactive antibiotics, the primary consideration would be the need for a resistance mechanism to protect the host cells from toxicity of the generated compounds. If the produced compound was toxic for *E. coli*, it would be essential to coexpress the self-resistance genes that usually exist within the native antibiotic gene clusters (Peirú et al. 2005; Watanabe et al. 2006; Zhang et al. 2010b). In terms of the valinomycin biosynthetic gene cluster from the native producer *S. tsusimaensis* ATCC 15141, no gene was deduced to play a self-resistance function (Cheng 2006; Jaitzig 2013). Therefore, it is necessary to test the toxicity of valinomycin on *E. coli* as a heterologous production host. An inhibiting effect on *E. coli* cell growth was evaluated from both externally and internally applied valinomycin. The results indicated that addition of valinomycin ranging from 10 to 100 mg L^{-1} to the culture has no growth inhibiting effect on the cells (see section 3.2.1). The possible reason is that *E. coli* is a Gram-negative bacterium which has two membranes and the outer membrane can prevent access of valinomycin to inside of the cell (Ryabova et al. 1975; Tempelaars et al. 2011). To our surprise, valinomycin formed within the cells did not obviously inhibit cell growth even though no resistance gene was coexpressed (Figure 3.8). The reduced cell density compared to the plasmid-free control strain is mainly due to the metabolic burden of the expression of the large VlmSyn rather than intracellular formed valinomycin. The reason why valinomycin does not depolarize the cell membrane potential of the inner membrane resulting in cell death is not clear. Further investigation could be carried out using flow cytometry to monitor and clarify the changes of the membrane potential of the growing cells. The results of the resistance assay suggest that *E. coli* can tolerate external and internal valinomycin and thus has the potential as a heterologous host for valinomycin overproduction.

For the reconstituted natural product biosynthesis in *E. coli*, another major issue needs to be addressed: the availability of biosynthetic precursors. Since the *E. coli* metabolic pathways and therefore the resulting metabolites may differ from the

native producer strains, indispensable precursors might be lacking in the *E. coli* metabolites pool. In that case they have to be supplied for the biosynthesis through basically two ways, either exogenous feeding or engineering of *E. coli* metabolic pathways to afford precursors (Murli et al. 2003; Pfeifer et al. 2001; Pfeifer et al. 2003; Zhang et al. 2010b). The precursors of valinomycin biosynthesis were proposed to be L-valine, D-α-hydroxyisovaleric acid, L-threonine, L-alanine and lactic acid in earlier studies with no consensus from different researches (Anke and Lipmann 1977; MacDonald 1960; MacDonald and Slater 1968; Ristow et al. 1974). In 2006, the valinomycin gene cluster was cloned and sequenced, and a four modular NRPS VlmSyn was rationally proposed (Cheng 2006; Magarvey et al. 2006). Based on the VlmSyn model, the three precursors of valinomycin were deduced to be pyruvate, α-ketoisovalerate and L-valine (Magarvey et al. 2006), which were confirmed experimentally with purified VlmSyn (Jaitzig 2013). Fortunately, the three precursors are native metabolites of *E. coli* involved in the branched chain amino acid metabolic pathway of L-valine (Figure 4.1). This confers *E. coli* as a suitable surrogate host to produce valinomycin without precursor feeding or further pathway engineering.

In the present study, the highest valinomycin titer reached 13 mg L^{-1} in *E. coli*, which is comparable to the productivity of several native *Streptomyces* producers (Table 1.3) (Matter et al. 2009). Therefore, *E. coli* is a competitive host compared to the native valinomycin producers since (i) *E. coli* needs much shorter cultivation times (2 d) compared to *Streptomyces* strains (6 d) to reach similar titers, (ii) *E. coli* needs simple carbon and nitrogen sources, and mild cultivation conditions, (iii) *E. coli* displays rapid growth rates, and (iv) *E. coli* cultivations can be easily scaled up to high cell densities in a large bioreactor. These advantages of *E. coli* will pave the way for developing an economical and feasible platform for valinomycin mass production.

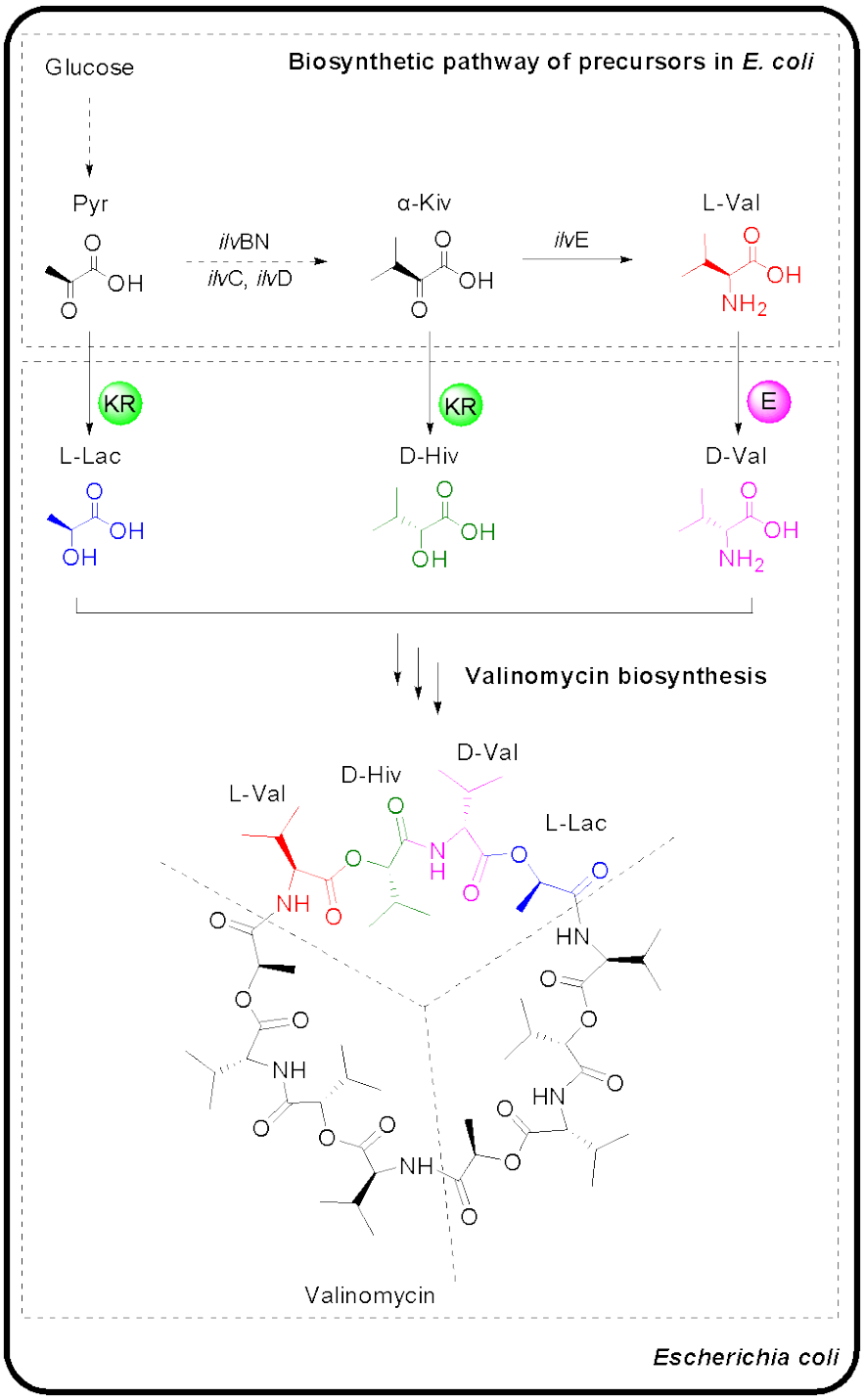

Figure 4.1 The biosynthetic pathway of valinomycin in the host *E. coli*. KR, ketoreductase; E, epimerase; *ilvBN*, acetohydroxy acid synthase I; *ilvC*, acetohydroxy acid isomeroreductase; *ilvD*, dihydroxy acid dehydratase; *ilvE*, branched chain amino acid aminotransferase, Pyr, pyruvate; L-Lac, lactate; α-Kiv, α-ketoisovalerate; D-Hiv, D-hydroxyisovalerate; L-Val, L-valine; D-Val, D-valine.

4.3. Enhancement of valinomycin production through small-scale high cell density fed-batch cultivation

The main aim of this work was to enhance valinomycin production through bioprocess optimization. Initially, batch and fed-batch type of cultivations were employed to produce valinomycin in shake flasks for comparison. For batch cultivation, the typical rich TB medium was used. For fed-batch production, the enzyme-based glucose delivery EnBase cultivation system was employed, which provides a controlled growth environment and optional nutrients for high cell density cultivation and consequently high biomolecules production. This fed-batch-like system has been reported to effectively improve expression yields of small recombinant proteins (<50 kDa) including alcohol dehydrogenase (Krause et al. 2010; Ukkonen et al. 2011), eukaryotic ribonuclease inhibitor (Šiurkus et al. 2010), and thermostable purine nucleoside phosphorylase (Zhou et al. 2013). In this work, we could show that this system can also be used to produce the large dimeric protein, valinomycin synthetase (654 kDa), and even the resultant antibiotic product valinomycin. During the whole cultivation process, a stable pH level around 7.0 without any external control was maintained (Figure 3.15), whereas in TB batch cultivation the pH gradually increased from initially 7.0 to 8.5, which exceeds the optimal pH range of *E. coli* growth (data not shown). This finding is in agreement with a previous report, suggesting EnBase medium is a good self-buffered system to cultivate *E. coli* cells with different kinds of recombinant proteins (Krause et al. 2010).

Interestingly, valinomycin was notably accumulated within the exponential growth phase in TB batch cultivations, accounting for 75 % of the total yield (Figure 3.10). In contrast, in EnBase fed-batch type cultivations, valinomycin was mainly produced in the growth limiting phase after nutrients boosting (Figures 3.11 and 3.15). We assume the difference can be attributed to the different cultivation modes. In the TB batch mode, we add IPTG to induce the expression of Vlm1 and Vlm2 at the mid-exponential growth phase (~3 h after inoculation) resulting in valinomycin

biosynthesis. Afterwards, more and more nutrients are consumed by the cells and they have to use the remaining nutrients to support their own metabolism maintenance rather than heterologous proteins synthesis and valinomycin formation. In addition, the large enzymes might lose catalytic activity due to denaturation and formation of insoluble aggregates in an unsuitable intracellular physiological environment. In the EnBase fed-batch mode, firstly, Vlm1 and Vlm2 can be expressed in high yields without IPTG induction due to leaky expression (data not shown). The boosting additives contain a lot of complex molecules that may gently induce the protein expression avoiding the formation of more insoluble aggregates. Secondly, nutrients boosting could rapidly promote cells to high densities followed by the glucose limitation phase where cells obtain their energy mainly from the released glucose and more nutrients (e.g., amino acids) are available. Therefore, *E. coli* cells have enough energy not only to cover their maintenance requirements, but also for valinomycin biosynthesis during the longer fed-batch process.

According to the DoE results, we could show that nutrients boosting has a significantly positive effect on valinomycin yield (Table 3.2). Although *E. coli* cells can also grow up to high cell density without nutrients boosting, valinomycin yields were much lower without boosting. The boosting effect might be related to the supply of amino acids, vitamins and cofactors to support efficient protein expression and provide additional precursors (e.g., L-valine) for valinomycin biosynthesis. Thus the following discussion is just based on the boosting group. In EnBase, the glucose feeding rate depends on the enzyme concentration. Within the tested range (0 to 6 U L^{-1}), a higher enzyme concentration gave rise to a higher valinomycin titer, but not a higher cell density. When the enzyme concentrations were increased from 1.5 to 9 U L^{-1}, the specific valinomycin yields were improved approximately two fold. This suggests that *E. coli* cells only need a certain amount of glucose for self-maintenance during the production phase. If more glucose is released by more enzyme (still at limiting concentrations), these glucose will enter into the branched chain amino acids metabolic pathway and highlight the L-valine synthesis route where pyruvate and

α-ketoisovalerate, the other two precursors in the valinomycin biosynthesis, are also involved (Figure 4.1). Consequently, more enzyme leads to more precursors for valinomycin formation. However, if the enzyme concentration is higher than 9 U L^{-1}, cell growth is strongly inhibited leading to a 3 and 16 times decrease in cell density and valinomycin titer, respectively (Figures 3.18 and 3.19). A possible explanation would be that high enzyme concentration causes glucose overfeeding, which results in the by-product acetic acid accumulation and medium acidification impairing the cultivation and the recombinant proteins production (Han et al. 1992; Jensen and Carlsen 1990; Kleman and Strohl 1994). In addition, compared to the batch cultivation, glucose polymer feeding dramatically improved the volumetric (33-fold) and even specific (5.2-fold) yields of valinomycin, probably due to a higher flux of glucose into the precursors metabolic pathways. Last but not least, for a high valinomycin yield it is very important to maintain aerobic conditions during the whole cultivation. Thus a maximum oxygen transfer rate is proposed. In our case lower culture volume allowed a better oxygen supply and thus contributed to higher cell density and valinomycin titers (Figure 3.14).

In this study, we could show that small-scale fed-batch cultivations can easily reach high cell densities and significantly improve valinomycin titers up to mg per liter levels compared to the low levels (µg per liter) obtained in batch cultivations. Moreover, the reliable optimization processes for enhanced valinomycin production could offer a reasonable route for the production of other complex natural products in *E. coli*.

4.4. Function of TEII on valinomycin improvement

Type II thioesterase (TEII) is a repair enzyme that usually exists in the NRPS gene cluster being responsible for regeneration of the functionality of NRPS through either hydrolysis of the misacylated thiol groups or incorrectly loaded monomers (Figure 1.13) (Schwarzer et al. 2002; Yeh et al. 2004). Deletion of TEII-encoding gene from the gene cluster can lead to a drastic reduction of the product yield in the wild-type producer (Zhou et al. 2008). On the contrary, coexpression of TEII and the relevant gene clusters in a heterologous host increases several folds of the final product yield (Pfeifer et al. 2002; Pfeifer et al. 2003; Tang et al. 1999). Such discrete TEII gene fragment was also identified from upstream of the VlmSyn gene cluster (Cheng 2006), and therefore, we thought to enhance valinomycin production via coexpression of TEII and VlmSyn in the heterologous host *E. coli*.

TEII was cloned into an expression vector carrying a RSF *ori* and transformed into the strain *E. coli* BJJ01. Initially, TEII was singly expressed using TB medium. With IPTG induction from 20 to 100 µM, TEII could be expressed in a similar level, whereas almost in insoluble form (Figure 3.23B). TEII was also expressed to a relative high level without IPTG induction since a leaky promoter was used in the plasmid (Figure 3.23B). Although TEII was mainly expressed in insoluble form, less soluble TEII was confirmed by western blot detection (data not shown). In order to improve the expression level of soluble TEII, we used the EnBase cultivation system which could improve the yield and quality of recombinant proteins compared to TB medium (Krause et al. 2010; Ukkonen et al. 2011). With EnBase medium, the total expression yields of TEII were significantly increased compared to TB cultivations, however, the soluble TEII was not improved (Figure 3.24B). Our TEII expression results showed a similar phenomenon to some other TEIIs, which could also be expressed in soluble form in *E. coli*, whereas with a very lower yield (Kotowska et al. 2009; Schwarzer et al. 2002).

Although TEII only can be expressed in very less soluble form, it was coexpressed with VlmSyn to investigate valinomycin production. When TEII was expressed in the strain BJJ01/pCTUT7-Vlm1+pKS01-Vlm2, almost no valinomycin was produced (data not shown). SDS-PAGE analysis revealed that when the three proteins were expressed together in one cell, Vlm2 was not expressed at all, while Vlm1 and TEII were expressed mainly in insoluble form (Figure 3.25B). This can be explained by the incompatible VlmSyn expression plasmids that pCTUT7 and pKS01 carry the same pBR322 *ori* making them cannot coexistence with a third TEII expression vector with RSF *ori*. To overcome the problem of plasmid instability and loss, pJL10-TEII was transformed into the strain BJJ01/pJL03-Vlm1+pJL07-Vlm2. These three plasmids have compatible *ori*s p15A (pJL03), pBR322 (pJL07) and RSF (pJL10), and thus could stably coexist in a single cell. Interestingly, SDS-PAGE gel indicated that Vlm1 and Vlm2 were expressed mostly in soluble form, while no obvious TEII band can be observed on the gel even in the insoluble fraction (Figure 3.25B). Nevertheless, TEII coexpression with pJL03-Vlm1 and pJL07-Vlm2 remarkably enhanced volumetric valinomycin titer up to 3.3 mg L^{-1}, which is >6.5-fold higher than that obtained in the control BJJ01/pJL03-Vlm1+pJL07-Vlm2 (0.5 mg L^{-1}) and an approximately two-fold increase compared to the strain BJJ01/pCTUT7-Vlm1+pKS01-Vlm2 (Figure 3.27). Glucose polymer feeding of BJJ01/pJL03-Vlm1+pJL07-Vlm2+pJL10-TEII dramatically increased the cell density with a final OD_{600} of 55 and the volumetric valinomycin titer of 13 mg L^{-1} (Figure 3.28D), which is a 43-fold increase compared to the initial TB batch production. Therefore, the strain BJJ01/pJL03-Vlm1+pJL07-Vlm2+pJL10-TEII would be a good candidate for the following large scale bioreactor valinomycin production since pCTUT7-Vlm1 and pKS01-Vlm2 cannot coexist well in the large bioreactor fermentation (data not shown).

In this study, we present an *in vivo* example to prove the repairing function of TEII in heterologous valinomycin production. While the exact working mechanism of valinomycin TEII is currently unknown. Therefore, more work should be carried out in the future to clarify the biochemical functions of TEII on valinomycin improvement.

5. Conclusions and outlook

5.1. Conclusions

In the present work, we used *E. coli* as a platform for valinomycin production with productivity enhancement through multiple strategies including strain improvement and bioprocess optimization. To realize heterologous biosynthesis of valinomycin in *E. coli*, nine new expression plasmids were constructed and the large heterodimeric valinomycin synthetase, Vlm1 (374 kDa) and Vlm2 (280 kDa), were coexpressed with different compatible plasmid combinations. Based on the protein expression level and the valinomycin productivity, the original pCTUT7-Vlm1 and pKS01-Vlm2 were found to be the best combination for valinomycin production in small scale.

Different cultivation modes impact significantly on valinomycin production. The TB batch cultivations produced modest valinomycin with the yields in µg per liter due to the low cell densities. In contrast, by switching a batch to an enzyme-based fed-batch mode in shake flasks, the valinomycin titers were notably increased, reaching mg per liter levels of product. Therefore, the enzyme-based cultivation system was used for the following optimization.

A design of experiments (DoE) guided optimization was implemented in parallel in milliliter-scale 24-well plates with online monitoring of oxygen and pH. The online data showed that the enzyme-based cultivation system can maintain a very stable pH level (~7.0), which is close to the optimal pH for *E. coli* growth. The results indicated that nutrients boosting has a significantly positive effect on valinomycin yields. Within the tested range from 0 to 6 U L^{-1}, a higher enzyme concentration gives rise to higher valinomycin titers. Further investigations suggested that 9 U L^{-1} is the best enzyme concentration for valinomycin production in our study. Lower culture volume allows better oxygen supply, contributing to higher cell density and valinomycin titers.

Glucose polymer feeding dramatically promoted the volumetric valinomycin titer up to 10 mg L^{-1}, which is a 33-fold increase compared to TB batch production. The specific yield of valinomycin with glucose polymer feeding reached 182 µg L^{-1} OD_{600}^{-1}, indicating a 5.2-fold improvement compared to the initial batch cultivation with a specific yield of 35 µg L^{-1} OD_{600}^{-1}.

Coexpression of the repairing enzyme type II thioesterase (TEII) and valinomycin synthetase further improved the valinomycin titer of 43-fold compared to the initial batch cultivations with the maximum yield of 13 mg L^{-1}. In this study, we presented an *in vivo* example to prove the repairing function of TEII in heterologous valinomycin production in *E. coli*.

Fed-batch cultivation in lab-scale bioreactors confirmed that the valinomycin production in the mg per liter range is also possible in pure glucose based mineral salt medium and that this process reacts robust to nutrient oscillations. This might suggest that a scaling of the process to large industrial scale should be possible.

5.2. Outlook

In this work, we have achieved a reasonable valinomycin productivity using the surrogate host *E. coli* through feasible approaches from strain improvement to bioprocess optimization. Further work still could mainly be carried out from two aspects for enhanced valinomycin production: strain engineering and bioprocess engineering.

Since the repairing enzyme TEII has a positive effect on valinomycin formation, the gene fragment of TEII could be integrated into the chromosome of *E. coli*, reducing the current expression system from three plasmids to two plasmids. Although in this study no obvious inhibiting effect of internal valinomycin on *E. coli* was observed, more higher valinomycin in the cells might inhibit cell growth and thus impede further product formation. To transport valinomycin from inside to outside of the cell, a possible strategy is to upregulate the gene expression of the relevant multidrug

efflux pump, for example, the AcrAB-TolC system, in *E. coli*.

Modest valinomycin yields were reached in this work through the preliminary production in a lab-scale bioreactor. Therefore, it would be more interesting to further investigate and optimize the scalable production processes. The three precursors of valinomycin involved in the primary metabolism of *E. coli* may be significantly increased through bioprocess engineering, finally leading to overproduction of valinomycin.

6. Appendix

6.1. Vector maps

6.1.1. Destination vector maps

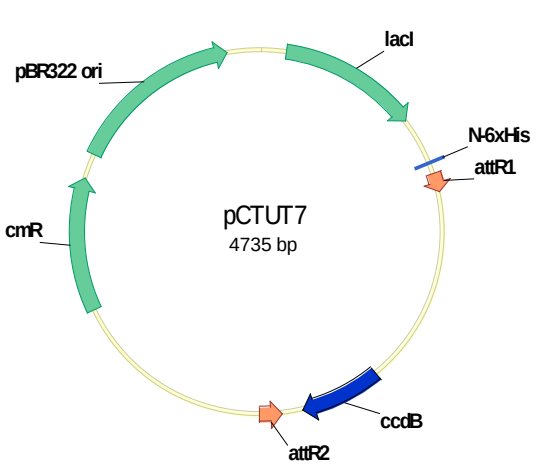

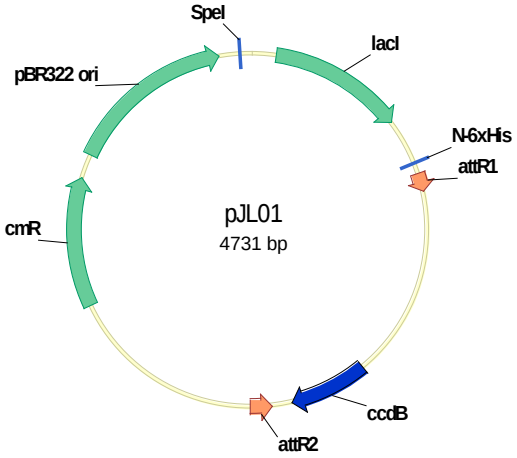

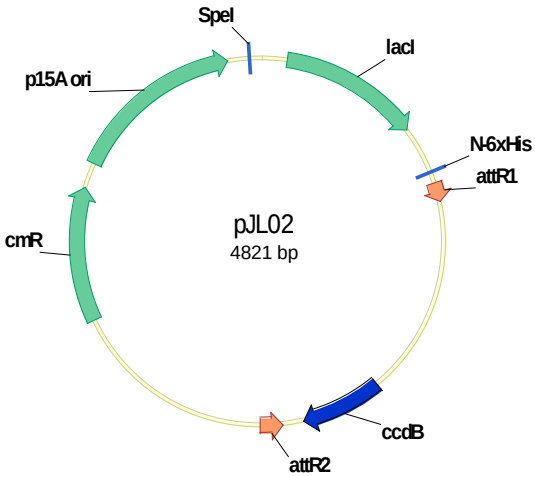

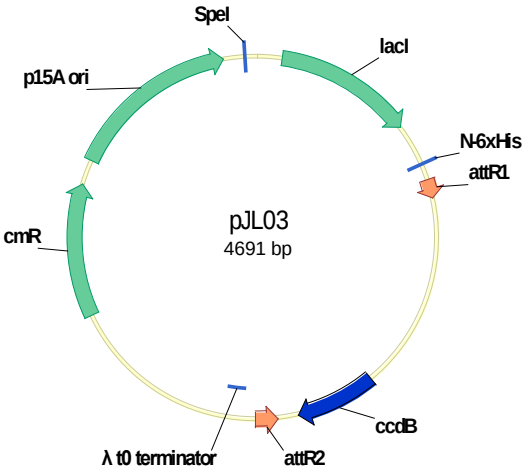

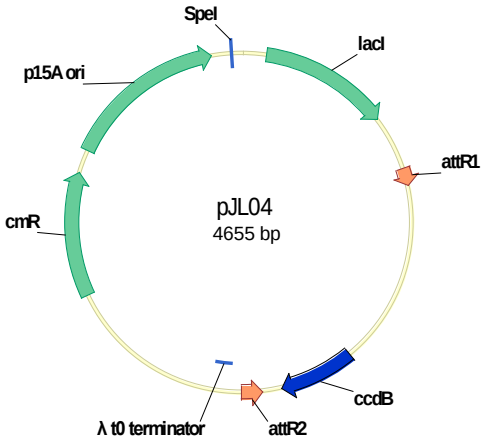

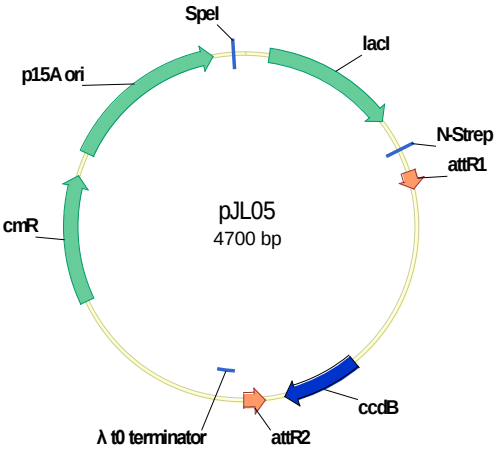

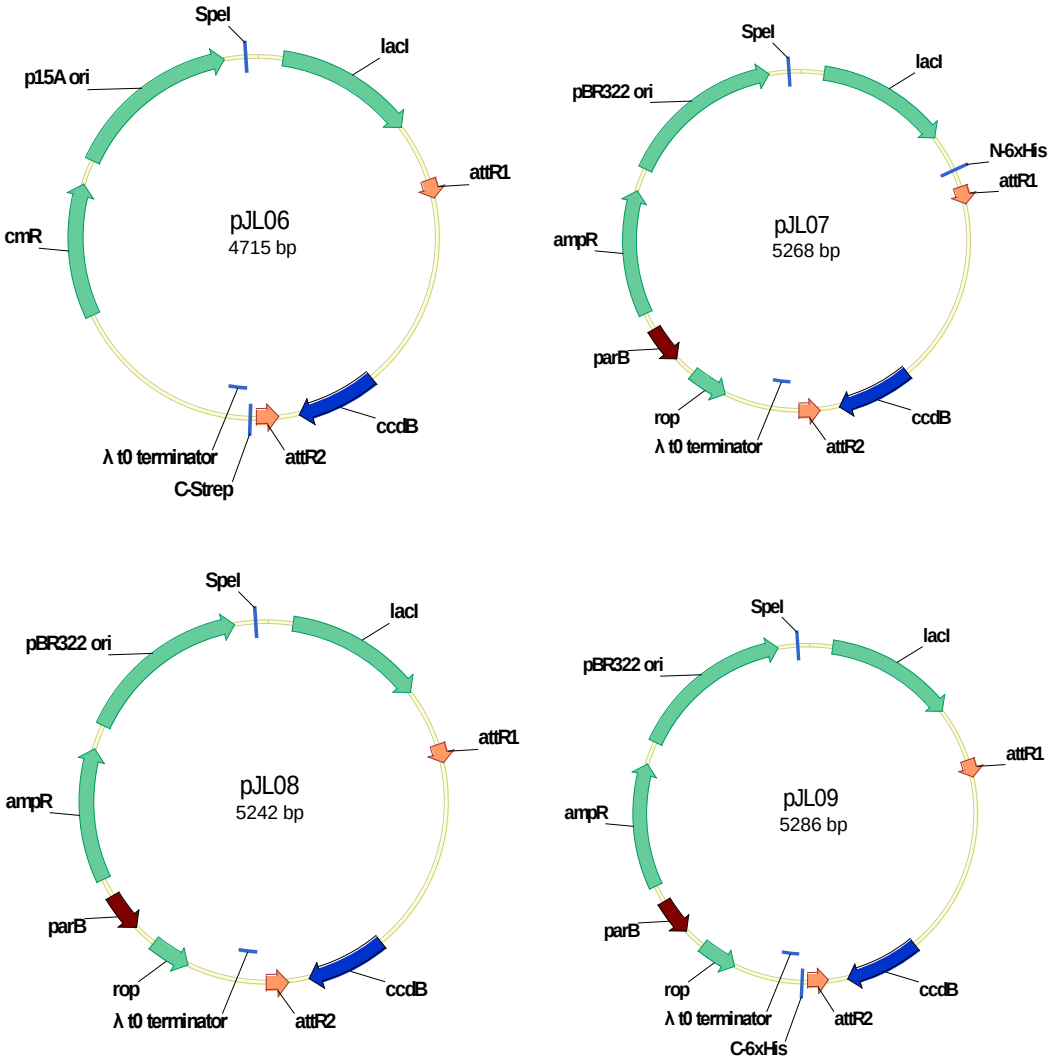

6.1.2. Expression vector map of pJL10-TEII

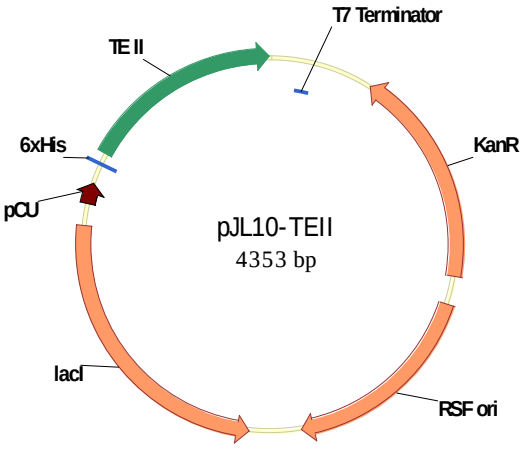

6.2. Cell growth curves and online data of DoE optimization

The figures shown in this section were generated from the experiment of DoE optimization in the 24-well plate. For details, see sections 2.6.5 and 3.5.

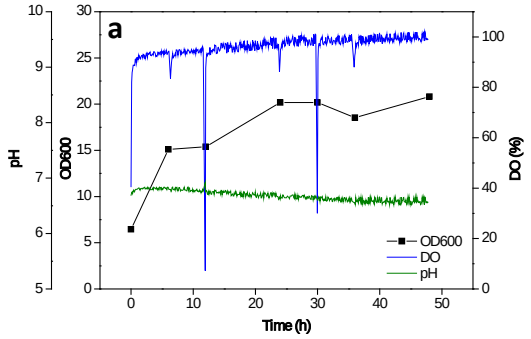

Enzyme: 0 U L^{-1}, Boosting: No, Volume: 0.5 mL

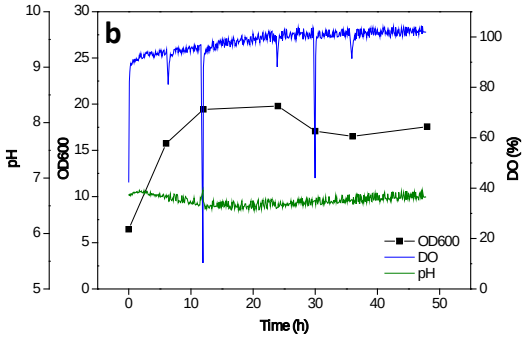

Enzyme: 6 U L^{-1}, Boosting: No, Volume: 0.5 mL

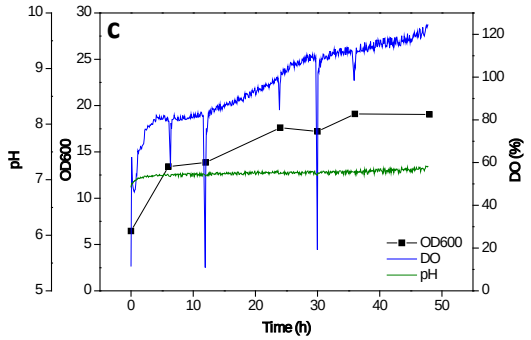

Enzyme: 0 U L^{-1}, Boosting: No, Volume: 1.5 mL

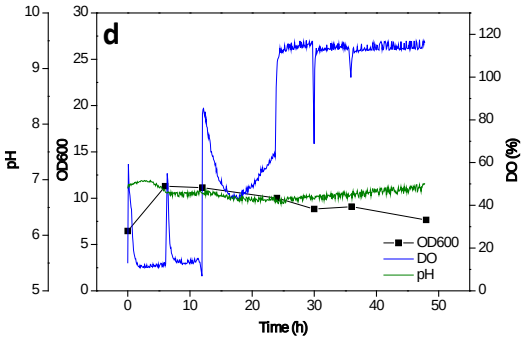

Enzyme: 6 U L^{-1}, Boosting: No, Volume: 1.5 mL

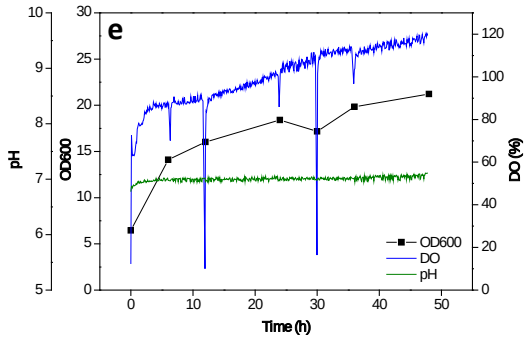

Enzyme: 0 U L^{-1}, Boosting: No, Volume: 1.167 mL

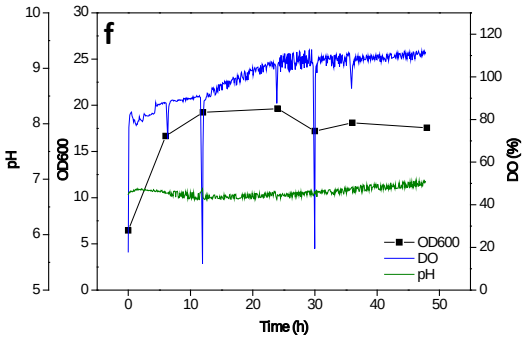

Enzyme: 6 U L^{-1}, Boosting: No, Volume: 0.833 mL

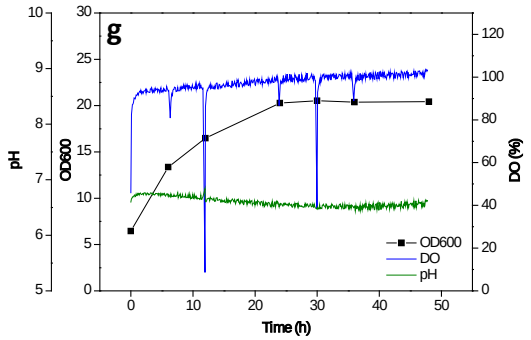

Enzyme: 2 U L^{-1}, Boosting: No, Volume: 0.5 mL

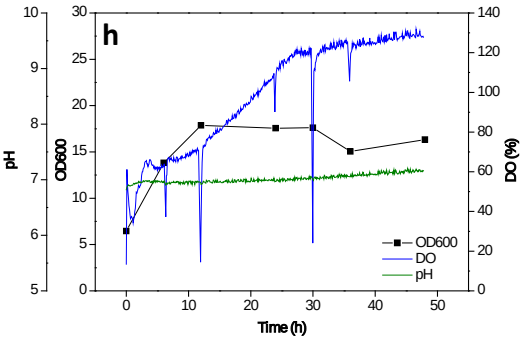

Enzyme: 4 U L^{-1}, Boosting: No, Volume: 1.5 mL

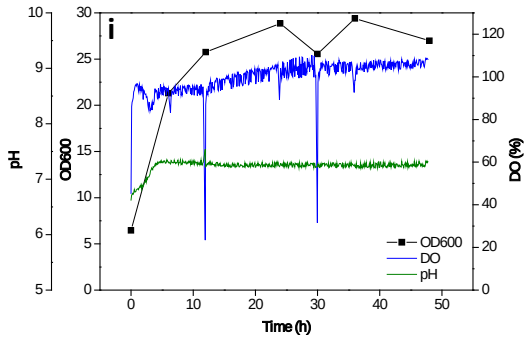

Enzyme: 0 U L^{-1}, Boosting: Yes, Volume: 0.5 mL

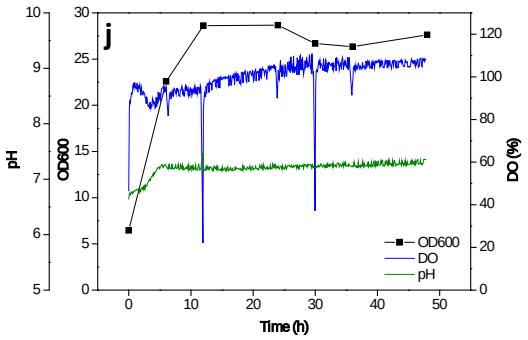

Enzyme: 6 U L^{-1}, Boosting: Yes, Volume: 0.5 mL

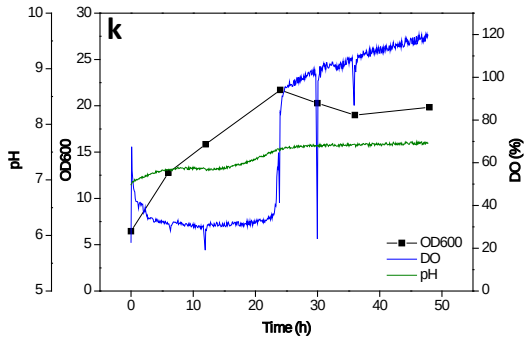

Enzyme: 0 U L^{-1}, Boosting: Yes, Volume: 1.5 mL

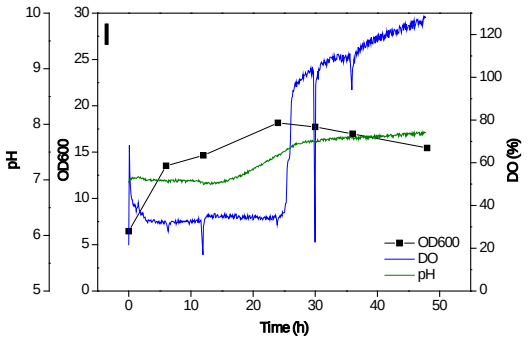

Enzyme: 6 U L^{-1}, Boosting: Yes, Volume: 1.5 mL

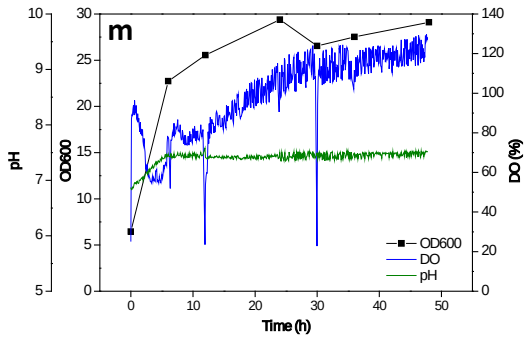

Enzyme: 0 U L^{-1}, Boosting: Yes, Volume: 0.833 mL

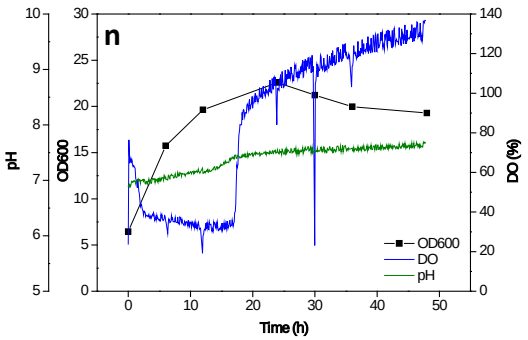

Enzyme: 6 U L^{-1}, Boosting: Yes, Volume: 1.167 mL

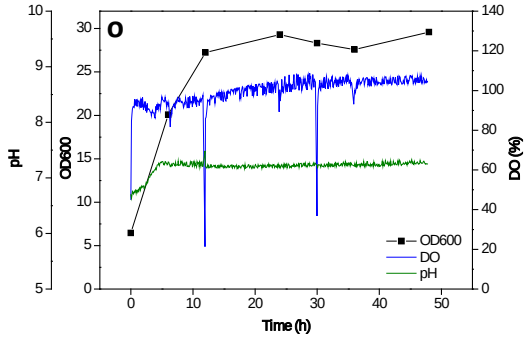

Enzyme: 4 U L^{-1}, Boosting: Yes, Volume: 0.5 mL

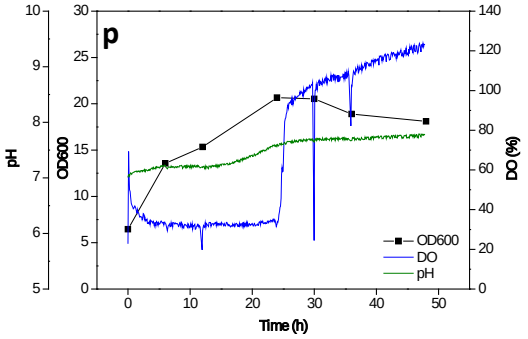

Enzyme: 2 U L^{-1}, Boosting: Yes, Volume: 1.5 mL

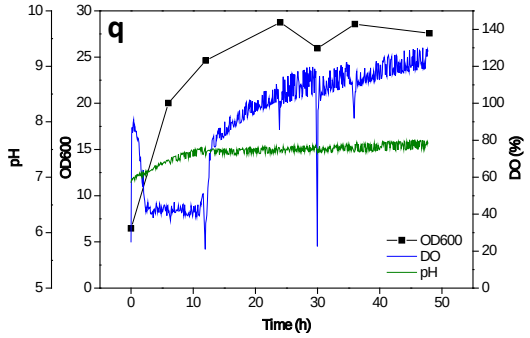

Enzyme: 3 U L^{-1}, Boosting: Yes, Volume: 1 mL

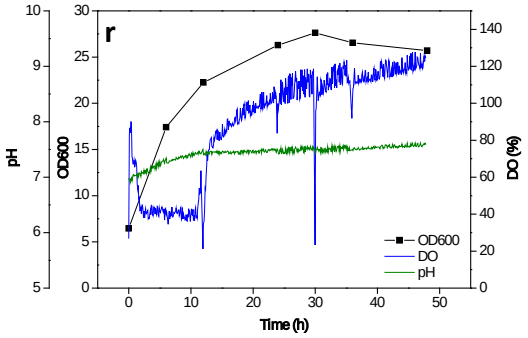

Enzyme: 3 U L^{-1}, Boosting: Yes, Volume: 1 mL

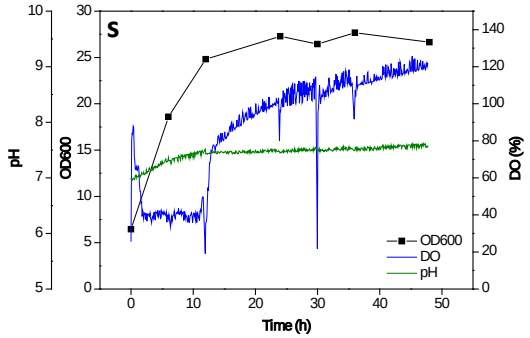

Enzyme: 3 U L^{-1}, Boosting: Yes, Volume: 1 mL

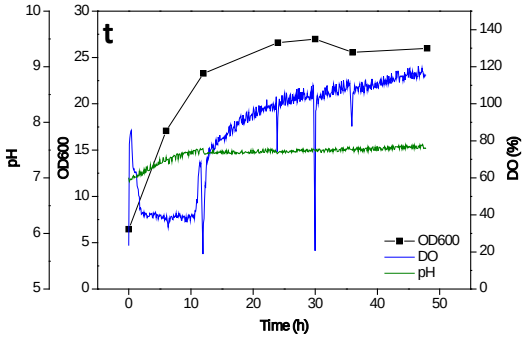

Enzyme: 3 U L^{-1}, Boosting: Yes, Volume: 1 mL

6.3. Investigation of enzyme concentration without boosting

This experiment was performed in the 24-well plate with online measurement of DO and pH. Cells were cultivated at 30 °C in EnBase Flo medium without nutrients boosting. The culture volume per well was 1 mL. For details, see sections 2.6.6 and 3.6.1.

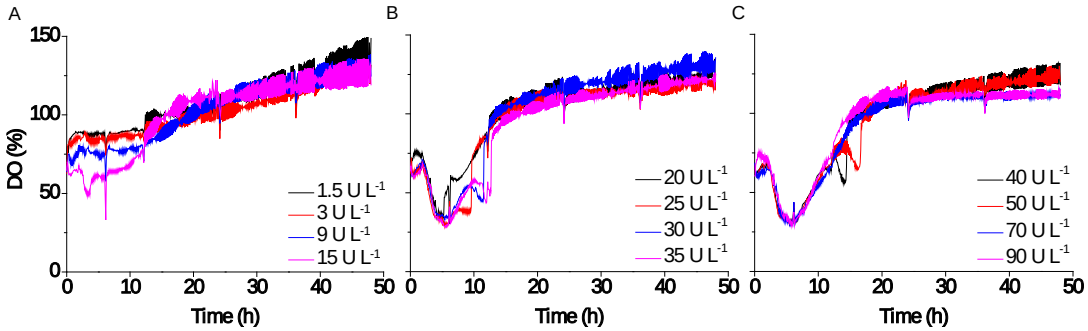

Online measurement of oxygen in the 24-well plate.

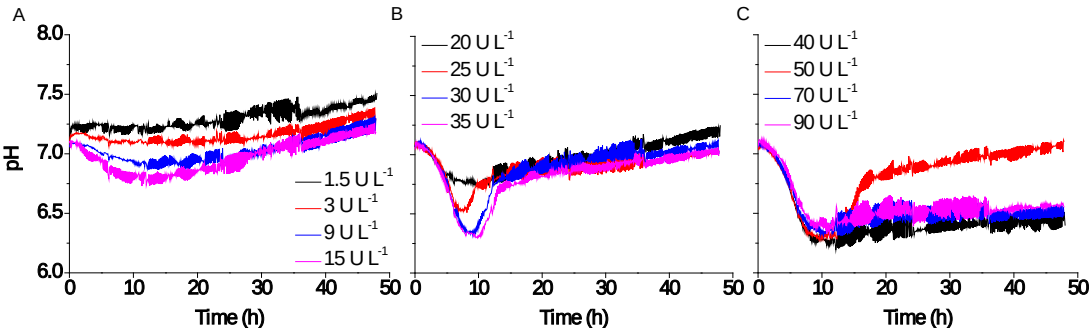

Online measurement of pH in the 24-well plate.

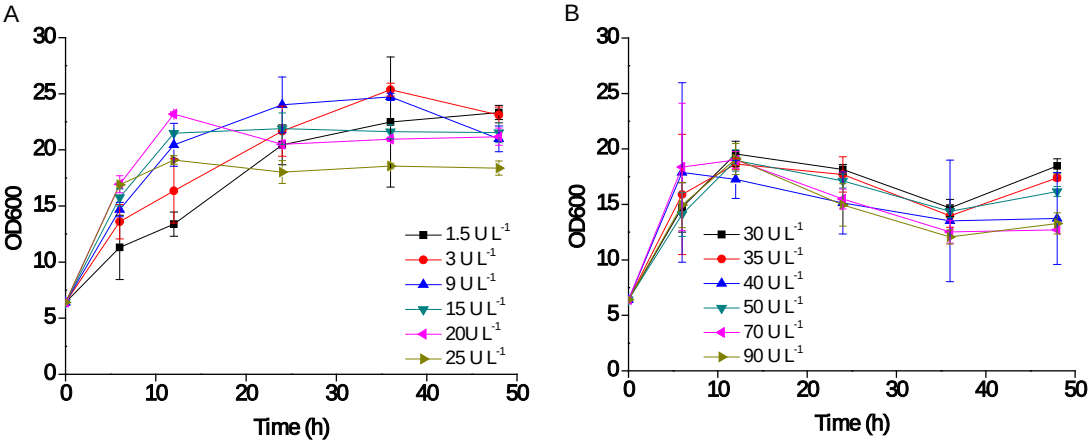

Cell growth curves with different enzyme concentrations in EnBase Flo medium without boosting.

6.4. Two-compartment reactor system

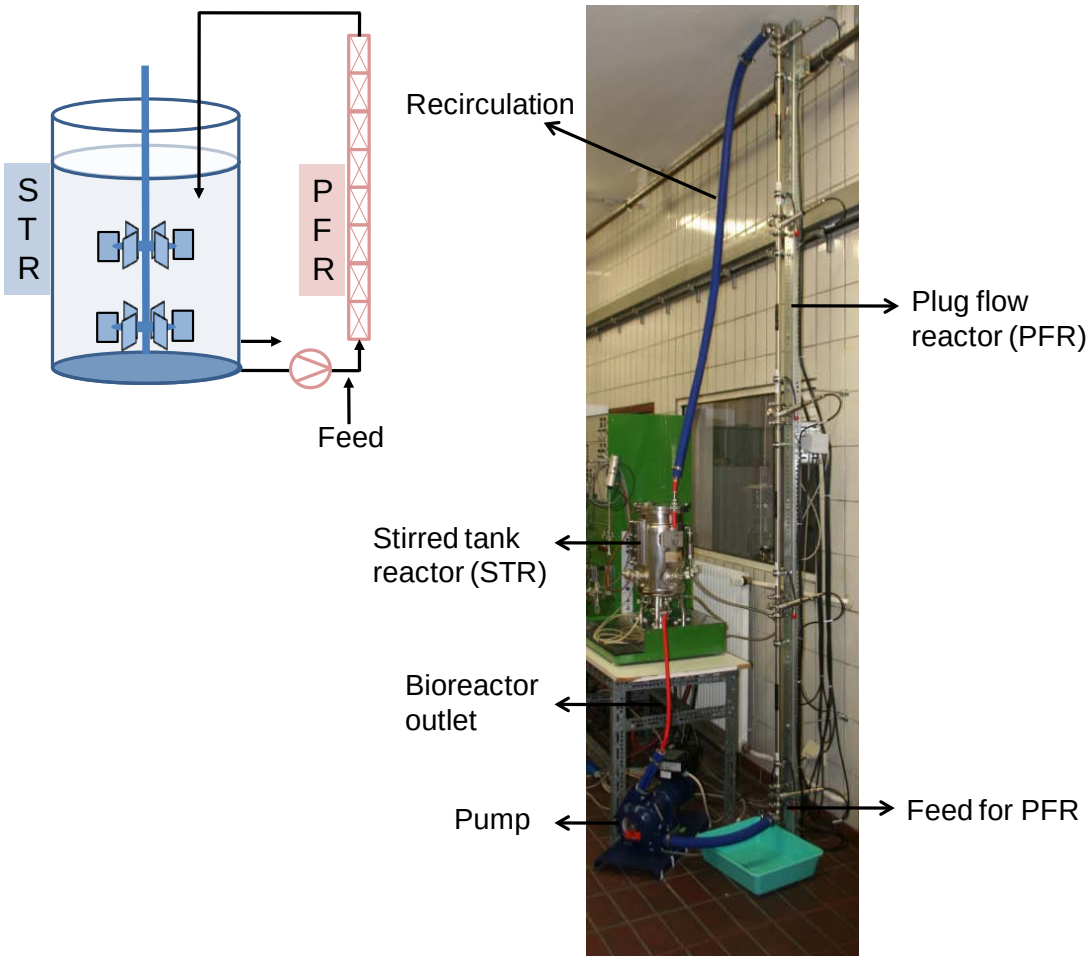

7. References

Abdalah R, Wei L, Francis K, Yu SP (2006) Valinomycin-induced apoptosis in Chinese hamster ovary cells. Neurosci Lett 405(1–2):68-73

Altendorf K, Epstein W, Löhmann A (1986) Valinomycin-induced cation transport in vesicles does not reflect the activity of K^+ transport systems in *Escherichia coli*. J Bacteriol 166(1):334-337

Aminov RI (2010) A brief history of the antibiotic era: lessons learned and challenges for the future. Front Microbiol 1:134

Andreoli TE, Tieffenberg M, Tosteson DC (1967) The effect of valinomycin on the ionic permeability of thin lipid membranes. J Gen Physiol 50(11):2527-2545

Angus TA (1968) Similarity of effect of valinomycin and *Bacillus thuringiensis* parasporal protein in larvae of *Bombyx mori*. J Invertebr Pathol 11(1):145-146

Anke T, Lipmann F (1977) Studies on the biosynthesis of valinomycin. FEBS lett 82(2):337-340

Asher IM, Rothschild KJ, Stanley HE (1974) Raman spectroscopic study of the valinomycin-KSCN complex. J Mol Biol 89(1):205-222

Balunas MJ, Kinghorn AD (2005) Drug discovery from medicinal plants. Life Sci 78(5):431-441

Belshaw PJ, Walsh CT, Stachelhaus T (1999) Aminoacyl-CoAs as probes of condensation domain selectivity in nonribosomal peptide synthesis. Science 284(5413):486-489

Bergendahl V, Linne U, Marahiel MA (2002) Mutational analysis of the C-domain in nonribosomal peptide synthesis. Eur J Biochem 269(2):620-629

Boddy CN, Hotta K, Tse ML, Watts RE, Khosla C (2004) Precursor-directed biosynthesis of epothilone in *Escherichia coli*. J Am Chem Soc 126(24):7436-7437

Boghigian BA, Zhang H, Pfeifer BA (2011) Multi-factorial engineering of heterologous polyketide production in *Escherichia coli* reveals complex pathway interactions. Biotechnol Bioeng 108(6):1360-1371

Brockmann H, Geeren H (1957) Valinomycin II. Antibiotika aus Actinomyceten XXXVII. Die konstitution des Valinomycins. Justus Liebigs Annalen Der Chemie 603(1):216-232

Brockmann H, Schmidt-Kastner G (1955) Valinomycin I, XXVII. Mitteil. über Antibiotica aus Actinomyceten. Chemische Berichte 88(1):57-61

Bruner SD, Weber T, Kohli RM, Schwarzer D, Marahiel MA, Walsh CT, Stubbs MT (2002) Structural basis for the cyclization of the lipopeptide antibiotic surfactin by the thioesterase domain SrfTE. Structure 10(3):301-310

Caboche S, Leclère V, Pupin M, Kucherov G, Jacques P (2010) Diversity of monomers in nonribosomal peptides: towards the prediction of origin and biological activity. J Bacteriol 192(19):5143-5150

Caboche S, Pupin M, Leclère V, Fontaine A, Jacques P, Kucherov G (2008) NORINE: a database of nonribosomal peptides. Nucleic Acids Res 36(suppl 1):D326-D331

Cane DE, Walsh CT (1999) The parallel and convergent universes of polyketide synthases and nonribosomal peptide synthetases. Chem Biol 6(12):R319-R325

Cane DE, Walsh CT, Khosla C (1998) Harnessing the biosynthetic code: combinations, permutations, and mutations. Science 282(5386):63-68

Cesareni G, Muesing MA, Polisky B (1982) Control of ColE1 DNA replication: the rop gene

product negatively affects transcription from the replication primer promoter. Proc Natl Acad Sci USA 79(20):6313-6317

Challis GL, Ravel J, Townsend CA (2000) Predictive, structure-based model of amino acid recognition by nonribosomal peptide synthetase adenylation domains. Chem Biol 7(3):211-224

Cheng Y-Q (2006) Deciphering the biosynthetic codes for the potent anti-SARS-CoV cyclodepsipeptide valinomycin in *Streptomyces tsusimaensis* ATCC 15141. ChemBioChem 7(3):471-477

Chin Y-W, Balunas M, Chai H, Kinghorn AD (2006) Drug discovery from natural sources. AAPS J 8(2):E239-E253

Conly J, Johnston B (2005) Where are all the new antibiotics? The new antibiotic paradox. Can J Infect Dis Med Microbiol 16(3):159-160

Conti E, Stachelhaus T, Marahiel MA, Brick P (1997) Structural basis for the activation of phenylalanine in the non-ribosomal biosynthesis of gramicidin S. EMBO J 16(14):4174-4183

Cragg GM, Newman DJ, Snader KM (1997) Natural products in drug discovery and development. J Nat Prod 60(1):52-60

Crump MP, Crosby J, Dempsey CE, Parkinson JA, Murray M, Hopwood DA, Simpson TJ (1997) Solution structure of the actinorhodin polyketide synthase acyl carrier protein from *Streptomyces coelicolor* A3(2). Biochemistry 36(20):6000-6008

Crusemann M, Kohlhaas C, Piel J (2013) Evolution-guided engineering of nonribosomal peptide synthetase adenylation domains. Chem Sci 4(3):1041-1045

Daoud S, Forde N (1991) Synergistic cytotoxic actions of cisplatin and liposomal valinomycin on human ovarian carcinoma cells. Cancer Chemother Pharmacol 28(5):370-376

Daoud SS, Juliano RL (1986) Reduced toxicity and enhanced antitumor effects in mice of the ionophoric drug valinomycin when incorporated in liposomes. Cancer Res 46(11):5518-5523

Daoud SS, Juliano RL (1989) Modulation of doxorubicin resistance by valinomycin (NSC 122023) and liposomal valinomycin in Chinese hamster ovary cells. Cancer Res 49(10):2661-2667

Deckers CLP, Lyons AB, Samuel K, Sanderson A, Maddy AH (1993) Alternative pathways of apoptosis induced by methylprednisolone and valinomycin analyzed by flow cytometry. Exp Cell Res 208(2):362-370

Dias DA, Urban S, Roessner U (2012) A historical overview of natural products in drug discovery. Metabolites 2(2):303-336

Du L, Lou L (2010) PKS and NRPS release mechanisms. Nat Prod Rep 27(2):255-278

Enfors SO, Jahic M, Rozkov A, Xu B, Hecker M, Jürgen B, Krüger E, Schweder T, Hamer G, O'Beirne D, Noisommit-Rizzi N, Reuss M, Boone L, Hewitt C, McFarlane C, Nienow A, Kovacs T, Trägårdh C, Fuchs L, Revstedt J, Friberg PC, Hjertager B, Blomsten G, Skogman H, Hjort S, Hoeks F, Lin HY, Neubauer P, van der Lans R, Luyben K, Vrabel P, Manelius Å (2001) Physiological responses to mixing in large scale bioreactors. J Biotechnol 85(2):175-185

Evans Bradley S, Chen Y, Metcalf William W, Zhao H, Kelleher Neil L (2011) Directed evolution of the nonribosomal peptide synthetase AdmK generates new andrimid derivatives

in vivo. Chem Biol 18(5):601-607

Faulkner DJ (2002) Marine natural products. Nat Prod Rep 19(1):1-48

Felnagle EA, Jackson EE, Chan YA, Podevels AM, Berti AD, McMahon MD, Thomas MG (2008) Nonribosomal peptide synthetases involved in the production of medically relevant natural products. Mol Pharmaceut 5(2):191-211

Finking R, Marahiel MA (2004) Biosynthesis of nonribosomal peptides. Annu Rev Microbiol 58:453-488

Fischbach MA, Walsh CT (2006) Assembly-line enzymology for polyketide and nonribosomal peptide antibiotics: logic, machinery, and mechanisms. Chem Rev 106(8):3468-3496

Fowler AV, Zabin I (1966) Effects of dimethylsulfoxide on the lactose operon in *Escherichia coli*. J Bacteriol 92(2):353-357

Furlong IJ, Lopez Mediavilla C, Ascaso R, Lopez Rivas A, Collins MK (1998) Induction of apoptosis by valinomycin: mitochondrial permeability transition causes intracellular acidification. Cell Death Differ 5(3):214-221

Gaitatzis N, Kunze B, Müller R (2001) In vitro reconstitution of the myxochelin biosynthetic machinery of *Stigmatella aurantiaca* Sg a15: biochemical characterization of a reductive release mechanism from nonribosomal peptide synthetases. Proc Natl Acad Sci USA 98(20):11136-11141

Gao X, Haynes SW, Ames BD, Wang P, Vien LP, Walsh CT, Tang Y (2012) Cyclization of fungal nonribosomal peptides by a terminal condensation-like domain. Nat Chem Biol 8(10):823-830

Gerdes K (1988) The parB (hok/sok) locus of plasmid R1: A general purpose plasmid stabilization system. Nat Biotech 6(12):1402-1405

Glazyrina J, Krause M, Junne S, Glauche F, Strom D, Neubauer P (2012) Glucose-limited high cell density cultivations from small to pilot plant scale using an enzyme-controlled glucose delivery system. New Biotechnol 29(2):235-242

Gruenewald S, Mootz HD, Stehmeier P, Stachelhaus T (2004) In vivo production of artificial nonribosomal peptide products in the heterologous host *Escherichia coli*. Appl Environ Microbiol 70(6):3282-3291

Guenzi E, Galli G, Grgurina I, Gross DC, Grandi G (1998) Characterization of the syringomycin synthetase gene cluster: a link between prokaryotic and eukaryotic peptide synthetases. J Biol Chem 273(49):32857-32863

Haefner B (2003) Drugs from the deep: marine natural products as drug candidates. Drug Discov Today 8(12):536-544

Halsey CM, Benham DA, JiJi RD, Cooley JW (2012) Influence of the lipid environment on valinomycin structure and cation complex formation. Spectrochim Acta A Mol Biomol Spectrosc 96(0):200-206

Hamilton G, Baskett T (2000) In the arms of morpheus: the development of morphine for postoperative pain relief. Can J Anesth 47(4):367-374

Han K, Lim HC, Hong J (1992) Acetic acid formation in *Escherichia coli* fermentation. Biotechnol Bioeng 39(6):663-671

Hartley JL, Temple GF, Brasch MA (2000) DNA cloning using in vitro site-specific recombination. Genome Res 10(11):1788-1795

Heisey RM, Huang J, Mishra SK, Keller JE, Miller JR, Putnam AR, D'Silva TDJ (1988) Production

of valinomycin, an insecticidal antibiotic, by *Streptomyces griseus* var. *flexipertum* var. nov. J Agric Food Chem 36(6):1283-1286

Holak TA, Kearsley SK, Kim Y, Prestegard JH (1988) Three-dimensional structure of acyl carrier protein determined by NMR pseudoenergy and distance geometry calculations. Biochemistry 27(16):6135-6142

Horton RM, Hunt HD, Ho SN, Pullen JK, Pease LR (1989) Engineering hybrid genes without the use of restriction enzymes: gene splicing by overlap extension. Gene 77(1):61-68

Hur GH, Vickery CR, Burkart MD (2012) Explorations of catalytic domains in non-ribosomal peptide synthetase enzymology. Nat Prod Rep 29(10):1074-1098

Inai Y, Yabuki M, Kanno T, Akiyama J, Yasuda T, Utsumi K (1997) Valinomycin induces apoptosis of ascites hepatoma cells (AH-130) in relation to mitochondrial membrane potential. Cell Struct Funct 22(5):555-563

Jaitzig J (2013) Reconstituted nonribosomal biosynthesis of the peptide antibiotic valinomycin in *Escherichia coli* as a whole-cell biocatalyst. Doctor thesis, Technischen Universität Berlin

Jensen EB, Carlsen S (1990) Production of recombinant human growth hormone in *Escherichia coli*: expression of different precursors and physiological effects of glucose, acetate, and salts. Biotechnol Bioeng 36(1):1-11

Ji H-F, Li X-J, Zhang H-Y (2009) Natural products and drug discovery. EMBO Rep 10(3):194-200

Julien B, Shah S, Ziermann R, Goldman R, Katz L, Khosla C (2000) Isolation and characterization of the epothilone biosynthetic gene cluster from *Sorangium cellulosum*. Gene 249(1–2):153-160

Junge W, Schmid R (1971) The mechanism of action of valinomycin on the thylakoid membrane. J Membrane Biol 4(1):179-192

Karuppannan AK, Wu KX, Qiang J, Chu JJ-H, Kwang J (2012) Natural compounds inhibiting the replication of Porcine reproductive and respiratory syndrome virus. Antiviral Res 94(2):188-194

Kealey JT, Liu L, Santi DV, Betlach MC, Barr PJ (1998) Production of a polyketide natural product in nonpolyketide-producing prokaryotic and eukaryotic hosts. Proc Natl Acad Sci USA 95(2):505-509

Keating TA, Ehmann DE, Kohli RM, Marshall CG, Trauger JW, Walsh CT (2001) Chain termination steps in nonribosomal peptide synthetase assembly lines: directed acyl-S-enzyme breakdown in antibiotic and siderophore biosynthesis. ChemBioChem 2(2):99-107

Keating TA, Marshall CG, Walsh CT (2000a) Reconstitution and characterization of the vibrio cholerae vibriobactin synthetase from VibB, VibE, VibF, and VibH. Biochemistry 39(50):15522-15530

Keating TA, Marshall CG, Walsh CT, Keating AE (2002) The structure of VibH represents nonribosomal peptide synthetase condensation, cyclization and epimerization domains. Nat Struct Mol Biol 9(7):522-526

Keating TA, Suo Z, Ehmann DE, Walsh CT (2000b) Selectivity of the yersiniabactin synthetase adenylation domain in the two-step process of amino acid activation and transfer to a holo-carrier protein domain. Biochemistry 39(9):2297-2306

Kinghorn AD, Pan L, Fletcher JN, Chai H (2011) The relevance of higher plants in lead

compound discovery programs. J Nat Prod 74(6):1539-1555

Kleman GL, Strohl WR (1994) Acetate metabolism by *Escherichia coli* in high-cell-density fermentation. Appl Environ Microbiol 60(11):3952-3958

Koglin A, Lohr F, Bernhard F, Rogov VV, Frueh DP, Strieter ER, Mofid MR, Guntert P, Wagner G, Walsh CT, Marahiel MA, Dotsch V (2008) Structural basis for the selectivity of the external thioesterase of the surfactin synthetase. Nature 454(7206):907-911

Konz D, Klens A, Schörgendorfer K, Marahiel MA (1997) The bacitracin biosynthesis operon of *Bacillus licheniformis* ATCC 10716: molecular characterization of three multi-modular peptide synthetases. Chem Biol 4(12):927-937

Konz D, Marahiel MA (1999) How do peptide synthetases generate structural diversity? Chem Biol 6(2):R39-R48

Kotowska M, Pawlik K, Smulczyk-Krawczyszyn A, Bartosz-Bechowski H, Kuczek K (2009) Type II thioesterase ScoT, associated with *Streptomyces coelicolor* A3(2) modular polyketide synthase Cpk, hydrolyzes acyl residues and has a preference for propionate. Appl Environ Microbiol 75(4):887-896

Kraft M, Knüpfer U, Wenderoth R, Kacholdt A, Pietschmann P, Hock B, Horn U (2007) A dual expression platform to optimize the soluble production of heterologous proteins in the periplasm of *Escherichia coli*. Appl Microbiol Biotechnol 76(6):1413-1422

Krause M, Ukkonen K, Haataja T, Ruottinen M, Glumoff T, Neubauer A, Neubauer P, Vasala A (2010) A novel fed-batch based cultivation method provides high cell-density and improves yield of soluble recombinant proteins in shaken cultures. Microb Cell Fact 9:11

Ladeuze S, Lentz N, Delbrassinne L, Hu X, Mahillon J (2011) Antifungal activity displayed by cereulide, the emetic toxin produced by *Bacillus cereus*. Appl Environ Microbiol 77(7):2555-2558

Lambalot RH, Gehring AM, Flugel RS, Zuber P, LaCelle M, Marahiel MA, Reid R, Khosla C, Walsh CT (1996) A new enzyme superfamily — the phosphopantetheinyl transferases. Chem Biol 3(11):923-936

Lau J, Tran C, Licari P, Galazzo J (2004) Development of a high cell-density fed-batch bioprocess for the heterologous production of 6-deoxyerythronolide B in *Escherichia coli*. J Biotechnol 110(1):95-103

Li JW-H, Vederas JC (2009) Drug discovery and natural products: end of an era or an endless frontier? Science 325(5937):161-165

Luo L, Burkart MD, Stachelhaus T, Walsh CT (2001) Substrate recognition and selection by the initiation module PheATE of gramicidin S synthetase. J Am Chem Soc 123(45): 11208-11218

MacDonald JC (1960) Biosynthesis of valinomycin. Can J Microbiol 6(1):27-34

MacDonald JC, Slater GP (1968) Biosynthesis of valinomycin. Can J Biochem 46(6):573-578

Magarvey NA, Ehling-Schulz M, Walsh CT (2006) Characterization of the cereulide NRPS α-hydroxy acid specifying modules: activation of α-keto acids and chiral reduction on the assembly line. J Am Chem Soc 128(33):10698-10699

Marahiel MA (2009) Working outside the protein-synthesis rules: insights into non-ribosomal peptide synthesis. J Pept Sci 15(12):799-807

Marahiel MA, Stachelhaus T, Mootz HD (1997) Modular peptide synthetases involved in

nonribosomal peptide synthesis. Chem Rev 97(7):2651-2674

Matter AM, Hoot SB, Anderson PD, Neves SS, Cheng Y-Q (2009) Valinomycin biosynthetic gene cluster in *Streptomyces*: conservation, ecology and evolution. PLoS ONE 4(9):e7194

May JJ, Wendrich TM, Marahiel MA (2001) The dhb operon of *Bacillus subtilis* encodes the biosynthetic template for the catecholic siderophore 2,3-dihydroxybenzoate-glycine-threonine trimeric ester bacillibactin. J Biol Chem 276(10):7209-7217

Moore C, Pressman B (1964) Mechanism of action of valinomycin on mitochondria. Biochem Biophys Res Commun 15(6):562-567

Mootz HD, Schwarzer D, Marahiel MA (2002) Ways of assembling complex natural products on modular nonribosomal peptide synthetases. ChemBioChem 3(6):490-504

Murli S, Kennedy J, Dayem LC, Carney JR, Kealey JT (2003) Metabolic engineering of *Escherichia coli* for improved 6-deoxyerythronolide B production. J Ind Microbiol Biotechnol 30(8):500-509

Mutka SC, Carney JR, Liu Y, Kennedy J (2006) Heterologous production of epothilone C and D in *Escherichia coli*. Biochemistry 45(4):1321-1330

Neubauer P, Junne S (2010) Scale-down simulators for metabolic analysis of large-scale bioprocesses. Curr Opin Biotechnol 21(1):114-121

Newman DJ, Cragg GM (2007) Natural products as sources of new drugs over the last 25 years. J Nat Prod 70(3):461-477

Newman DJ, Cragg GM (2012) Natural products as sources of new drugs over the 30 years from 1981 to 2010. J Nat Prod 75(3):311-335

Newman DJ, Cragg GM, Snader KM (2003) Natural products as sources of new drugs over the period 1981−2002. J Nat Prod 66(7):1022-1037

Paananen A, Järvinen K, Sareneva T, Salkinoja-Salonen MS, Timonen T, Hölttä E (2005) Valinomycin-induced apoptosis of human NK cells is predominantly caspase independent. Toxicology 212(1):37-45

Paananen A, Mikkola R, Sareneva T, Matikainen S, Andersson M, Julkunen I, Salkinoja-Salonen MS, Timonen T (2000) Inhibition of human NK cell function by valinomycin, a toxin from *Streptomyces griseus* in indoor air. Infect Immun 68(1):165-169

Pansa MC, Natalizi GM, Bettini S (1973) Toxicity of valinomycin on insects. J Invertebr Pathol 22(2):148-152

Park CN, Lee JM, Lee D, Kim BS (2008) Antifungal activity of valinomycin, a peptide antibiotic produced by *Streptomyces* sp. strain M10 antagonistic to *Botrytis cinerea*. J Microbiol Biotechnol 18(5):880-840

Peirú S, Menzella HG, Rodríguez E, Carney J, Gramajo H (2005) Production of the potent antibacterial polyketide erythromycin C in *Escherichia coli*. Appl Environ Microbiol 71(5):2539-2547

Perkins JB, Guterman SK, Howitt CL, Williams VE, Pero J (1990) *Streptomyces* genes involved in biosynthesis of the peptide antibiotic valinomycin. J Bacteriol 172(6):3108-3116

Pettit GR, Tan R, Melody N, Kielty JM, Pettit RK, Herald DL, Tucker BE, Mallavia LP, Doubek DL, Schmidt JM (1999) Antineoplastic agents. Part 409: isolation and structure of montanastatin from a terrestrial actinomycete. Bioorg Med Chem 7(5):895-899

Pfeifer B, Hu Z, Licari P, Khosla C (2002) Process and metabolic strategies for improved production of *Escherichia coli*-derived 6-deoxyerythronolide B. Appl Environ Microbiol 68(7):3287-3292

Pfeifer BA, Admiraal SJ, Gramajo H, Cane DE, Khosla C (2001) Biosynthesis of complex polyketides in a metabolically engineered strain of *E. coli*. Science 291(5509):1790-1792

Pfeifer BA, Wang CCC, Walsh CT, Khosla C (2003) Biosynthesis of yersiniabactin, a complex polyketide-nonribosomal peptide, using *Escherichia coli* as a heterologous host. Appl Environ Microbiol 69(11):6698-6702

Pimentel-Elardo SM, Kozytska S, Bugni TS, Ireland CM, Moll H, Hentschel U (2010) Anti-parasitic compounds from *Streptomyces* sp. strains isolated from Mediterranean sponges. Mar Drugs 8(2):373-380

Pistorino M, Pfeifer BA (2009) Efficient experimental design and micro-scale medium enhancement of 6-deoxyerythronolide B production through *Escherichia coli*. Biotechnol Prog 25(5):1364-1371

Praseuth AP, Praseuth MB, Oguri H, Oikawa H, Watanabe K, Wang CCC (2008) Improved production of triostin A in engineered *Escherichia coli* with furnished quinoxaline chromophore by design of experiments in small-scale culture. Biotechnol Prog 24(1):134-139

Pressman BC (1965) Induced active transport of ions in mitochondria. Proc Natl Acad Sci USA 53(5):1076-1083

Quadri LEN, Weinreb PH, Lei M, Nakano MM, Zuber P, Walsh CT (1998) Characterization of Sfp, a *Bacillus subtilis* phosphopantetheinyl transferase for peptidyl carrier protein domains in peptide synthetases. Biochemistry 37(6):1585-1595

Ristow H, Salnikow J, Kleinkauf H (1974) Biosynthesis of valinomycin. FEBS lett 42(2):127-130

Ryabova ID, Gorneva GA, Ovchinnikov YA (1975) Effect of valinomycin on ion transport in bacterial cells and on bacterial growth. BBA-Biomembranes 401(1):109-118

Ryoo I-J, Park H-R, Choo S-J, Hwang J-H, Park Y-M, Bae K-H, Shin-Ya K, Yoo I-D (2006) Selective cytotoxic activity of valinomycin against HT-29 human colon carcinoma cells via down-regulation of GRP78. Biol Pharm Bull 29(4):817-820

Sambrook J, Russell DW (2001) Molecular cloning: a laboratory manual. 3rd ed. New York: Cold Spring Harbor Laboratory Press

Samel SA, Marahiel MA, Essen L-O (2008) How to tailor non-ribosomal peptide products-new clues about the structures and mechanisms of modifying enzymes. Mol Biosyst 4(5):387-393

Samel SA, Schoenafinger G, Knappe TA, Marahiel MA, Essen L-O (2007) Structural and functional insights into a peptide bond-forming bidomain from a nonribosomal peptide synthetase. Structure 15(7):781-792

Samel SA, Wagner B, Marahiel MA, Essen L-O (2006) The thioesterase somain of the fengycin biosynthesis cluster: a structural base for the macrocyclization of a non-ribosomal lipopeptide. J Mol Biol 359(4):876-889

Schmoock G, Pfennig F, Jewiarz J, Schlumbohm W, Laubinger W, Schauwecker F, Keller U (2005) Functional cross-talk between fatty acid synthesis and nonribosomal peptide synthesis in quinoxaline antibiotic-producing *Streptomycetes*. J Biol Chem 280(6):

4339-4349

Schwarzer D, Finking R, Marahiel MA (2003) Nonribosomal peptides: from genes to products. Nat Prod Rep 20(3):275-287

Schwarzer D, Mootz HD, Linne U, Marahiel MA (2002) Regeneration of misprimed nonribosomal peptide synthetases by type II thioesterases. Proc Natl Acad Sci USA 99(22):14083-14088

Schwarzer D, Mootz HD, Marahiel MA (2001) Exploring the impact of different thioesterase domains for the design of hybrid peptide synthetases. Chem Biol 8(10):997-1010

Seshachalam D, Frahm DH, Ferraro FM (1973) Cation reversal of inhibition of growth by valinomycin in *Streptococcus pyogenes* and *Clostridium sporogenes*. Antimicrob Agents Chemother 3(1):63-67

Shemyakin MM, Aldanova NA, Vinogradova EI, Feigina MY (1963a) The structure and total synthesis of valinomycin. Tetrahedron Lett 4(28):1921-1925

Shemyakin MM, Vinogradova EI, Feigina MY, Aldanova NA (1963b) On the structure of amidomycin and valinomycin. Tetrahedron Lett 4(6):351-356

Shemyakin MM, Vinogradova EI, Ryabova ID, Fonina LA, Sanasaryan AA (1973) Relationship between structure, stability of potassium complexes, and antimicrobial activity in a series of analogs of valinomycin. Chem Nat Compd 9(2):229-234

Šiurkus J, Panula-Perälä J, Horn U, Kraft M, Rimšeliene R, Neubauer P (2010) Novel approach of high cell density recombinant bioprocess development: optimisation and scale-up from microlitre to pilot scales while maintaining the fed-batch cultivation mode of *E. coli* cultures. Microb Cell Fact 9:35

Smith TAD, Blaylock MG (2007) Treatment of breast tumor cells In vitro with the mitochondrial membrane potential dissipater valinomycin increases 18F-FDG incorporation. J Nucl Med 48(8):1308-1312

Soini J, Falschlehner C, Liedert C, Bernhardt J, Vuoristo J, Neubauer P (2008) Norvaline is accumulated after a down-shift of oxygen in *Escherichia coli* W3110. Microb Cell Fact 7:30

Som T, Tomizawa J (1983) Regulatory regions of ColE1 that are involved in determination of plasmid copy number. Proc Natl Acad Sci USA 80(11):3232-3236

Spande TF, Garraffo HM, Edwards MW, Yeh HJC, Pannell L, Daly JW (1992) Epibatidine: a novel (chloropyridyl)azabicycloheptane with potent analgesic activity from an Ecuadoran poison frog. J Am Chem Soc 114(9):3475-3478

Stachelhaus T, Mootz HD, Bergendahl V, Marahiel MA (1998) Peptide bond formation in nonribosomal peptide biosynthesis: catalytic role of the condensation domain. J Biol Chem 273(35):22773-22781

Stachelhaus T, Mootz HD, Marahiel MA (1999) The specificity-conferring code of adenylation domains in nonribosomal peptide synthetases. Chem Biol 6(8):493-505

Stack D, Neville C, Doyle S (2007) Nonribosomal peptide synthesis in *Aspergillus fumigatus* and other fungi. Microbiology 153(5):1297-1306

Szeker K, Niemitalo O, Casteleijn MG, Juffer AH, Neubauer P (2011) High-temperature cultivation and 5' mRNA optimization are key factors for the efficient overexpression of thermostable *Deinococcus geothermalis* purine nucleoside phosphorylase in *Escherichia coli*. J Biotechnol 156(4):268-274

Tang L, Fu H, Betlach MC, McDaniel R (1999) Elucidating the mechanism of chain termination switching in the picromycin/methymycin polyketide synthase. Chem Biol 6(8):553-558

Tanovic A, Samel SA, Essen L-O, Marahiel MA (2008) Crystal structure of the termination module of a nonribosomal peptide synthetase. Science 321(5889):659-663

Tempelaars MH, Rodrigues S, Abee T (2011) Comparative analysis of antimicrobial activities of valinomycin and cereulide, the *Bacillus cereus* emetic toxin. Appl Environ Microbiol 77(8):2755-2762

Tolia NH, Joshua-Tor L (2006) Strategies for protein coexpression in *Escherichia coli*. Nat Meth 3(1):55-64

Twigg AJ, Sherratt D (1980) Trans-complementable copy-number mutants of plasmid ColE1. Nature 283:216-218

Ukkonen K, Vasala A, Ojamo H, Neubauer P (2011) High-yield production of biologically active recombinant protein in shake flask culture by combination of enzyme-based glucose delivery and increased oxygen transfer. Microb Cell Fact 10:107

von Döhren H, Keller U, Vater J, Zocher R (1997) Multifunctional peptide synthetases. Chem Rev 97(7):2675-2706

Walhout AJM, Temple GF, Brasch MA, Hartley JL, Lorson MA, van den Heuvel S, Vidal M (2000) GATEWAY recombinational cloning: application to the cloning of large numbers of open reading frames or ORFeomes. In: Jeremy Thorner SDE, John NA (eds) Methods Enzymol 328:575-592

Walsh CT (2004) Polyketide and nonribosomal peptide antibiotics: modularity and versatility. Science 303(5665):1805-1810

Walsh CT, Chen H, Keating TA, Hubbard BK, Losey HC, Luo L, Marshall CG, Miller DA, Patel HM (2001) Tailoring enzymes that modify nonribosomal peptides during and after chain elongation on NRPS assembly lines. Curr Opin Chem Biol 5(5):525-534

Walsh CT, Gehring AM, Weinreb PH, Quadri LEN, Flugel RS (1997) Post-translational modification of polyketide and nonribosomal peptide synthases. Curr Opin Chem Biol 1(3):309-315

Wang Y, Boghigian B, Pfeifer B (2007) Improving heterologous polyketide production in *Escherichia coli* by overexpression of an *S*-adenosylmethionine synthetase gene. Appl Microbiol Biotechnol 77(2):367-373

Wang Y, Pfeifer BA (2008) 6-Deoxyerythronolide B production through chromosomal localization of the deoxyerythronolide B synthase genes in *E. coli*. Metab Eng 10(1):33-38

Watanabe K, Hotta K, Nakaya M, Praseuth AP, Wang CCC, Inada D, Takahashi K, Fukushi E, Oguri H, Oikawa H (2009a) *Escherichia coli* allows efficient modular incorporation of newly isolated quinomycin biosynthetic enzyme into echinomycin biosynthetic pathway for rational design and synthesis of potent antibiotic unnatural natural product. J Am Chem Soc 131(26):9347-9353

Watanabe K, Hotta K, Praseuth AP, Koketsu K, Migita A, Boddy CN, Wang CCC, Oguri H, Oikawa H (2006) Total biosynthesis of antitumor nonribosomal peptides in *Escherichia coli*. Nat Chem Biol 2(8):423-428

Watanabe K, Hotta K, Praseuth AP, Searcey M, Wang CCC, Oguri H, Oikawa H (2009b)

Rationally engineered total biosynthesis of a synthetic analogue of a natural quinomycin depsipeptide in *Escherichia coli*. ChemBioChem 10(12):1965-1968

Weber G, Schörgendorfer K, Schneider-Scherzer E, Leitner E (1994) The peptide synthetase catalyzing cyclosporine production in *Tolypocladium niveum* is encoded by a giant 45.8-kilobase open reading frame. Curr Genet 26(2):120-125

Weber T, Baumgartner R, Renner C, Marahiel MA, Holak TA (2000) Solution structure of PCP, a prototype for the peptidyl carrier domains of modular peptide synthetases. Structure 8(4):407-418

Weber T, Marahiel MA (2001) Exploring the domain structure of modular nonribosomal peptide synthetases. Structure 9(1):R3-R9

Woodruff H (1980) Natural products from microorganisms. Science 208(4449):1225-1229

Wu C-Y, Jan J-T, Ma S-H, Kuo C-J, Juan H-F, Cheng Y-SE, Hsu H-H, Huang H-C, Wu D, Brik A, Liang F-S, Liu R-S, Fang J-M, Chen S-T, Liang P-H, Wong C-H (2004) Small molecules targeting severe acute respiratory syndrome human coronavirus. Proc Natl Acad Sci USA 101(27):10012-10017

Wulff EG, Mguni CM, Mansfeld-Giese K, Fels J, Lübeck M, Hockenhull J (2002) Biochemical and molecular characterization of *Bacillus amyloliquefaciens*, *B. subtilis* and *B. pumilus* isolates with distinct antagonistic potential against *Xanthomonas campestris* pv. campestris. Plant Pathol 51(5):574-584

Wyatt MA, Magarvey NA (2013) Optimizing dimodular nonribosomal peptide synthetases and natural dipeptides in an *Escherichia coli* heterologous host. Biochem Cell Biol 91:1-6

Yamasaki M, Nakamura K, Tamura N, Hwang S-J, Yoshikawa M, Sasaki N, Ohta H, Yamato O, Maede Y, Takiguchi M (2009) Effects and mechanisms of action of ionophorous antibiotics valinomycin and salinomycin-Na on *Babesia gibsoni* in vitro. J Parasitol 95(6):1532-1538

Yang W, Zhang L, Lu Z, Tao W, Zhai Z (2001) A new method for protein coexpression in *Escherichia coli* using two incompatible plasmids. Protein Expres Purif 22(3):472-478

Yeh E, Kohli RM, Bruner SD, Walsh CT (2004) Type II thioesterase restores activity of a NRPS module stalled with an aminoacyl-S-enzyme that cannot be elongated. ChemBioChem 5(9):1290-1293

Zhang H, Boghigian BA, Armando J, Pfeifer BA (2011) Methods and options for the heterologous production of complex natural products. Nat Prod Rep 28(1):125-151

Zhang H, Boghigian BA, Pfeifer BA (2010a) Investigating the role of native propionyl-CoA and methylmalonyl-CoA metabolism on heterologous polyketide production in *Escherichia coli*. Biotechnol Bioeng 105(3):567-573

Zhang H, Skalina K, Jiang M, Pfeifer BA (2012) Improved *E. coli* erythromycin A production through the application of metabolic and bioprocess engineering. Biotechnol Prog 28(1):292-296

Zhang H, Wang Y, Pfeifer BA (2008a) Bacterial hosts for natural product production. Mol Pharmaceut 5(2):212-225

Zhang H, Wang Y, Wu J, Skalina K, Pfeifer BA (2010b) Complete biosynthesis of erythromycin A and designed analogs using *E. coli* as a heterologous host. Chem Biol 17(11):1232-1240

Zhang W, Li Y, Tang Y (2008b) Engineered biosynthesis of bacterial aromatic polyketides in *Escherichia coli*. Proc Natl Acad Sci USA 105(52):20683-20688

Zhou X, Szeker K, Janocha B, Böhme T, Albrecht D, Mikhailopulo IA, Neubauer P (2013) Recombinant purine nucleoside phosphorylases from thermophiles: preparation, properties and activity towards purine and pyrimidine nucleosides. FEBS J 280(6):1475-1490

Zhou Y, Meng Q, You D, Li J, Chen S, Ding D, Zhou X, Zhou H, Bai L, Deng Z (2008) Selective removal of aberrant extender units by a type II thioesterase for efficient FR-008/candicidin biosynthesis in *Streptomyces* sp. strain FR-008. Appl Environ Microbiol 74(23):7235-7242

Acknowledgements

I would like to take this opportunity to sincerely appreciate all the people who have made contributions to this work and helps to my life in Berlin.

First of all, I would like to deeply thank my supervisor Prof. Dr. Peter Neubauer for accepting me to work in his group and giving me the interesting research project. I am greatly impressed by his inspired ideas and enthusiastic attitude towards science. His continuous support and encouragement always made me feeling confident to go forward. I also want to thank Prof. Dr. Roderich Süssmuth for his collaboration and allowing me to analyze all my samples in his group.

Especially, I would like to thank Jennifer Jaitzig for working together with me on the project, training me the molecular biology techniques and discussing the experimental designs. It was really a pleasant experience for me to work with her. In addition, I want to extend my gratitude to Lorenz Theuer for his contributions to my work. Furthermore, I am grateful to Dr. Stefan Junne, Eva Brand, Florian Glauche, Ping Lu, Basant El Kady and Qin Fan for their help during the bioreactor fermentation.

I am very grateful for the scholarship funded by the Berlin International Graduate School of Natural Sciences and Engineering (BIG-NSE) of the Cluster of Excellence “Unifying Concepts in Catalysis” (UniCat). Many thanks to Dr. Jean-Philippe Lonjaret for his excellent organizations of all the BIG-NSE activities. I also want to thank the PhD students from the BIG-NSE, Xiao Xie, Amandine Guiet, Arno Bergmann, Elham Baktash, Elisabeth Siebert, Florian Heims, Manar Arafeh, Pradip Dey, Fedaa al Masri, Florian Mayer, Heiner Schwarz, Rashed al Toma and Swantje Wiebalck, for their help and support.

I would like to express my gratitude to all the present and former members in Prof. Neubauer’s group. I thank Irmgard Maue-Mohn and Brigitte Burckhardt for their technical support. Herta Klein-Leuendorf for help with bureaucracy. Mirja Krause for

her always smiling greetings in the morning and endless encouragement in my hard times. Xinrui Zhou for her countless discussions with me from science to life. Dr. Kathleen Szeker for her kind help from laboratory experiment to outside conference. Friederike Hillig for perfectly translating German to English even though she was always busy with her huge data in the office. Dr. Nicolas Cruz-Bournazou for help with the experimental model design. I also want to thank Dr. Andreas Knepper, Erich Kielhorn, Julia Glazyrina, Anika Bockisch, Funda Cansu Ertem, Christian Reitz, Andri Hutari and all other colleagues for creating a great working environment.

I would like to thank Dr. Changzhu Wu for his helpful suggestions and positive discussions. Juan Li for her time to prepare a lot of yummy food. I also want to thank Gengwen Tan, Linyu Jiao and Xunhua Zhao for sharing some of their time with me in Berlin.

Finally, I would like to give my big thanks to my family. Without their understanding, support and unconditional love, I would not have been able to finish this study. I love you all forever!